

CANADIAN THESES ON MICROFICHE

THÈSES CANADIENNES SUR MICROFICHE



National Library of Canada
Collections Development Branch

Canadian Theses on
Microfiche Service

Ottawa, Canada
K1A 0N4

Bibliothèque nationale du Canada
Direction du développement des collections

Service des thèses canadiennes
sur microfiche

NOTICE

The quality of this microfiche is heavily dependent upon the quality of the original thesis submitted for microfilming. Every effort has been made to ensure the highest quality of reproduction possible.

If pages are missing, contact the university which granted the degree.

Some pages may have indistinct print especially if the original pages were typed with a poor typewriter ribbon or if the university sent us an inferior photocopy.

Previously copyrighted materials (journal articles, published tests, etc.) are not filmed.

Reproduction in full or in part of this film is governed by the Canadian Copyright Act, R.S.C. 1970, c. C-30. Please read the authorization forms which accompany this thesis.

**THIS DISSERTATION
HAS BEEN MICROFILMED
EXACTLY AS RECEIVED**

AVIS

La qualité de cette microfiche dépend grandement de la qualité de la thèse soumise au microfilmage. Nous avons tout fait pour assurer une qualité supérieure de reproduction.

S'il manque des pages, veuillez communiquer avec l'université qui a conféré le grade.

La qualité d'impression de certaines pages peut laisser à désirer, surtout si les pages originales ont été dactylographiées à l'aide d'un ruban usé ou si l'université nous a fait parvenir une photocopie de qualité inférieure.

Les documents qui font déjà l'objet d'un droit d'auteur (articles de revue, examens publiés, etc.) ne sont pas microfilmés.

La reproduction, même partielle, de ce microfilm est soumise à la Loi canadienne sur le droit d'auteur, SRC 1970, c. C-30. Veuillez prendre connaissance des formules d'autorisation qui accompagnent cette thèse.

**LA THÈSE A ÉTÉ
MICROFILMÉE TELLE QUE
NOUS L'AVONS REÇUE**

Canada



National Library
of Canada

Bibliothèque nationale
du Canada

Ottawa, Canada
K1A 0N4

TC -

ISBN 0-315-21203-9

CANADIAN THESES ON MICROFICHE SERVICE - SERVICE DES THÈSES CANADIENNES SUR MICROFICHE

PERMISSION TO MICROFILM - AUTORISATION DE MICROFILMER

• Please print or type - Écrire en lettres moulées ou dactylographier

AUTHOR - AUTEUR

Full Name of Author - Nom complet de l'auteur

William Mark McKinley

Date of Birth - Date de naissance

Aug 9 1958

Canadian Citizen - Citoyen canadien

Yes / Oui

No / Non

Country of Birth - Lieu de naissance

Canada

Permanent Address - Résidence fixe

11117 University Ave.
Edmonton, Alta.
Canada, T6G-1Y5

THESIS - THÈSE

Title of Thesis - Titre de la thèse

The Interaction of Masonry Veneer and Steel
Studs in Curtain Wall Construction

Degree for which thesis was presented
Grade pour lequel cette thèse fut présentée

M.Sc.

Year this degree conferred
Année d'obtention de ce grade

1985

University - Université

University of Alberta

Name of Supervisor - Nom du directeur de thèse

Dr. J. Warwark

AUTHORIZATION - AUTORISATION

Permission is hereby granted to the NATIONAL LIBRARY OF CANADA to
microfilm this thesis and to lend or sell copies of the film.

L'autorisation est, par la présente, accordée à la BIBLIOTHÈQUE NATIONALE
DU CANADA de microfilmer cette thèse et de prêter ou de vendre des ex-
emplaires du film.

The author reserves other publication rights, and neither the thesis nor exten-
sive extracts from it may be printed or otherwise reproduced without the
author's written permission.

L'auteur se réserve les autres droits de publication; ni la thèse ni de longs ex-
traits de celle-ci ne doivent être imprimés ou autrement reproduits sans
l'autorisation écrite de l'auteur.

ATTACH FORM TO THESIS - VEUILLEZ JOINDRE CE FORMULAIRE À LA THÈSE

Signature

W. M. McKinley

Date

April 15, 1985

THE UNIVERSITY OF ALBERTA

THE INTERACTION OF MASONRY VENEER AND STEEL STUDS IN CURTAIN
WALL CONSTRUCTION

by

William Mark McGinley



A THESIS

SUBMITTED TO THE FACULTY OF GRADUATE STUDIES AND RESEARCH
IN PARTIAL FULFILMENT OF THE REQUIREMENTS FOR THE DEGREE
OF Masters of Science

Department of Civil Engineering

EDMONTON, ALBERTA

SPRING 1985

THE UNIVERSITY OF ALBERTA

RELEASE FORM

NAME OF AUTHOR William Mark McGinley
TITLE OF THESIS THE INTERACTION OF MASONRY VENEER AND
STEEL STUDS IN CURTAIN WALL CONSTRUCTION
DEGREE FOR WHICH THESIS WAS PRESENTED Masters of Science
YEAR THIS DEGREE GRANTED SPRING 1985

Permission is hereby granted to THE UNIVERSITY OF ALBERTA LIBRARY to reproduce single copies of this thesis and to lend or sell such copies for private, scholarly or scientific research purposes only.

The author reserves other publication rights, and neither the thesis nor extensive extracts from it may be printed or otherwise reproduced without the author's written permission.

(SIGNED) *W.M. McGinley*.....

PERMANENT ADDRESS:

*.....11117.....University.....Ave.
.....Edmonton.....Alta.....
.....Canada.....T6G-1Y5*

DATED *April 4*.....1985

THE UNIVERSITY OF ALBERTA
FACULTY OF GRADUATE STUDIES AND RESEARCH

The undersigned certify that they have read, and recommend to the Faculty of Graduate Studies and Research, for acceptance, a thesis entitled THE INTERACTION OF MASONRY VENEER AND STEEL STUDS IN CURTAIN WALL CONSTRUCTION submitted by William Mark McGinley in partial fulfilment of the requirements for the degree of Masters of Science.

June
.....
Supervisor
Shonquorth
.....
W. J. Fitzpatrick
.....
W. H. H. H.
.....
Kennedy
.....

Date... *April 7* 1985

ABSTRACT

A three phase experimental program was conducted to evaluate the load deflection behaviour of laterally loaded brick veneer and steel stud curtain walls.

The first phase evaluated the interaction of the metal ties and steel studs. Effects of the wall cavity, tie type, stud type, relative displacement of the tie ends, and the tie location were investigated. The tie tests were performed on both short individual studs and larger wall sections.

Phase two evaluated the performance of the steel stud backing wall. The support settlement at the track and stud junction and the extent of the composite action between the steel studs and gyproc sheathing were investigated.

The final phase of the testing program evaluated the performance of sixteen, full sized, brick veneer and steel stud, curtain wall specimens subjected to a positive pressure loading. The effects of wall cavity, tie type, and stud type were investigated.

A semi-empirical model of the tie stiffness was developed and subsequently used for a direct stiffness analysis procedure to predict the behaviour of brick veneer and steel stud curtain walls.

ACKNOWLEDGEMENTS

This investigation was made possible by financial assistance and material donations provided by the Natural Sciences and Engineering Research Council of Canada, the Alberta Masonry Institute, and IXL Brick Ltd.

Dr. J. Warwaruk provided invaluable financial and technical support as supervisor of this investigation. The advice and technical assistance of Dr. M. Hatzinikolas and Prof. J. Longworth were also greatly appreciated.

The help of Thomas Casey with the computer generated plots contained in this report is hereby acknowledged.

The author would like to thank the Department of Civil Engineering for its financial support in the form of a Graduate Teaching Assistantship. He would also like to thank his wife, whose assistance in the production of this report proved invaluable.

Table of Contents

Chapter	Page
ABSTRACT	iv
ACKNOWLEDGEMENTS	v
LIST OF TABLES	vii
LIST OF FIGURES	viii
1. INTRODUCTION	1
2. A REVIEW OF CURRENT DESIGN PROCEDURES AND EXPERIMENTAL WORK	4
3. TESTING PROGRAM	8
3.1 Introduction	8
3.2 Tie Testing	8
3.2.1 Brick Tie and Steel Stud Tests	9
3.2.1.1 Specimen Description and Construction	9
3.2.1.2 Testing Apparatus and Procedures ..	12
3.2.2 Tie and Wall Section Tests	14
3.2.2.1 Specimen Description and Construction	14
3.2.2.2 Testing Apparatus and Procedures ..	16
3.3 Backing Wall Tests	19
3.3.1 Stud and Track Interaction	20
3.3.1.1 Specimen Description and Construction	20
3.3.1.2 Testing Apparatus and Procedures ..	21
3.3.2 Stud and Gyproc Interaction	21
3.3.2.1 Specimen Description and Fabrication	21
3.3.2.2 Testing Apparatus and Procedures ..	23
3.4 Full Sized Wall Tests	25

3.4.1	Specimen Description and Construction	25
3.4.2	Testing Apparatus and Procedures	32
4.	TEST RESULTS	39
4.1	Introduction	39
4.2	Tie Test Results	39
4.2.1	Short Stud and Tie Tests	40
4.2.1.1	Weak Tie Behaviour	40
4.2.1.2	Strong Tie Behaviour	45
4.2.2	Tie and Wall Section Tests	46
4.2.2.1	Weak Tie Behaviour	47
4.2.2.2	Strong Tie Behaviour	47
4.3	Backing Wall Test Results	49
4.3.1	Stud and Track Interaction	49
4.3.2	Gyproc and Stud Interaction	55
4.4	Results of the Full Sized Wall Tests	55
4.4.1	Series No.1	57
4.4.1.1	Series No.1 Wall No.1	57
4.4.1.2	Series No.1 Wall No.2	59
4.4.1.3	Series No.1 Wall No.3	59
4.4.1.4	Series No.1 Wall No.4	60
4.4.2	Series No.2	61
4.4.2.1	Series No.2 Wall No.1	61
4.4.2.2	Series No.2 Wall No.2	62
4.4.2.3	Series No.2 Wall No.3	62
4.4.2.4	Series No.2 Wall No.4	63
4.4.3	Series No.3	64
4.4.3.1	Series No.3 Wall No.1	64

4.4.3.2	Series No.3 Wall No.2	64
4.4.3.3	Series No.3 Wall No.3	65
4.4.3.4	Series No.3 Wall No.4	65
4.4.4	Series No.4	67
4.4.4.1	Series No.4 Wall No.1	67
4.4.4.2	Series No.4 Wall No.2	68
4.4.4.3	Series No.4 Wall No.3	70
4.4.4.4	Series No.4 Wall No.4	70
5.	ANALYSIS AND DISCUSSION	72
5.1.	Introduction	72
5.2	Evaluation of the Tie Tests	72
5.2.1	The Effects of the Tie Type	73
5.2.1.1	Junction Stiffness	73
5.2.1.2	Maximum Load	79
5.2.2	The Effect Of Stud Type	81
5.2.2.1	Junction Stiffness	81
5.2.2.2	Maximum Load	82
5.2.3	The Effect Of The Tie End Offset	83
5.2.3.1	Junction Stiffness	83
5.2.3.2	Maximum Load	85
5.2.4	The Effect Of Gap Size	86
5.2.4.1	Junction Stiffness	86
5.2.4.2	Maximum Load	87
5.2.5	Location Of Tie	87
5.2.5.1	Junction Stiffness	87
5.2.5.2	Maximum Load	89

5.2.6 Wall Section Tests Versus Short Stud Tests	89
5.2.6.1 Junction Stiffness	90
5.2.6.2 Maximum Load	90
5.3 The Evaluation of Gyproc, Track and Stud Interaction	91
5.4 Evaluation of Full Sized Wall Tests	94
5.4.1 Wall Performance	95
5.4.1.1 90 mm. 18 Gauge Walls	95
5.4.1.2 150 mm 20 Gauge Walls	101
5.5 Analytical Models	104
5.6 Evaluation of the Analytical Model	107
5.7 Evaluation of Current Design Procedures	115
6. CONCLUSIONS AND RECOMMENDATIONS	118
6.1 Conclusions	118
6.2 Recommendations	120
References	122
APPENDIX A - MATERIAL TESTS	124
APPENDIX B - LOAD DEFLECTION CURVES	132

List of Tables

Table		Page
3.1	A Summary of Tie Dimensions	10
3.2	A Summary of Full Sized Wall Specimens	33
4.1	Short Stud and Tie Test Results	41
4.2	Short Stud and Tie Test Results	42
4.3	Short Stud and Tie Test Results	43
4.4	Wall Section and Tie Test Results	50
4.5	Wall Section and Tie Test Results	51
5.1	Summary of Wall Failure Loads	97
Table A-1	Summary of Masonry Tests	125
Table A-2	Summary of Gyproc Tests	130

List of Figures

Figure		Page
3.1	Ties Tested	11
3.2	Studs Tested	11
3.3	Single Stud Tie Testing Apparatus	13
3.4	Measured Dimensions	15
3.5	Tie and Wall Section Testing Apparatus	17
3.6	Track-Stud Interaction Testing Apparatus	22
3.7	Wall Section Testing Apparatus and Specimen	24
3.8	Full Sized Wall Specimen	26
3.9	Full Sized Wall Specimen Details	27
3.10	Full Sized Wall Steel Track Secured	29
3.11	Full Sized Wall Studs and Bridging Assembled	29
3.12	Full Sized Wall Backing Wall Completed	30
3.13	Full Sized Wall Top Expansion Joint Detail	31
3.14	Full Sized Wall Specimen Completed	31
3.15	A Summary of Tie Patterns	34
3.16	Full Sized Wall Test Frame	35
3.17	The L.V.D.T.s Assembly	35
3.18	Location of the Measured Points of Deflection	37
4.1	Typical Weak Tie Behaviour (Short Stud Tests)	44
4.2	Typical Strong Tie Behaviour (Short Stud Tests)	44

Figure		Page
4.3	Typical Weak Tie Behaviour (Wall Section Tests)	48
4.4	Typical Strong Tie Behaviour (Wall Section Tests)	48
4.5	Track and Stud Interaction (18 gauge)	53
4.6	Track and Stud Interaction (20 gauge)	54
4.7	The Stud and Gyproc Wall Section Test Results	56
4.8	Buckled Ties in Wall Cavity	58
4.9	Failure of Stud Web	66
4.10	Typical Stud Flange Failure	69
5.1	Tie and Stud Junction	74
5.2	Variation of Slope With End Offset	84
5.3	Variation of Maximum Load With End Offset	84
5.4	Variation of the Junction Stiffness with Web Distance	88
5.5	True Load Deflection Curves for the Backing Walls	93
5.6	A Comparison of Brick Veneer Deflections	99
5.7	A Comparison of Steel Stud Deflections	100
5.8	Curtain Wall Direct Stiffness Model	106
5.9	A Comparison of Brick Veneer Deflections	109
5.10	A Comparison of Stud Wall Deflections	110

Figure		Page
5.11	A Comparison of Brick Veneer Deflections	112
5.12	A Comparison of Stud Wall Deflections	113
Figure A-1	Brick Prism Deflections - Series No.2	126
Figure A-2	Brick Prism Deflections - Series No.3	127
Figure A-3	Brick Prism Deflections - Series No.4	128
Figure A-4	Steel Tension Coupon Tests	131
Figure B-1	Brick Veneer Deflections - Series No.1 Wall No.1	133
Figure B-2	Stud Wall Deflections - Series No.1 Wall No.1	134
Figure B-3	Brick Veneer Deflections - Series No.1 Wall No.2	135
Figure B-4	Stud Wall Deflections - Series No.1 Wall No.2	136
Figure B-5	Brick Veneer Deflections - Series No.1 Wall No.3	137
Figure B-6	Stud Wall Deflections - Series No.1 Wall No.3	138
Figure B-7	Brick Veneer Deflections - Series No.1 Wall No.4	139
Figure B-8	Stud Wall Deflections - Series No.1 Wall No.4	140
Figure B-9	Brick Veneer Deflections - Series No.2 Wall No.1	141
Figure B-10	Stud Wall Deflections - Series No.2 Wall No.1	142
Figure B-11	Brick Veneer Deflections - Series No.2 Wall No.2	143

Figure	Page
Figure B-12 Stud Wall Deflections - Series No.2 Wall No.2	144
Figure B-13 Brick Veneer Deflections - Series No.2 Wall No.3	145
Figure B-14 Stud Wall Deflections - Series No.2 Wall No.3	146
Figure B-15 Brick Veneer Deflections - Series No.2 Wall No.4	147
Figure B-16 Stud Wall Deflections - Series No.2 Wall No.4	148
Figure B-17 Brick Veneer Deflections - Series No.3 Wall No.1	149
Figure B-18 Stud Wall Deflections - Series No.3 Wall No.1	150
Figure B-19 Brick Veneer Deflections - Series No.3 Wall No.2	151
Figure B-20 Stud Wall Deflections - Series No.3 Wall No.2	152
Figure B-21 Brick Veneer Deflections - Series No.3 Wall No.3	153
Figure B-22 Stud Wall Deflections - Series No.3 Wall No.3	154
Figure B-23 Brick Veneer Deflections - Series No.3 Wall No.4	155
Figure B-24 Stud Wall Deflections - Series No.3 Wall No.4	156
Figure B-25 Brick Veneer Deflections - Series No.4 Wall No.1	157
Figure B-26 Stud Wall Deflections - Series No.4 Wall No.1	158
Figure B-27 Brick Veneer Deflections - Series No.4 Wall No.2	159
Figure B-28 Stud Wall Deflections - Series No.4 Wall No.2	160

Figure	Page
Figure B-29	Brick Veneer Deflections - Series No.4 Wall No.3161
Figure B-30	Stud Wall Deflections - Series No.4 Wall No.3162
Figure B-31	Brick Veneer Deflections - Series No.4 Wall No.4163
Figure B-32	Stud Wall Deflections - Series No.4 Wall No.4164
Figure B-33	Brick Veneer Deflections - Series No.1 Wall No.1 With Analysis165
Figure B-34	Stud Wall Deflections - Series No.1 Wall No.1 With Analysis166
Figure B-35	Brick Veneer Deflections - Series No.2 Wall No.2 With Analysis167
Figure B-36	Stud Wall Deflections - Series No.2 Wall No.2 With Analysis168
Figure B-37	Brick Veneer Deflections - Series No.3 Wall No.2 With Analysis169
Figure B-38	Stud Wall Deflections - Series No.3 Wall No.2 With Analysis170
Figure B-39	Brick Veneer Deflections - Series No.4 Wall No.4 With Analysis171
Figure B-40	Stud Wall Deflections - Series No.4 Wall No.4 With Analysis172

1. INTRODUCTION

The use of masonry veneer with steel stud backing walls, for curtain wall construction, has gained in popularity in the past few years. The steel stud backing wall is quick to erect and easy to insulate. When compared to a backing wall comprised of concrete blocks, the steel stud walls are much lighter, require no additional stud inner wall and are easily modified for openings. Thus, this type of wall system provides an economical and lightweight alternative to the double wythe masonry cavity wall system.

The brick veneer and steel stud wall system is particularly useful as a durable cladding for high-rise construction. For this type of application, each lift of brick veneer is supported on a steel shelf angle which is attached to the building frame at floor level. The steel stud backing wall spans between each floor slab.

A masonry veneer and steel stud curtain wall consists of an exterior wythe of brick connected to a steel stud backing wall by corrosion resisting metal ties. The airspace over which the ties span is currently limited to 25 mm. The steel stud backing wall is usually sheathed on both sides by gypsum wallboard.

A wide variety of metal ties is available for the connection of brick veneer and steel stud backing. These types of ties range from corrugated metal strip ties to heavy gauge wire ties with adjustable connections to allow for vertical movements.

Until recently, the brick veneer and the steel stud wall systems had been used quite successfully. However, application of this wall system for wall heights exceeding 2700 mm., and with larger cavities for extra insulation, has resulted in unsatisfactory performance. There is, therefore, a lack of confidence in the current methods of wall design.

The masonry veneer and steel stud curtain wall system is an efficient form of cladding. Therefore, the uncertainty in the performance of the walls resulting from currently accepted design practices requires investigation.

Presented are the results of an experimental investigation conducted on masonry veneer and steel stud curtain walls. The goal of this investigation was to provide data on performance of the masonry veneer and steel stud curtain walls in a variety of configurations. The adequacy of current design methods is evaluated for both larger than standard wall height and larger than standard gap. As part of the investigation, the effects of tie type, stud type, and tie configuration on the load deflection behaviour of the masonry veneer and steel stud wall system are also evaluated.

To better understand the behaviour of the wall system, the interaction of each of the system's component parts was investigated. Tests were performed on the steel stud and tie junction and on the steel stud and gypsum wallboard backing wall.

A review of the currently accepted design methods and recent experimental work is presented in the second chapter. Subsequent chapters present a summary of the experimental program and its results, a discussion of the test results and a review of analytical techniques developed to model the behaviour of the masonry veneer and steel stud walls. Finally an evaluation of the adequacy of current design methods is presented.

2. A REVIEW, OF CURRENT DESIGN PROCEDURES AND EXPERIMENTAL WORK

Masonry veneer walls are currently designed almost exclusively using loading tables provided by various steel stud manufacturers. These tables ignore the strength of the brick veneer and simply assume that the steel studs will resist the entire wind load. Hence, the steel studs used in this experimental investigation were designed, according to the CSA Standard S-136 (1974), to resist the full wind loading. The maximum deflection of the steel studs was limited to $L/360$.

The spacing of the ties, the tie type and the maximum gap recommended for use in masonry veneer walls are governed by empirically derived limits specified in CSA Standard CAN3-S304-M78'. This standard limits the total height of brick veneer allowed in each lift of wall to 3.6 m.. It further limits the gap to 25 mm. and the minimum gauge of corrugated tie that can be used to 28. Maximum vertical tie spacing varies with the maximum horizontal tie spacing; for a 400 mm. horizontal spacing, the maximum vertical spacing is 600 mm. and, for a horizontal spacing of 600 mm., the maximum vertical spacing is 500 mm..

CSA Standard CAN3-A37-M84² recommends different spacing limits for corrugated ties. The new limits are 400 mm. horizontal for a 600 mm. vertical spacing, and 600 mm. horizontal for a 400 mm. vertical spacing. This Code requires that non standard ties be tested using a typical

tie and stud assembly. The total deflection of this assembly must not cause cracking of the brick veneer.

The interaction of the brick veneer and the steel studs has been largely ignored in the evaluation of the behaviour of curtain walls. The Brick Institute of America³, however, postulates that if the ties are arranged so that the studs and brick deflect equally then the wind load can be distributed according to the relative stiffness (EI) of the two walls. Because the stiffer brick veneer will be required to resist a large portion of the wind load, the Brick Institute of America suggests that the present deflection limits are not adequate and, accordingly, recommends a deflection limit of $L/600$ to $L/720$.

The distribution of load, as a function of the relative stiffness, is used for the design of cavity walls comprised of two wythes of masonry. In cavity walls, the relative stiffnesses of the two wythes are of the same order of magnitude. However, in a curtain wall, the brick veneer is considerably stiffer than the steel stud backing wall. Furthermore, the support conditions and span lengths of the stud and brick veneer differ. These factors argue against the equal deflection of the backup and veneer. Tests on full-sized curtain wall specimens conducted by Arumala and Brown⁴ at Clemson University, confirmed the inadequacies of load distribution by relative stiffness. They found that the end conditions, the difference in the span of the two wythes, and the tie stiffness affect the distribution of

lateral load as much as the relative stiffnesses of the brick and the studs. Thus while the behaviour of the curtain wall is greatly affected by the interaction of the veneer and the steel studs there are many other factors which also have a significant effect on the wall's behaviour.

The analysis by Arumala and Brown of the results of their full sized wall tests indicated that there is little or no interaction between the studs and gyproc sheathings in the backing wall. Their analysis also indicated that the compressible filler in the top expansion joint provided negligible restraint to the movement of the wall. With the large differential movement allowed at the top of the brick veneer, the stress in the brick was reduced and the brick walls were able to reach their design load. The safety factors for the walls ranged from 1.2 to 3.0. These factors of safety are lower than those generally used for masonry design.

In the Arumala and Brown study, the load deflection behaviour of the ties was studied for ties tested in isolation from the rest of the backing wall. The ties were tested between a brick prism and a steel plate. A stiffness factor was derived from the slope of the load deflection plot for each of the ties. This stiffness factor was then used as a spring constant in their mathematical model of the frame action of the walls. Their model and testing ignored the interaction between the flange of the steel stud, tie and gyproc.

There is still relatively little information on the behaviour of brick veneer and steel stud curtain walls. The effects of the tie type, stud stiffness, cavity size, and tie spacing on the wall's performance need further investigation. In particular, the interaction of the tie, steel stud and gyproc must be investigated.

3. TESTING PROGRAM

3.1 Introduction

A typical masonry veneer curtain wall consists of brick veneer, steel ties and a gyproc and steel stud backing wall. To better understand the behaviour of masonry and steel stud walls an extensive experimental program was conducted at the University of Alberta's Structures lab. The behaviour of the ties, the brick and the studs was studied, both in isolation and in combination.

The following sections describe the testing program conducted on the major structural components of these walls. The first section describes the experiments performed on the steel ties. Subsequent sections report the testing program carried out on the backing wall and full sized wall sections. The tests conducted on the brick veneer are presented in Appendix A.

3.2 Tie Testing

The purpose of the tie tests was to record the load deflection behaviour and mode of failure of different types of ties under a compressive axial load. A linear approximation of this behaviour was then used in a mathematical analysis of the load-deflection behaviour of the full sized wall sections.

Wall ties do not act in isolation. They interact with the brick, the steel studs, and the gyproc panels. Previous

studies have examined the interaction of ties and masonry. Results indicated that below the pullout load the masonry has little effect on the behaviour of the steel ties. The steel studs, however, have an open section and, as a result, have a significant effect on the behaviour of the ties.

The gypsum panels provide restraint to the flange of the steel stud so that they also affect the performance of the ties. To evaluate the contribution of each of these components to the behaviour of the ties, two series of tests were conducted on a selection of ties. In the first series the ties were tested on short lengths of a single stud and in the second series the ties were tested on a full width wall section.

3.2.1 Brick Tie and Steel Stud Tests

3.2.1.1 Specimen Description and Construction

There were two major parameters in this experimental program, namely the tie type and the stud type. Five different ties were tested; 24, 22, and 16 gauge corrugated strip ties, a 6 gauge adjustable rod "V" tie and a 9 gauge wire ladder tie. Table 3.1 describes these ties in more detail. The two studs used were a 18 gauge 90 mm. (3 5/8 in.) and a 20 gauge 150 mm. (6 in.) steel stud. The ties and studs are shown in Figures 3.1 and 3.2 respectively.

A 450 mm. length of steel stud was cut and the ties were fastened to the centre of the stud flange at

Table 3.1 A Summary of Tie Dimensions

A DESCRIPTION OF THE TIES USED IN THIS PROGRAM	
Tie Type	Description
24 gauge corrugated	width= 25 mm., length= 205 mm., thickness= 0.66 mm.
22 gauge corrugated	width= 25 mm., length= 205 mm., thickness= 0.78 mm.
16 gauge corrugated	width= 25 mm., length= 190 mm., thickness= 1.50 mm.
Ladder	wire diameter= 3.66 mm., cross pieces arranged in ladder fashion between longitudinal wires 100 mm. apart. The cross pieces are at 380 mm. O.C.
"T" B.L.319 adjustable veneer tie	wire diameter= 4.75 mm., spacing of wire= 8 mm., adjustment height= 50 mm., length= 120 mm., and a cross "T" width= 110. mm.
"V"	wire diameter= 4.75 mm., dimensions of "V" are 40 mm. and 90 mm., length= 75 mm., 18 gauge clip with a 30 mm. adjustment, and a 16 gauge backing

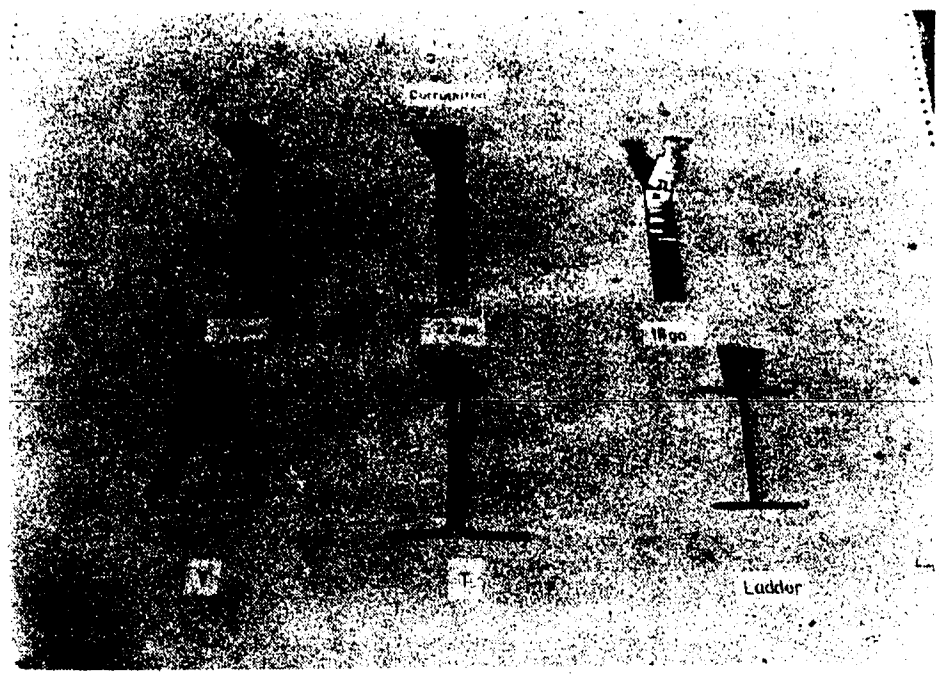


Figure 3.1 Ties Tested

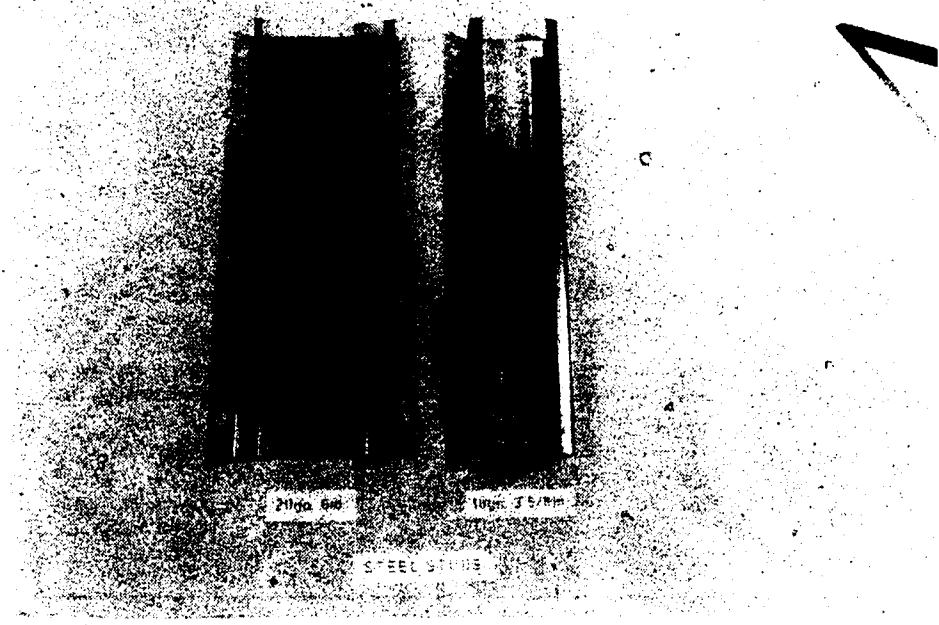


Figure 3.2 Studs Tested

mid-height. A small pad of gyproc was placed between the tie and the stud before the tie was fastened down. A single No. 10 self-drilling sheet metal screw was used to attach all but the "V" ties. Each screw was located as close as possible to the tie bend. The "V" ties were fastened by two hex head, number 6, self-drilling screws.

The stud and tie assembly was then bolted to the supports of the testing apparatus. Two 75 mm. long, wood bearing stiffeners were used at the supports to preclude any bending of the stud flange by the clamping force of the fastening bolts.

3.2.1.2 Testing Apparatus and Procedures

The testing apparatus consists of a single-acting loading jack, clamping mechanism, adjustable travel guide, load cell, and a linear variable differential transducer. Figure 3.3 is a schematic drawing of the testing unit. A 200 lb. (W) weight was placed on the clamp to preclude any upward movement as the tie buckled. The increase in friction between the clamp and guide, due to this added weight, was found to be negligible.

After the stud and tie assembly was bolted to the cross-members, the tie was placed in the clamping mechanism and securely fastened. A backing plate was used with the V, T, 16 gauge corrugated, and ladder ties so that slipping of the tie within the clamping

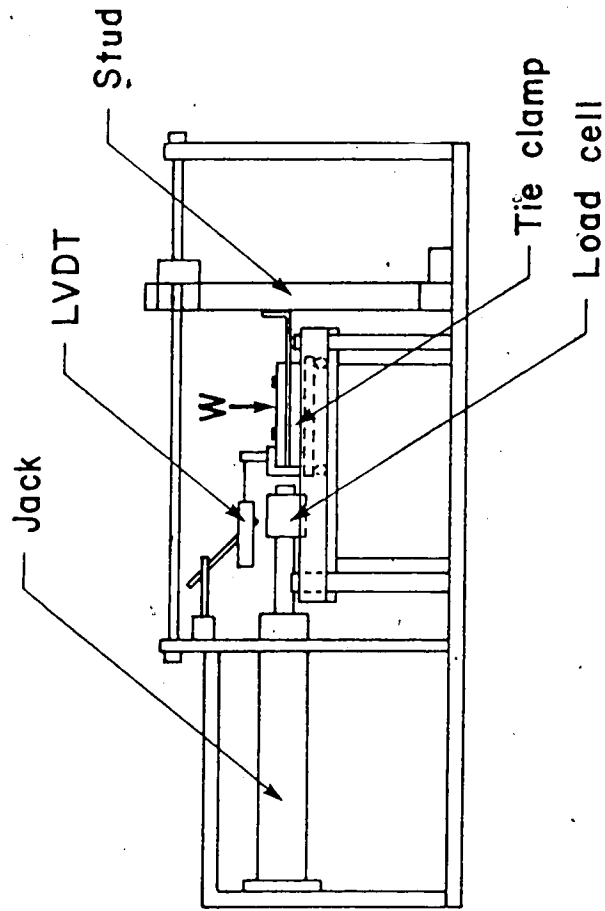


Figure 3.3 Single Stud Tie Testing Apparatus

mechanism was prevented. The ties were clamped to simulate the restraint that brick veneer provides.

A compressive load was then applied to the clamped tie via a hand operated pump and the loading jack. A transducer measured the axial deflection of the clamped end of the tie. The output from the load cell and the transducer were plotted as the test proceeded. A load-deflection curve and a maximum load was generated for each specimen.

All the ties were tested on the 16 gauge, 90 mm. studs. In addition to these tests the end offset (d) was varied for the 16, 22, and 24 gauge corrugated and ladder ties (see Figure 3.4). The gap (c1) was kept at a constant 50 mm for all tests. The 22 gauge corrugated ties were also tested using a gap of 25 mm.

The 16 gauge and 22 gauge corrugated ties were tested on the 150 mm. 20 gauge steel stud. In these tests, the gap was kept at a constant 50 mm. and the end offset was as close to zero as possible .

3.2.2 Tie and Wall Section Tests

3.2.2.1 Specimen Description and Construction

In this phase of testing, a 1210 mm. long by a 1210 mm. wide wall section was used as a backing for the tie tests. This wall section consisted of three steel studs spaced at 400 mm. on centre, sheathed on both sides by 12 mm. sheets of gyproc. The gyproc was fastened to the

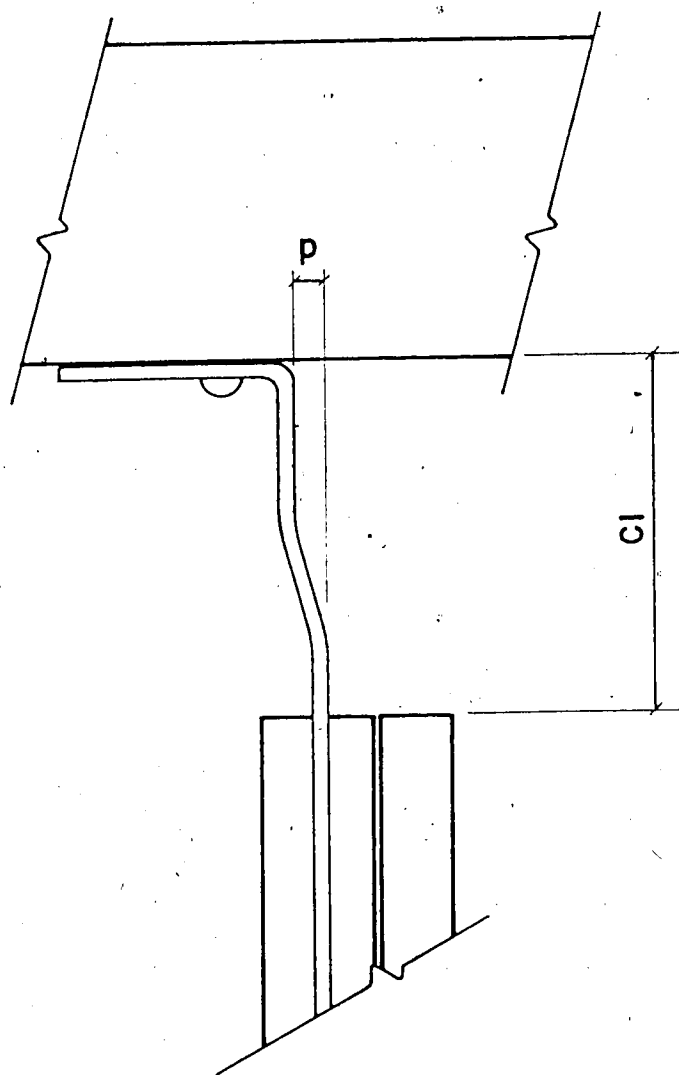


Figure 3.4 Measured Dimensions

studs by 38 mm. (1 1/2 in.), "Teck", self-drilling, flat head screws at 600 mm. centres. The studs were attached to the supporting channels using the manufacturer's standard steel track for each gauge of stud.

After the wall sections were fabricated in the testing frame, the ties were fastened to the studs. On each wall section, the outlines of the studs were accurately established. Each outline was clearly marked on the gyproc so that the location of the screw, with respect to the stud web, could be measured later.

Three wall sections were fabricated, two using the 18 gauge 90 mm. studs and one using the 20 gauge 150 mm. studs. Only three types of ties were tested in this phase of the experimental program. They were the B.L. 319 "T" ties, and the 22 and 16 gauge corrugated strip ties.

3.2.2.2 Testing Apparatus and Procedures

The apparatus used to test the veneer ties and wall sections is shown in Figure 3.5. This testing frame consisted of a double-acting jack, tie clamp, adjustable clamp guide, load cell, two linear variable differential transducers, and the supporting channels for the wall sections.

After the wall section was built, the ties were fastened to the center stud. While the vertical position of the ties in the wall varied with each tie tested, all ties were tested within 200 mm. of mid-height. The tie



Figure 3.5 Tie and Wall Section Testing Apparatus

was then clamped and measurements of its location and gap were made. The offset of the tie ends was kept at a constant value of zero.

One transducer, located at the back side of the wall section, was positioned so that it was at the same height as the tie. Thus, a measurement of the beam deflection of the stud was made. A second transducer measured the deflection of the clamped end of the tie. By taking the difference between these two deflections, an accurate reading of the overall deflection behaviour of the tie-stud junction was obtained.

A compressive load was applied to the ties using a hand hydraulic pump to actuate the jack. The load cell output, as well as the output from both transducers, was plotted using a three channel plotter. Load-deflection curves were obtained for all specimens tested.

When the 22 gauge corrugated ties were tested, the same backing was re-used for a series of tie tests. Each subsequent tie was fastened to the stud on an undamaged area of the gyproc. This procedure was repeated until all but one area of the gyproc in the centre region of the middle stud had been used.

The 16 gauge corrugated ties or the "T" ties were tested on the the wall sections after the 22 gauge tie tests were completed. As the studs failed during the testing of these stiff ties, only one tie was tested on each of the studs in the backing wall.

The 16 and 22 gauge corrugated ties were tested on the 90 mm. and 150 mm. stud walls. The "T" ties were tested only on the 90 mm. backing wall section.

The final variable investigated in this phase of the testing program was the location of the tie fastening screw on the stud flange, relative to the stud web. Except for the tests where the location of the corrugated ties was purposely varied, the ties were placed as close as possible to the centre of stud flange without measuring. The effect of the location of the screws was investigated on both the 90 mm. and 150 mm. stud wall sections.

3.3 Backing Wall Tests

The next phase of the testing program evaluated the structural behaviour of the backing wall. This wall consists of track, studs and gyproc sheathing. The load-deflection behavior of each of these components was investigated in the following series of experiments.

The flexural behaviour of the gyproc panels was evaluated by loading 100 mm. by 780 mm. strips of gyproc as beams and observing their behavior. The procedures used, and the results obtained from these tests, are reported in Appendix A.

During earlier tests, it was noted that the flange of the steel track used to fasten the studs to the structural supports underwent significant deflection upon loading. The

first series of tests in this section attempted to quantify this effect.

One of the most important purposes of this phase of the testing program was to determine whether there was any composite action between the steel studs and the gyproc sheathing. The second series of tests was conducted to determine the extent of this composite action. In later analysis, an accurate value for the Young's Modulus (E) of the steel studs was required. A set of tension coupons was cut from the stud metal and tested. The results of these tests are reported in Appendix A.

3.3.1 Stud and Track Interaction

3.3.1.1 Specimen Description and Construction

The deflection of the studs, within their supporting track, was investigated in this section of the experimental program.

Each specimen consisted of a 470 mm. length of stud fixed between two 300 mm. sections of track. A 200 mm. wood bearing stiffener was placed at midspan of each of the studs. The stiffener was used to preclude buckling of the stud upon loading of the specimen.

Four specimens were fabricated, two from the 18 gauge 90 mm. studs and two from the 20 gauge 150 mm. steel studs.

3.3.1.2 Testing Apparatus and Procedures

Each track and stud assembly was placed between a pair of fixed channels. The track was fastened using 12 mm. grade 2 capscrews spaced at 200 mm. centres. Two metric dial gauges were then set at 30 mm. from the each end of the specimen. The loading apparatus, a single-action jack and load cell, was then located over midspan (see Figure 3.6).

Using a hand hydraulic pump to actuate the jack, the specimen was loaded at its centre. Static loads and deflections were recorded up to the specimen's failure.

3.3.2 Stud and Gyproc Interaction

3.3.2.1 Specimen Description and Fabrication

Three specimens were fabricated and tested in this series of experiments. The specimens were constructed to model a typical section of the gyproc and the steel stud backing wall. All of the walls were built using the 90 mm., 18 gauge, steel studs. Before the wall sections were assembled, the dimensions of each stud were accurately measured.

Two of the wall sections were identical. Both consisted of 2 steel studs spaced at 400 mm. on centre sheathed by 12 mm. gyproc on both sides. Standard 18 gauge track was attached to the ends of the steel studs. The gyproc was fastened to the studs using "Teck" screws, at a 600 mm spacing. Two lines of 12 mm channel

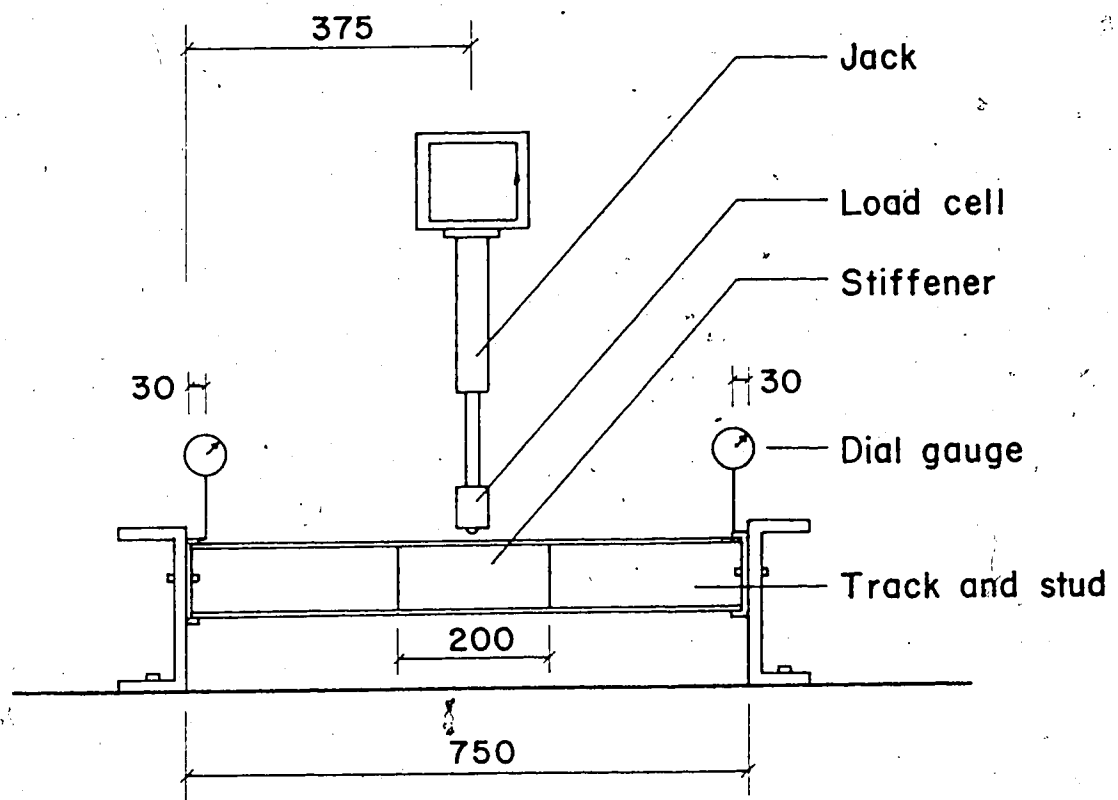


Figure 3.6 Track-Stud Interaction Testing Apparatus

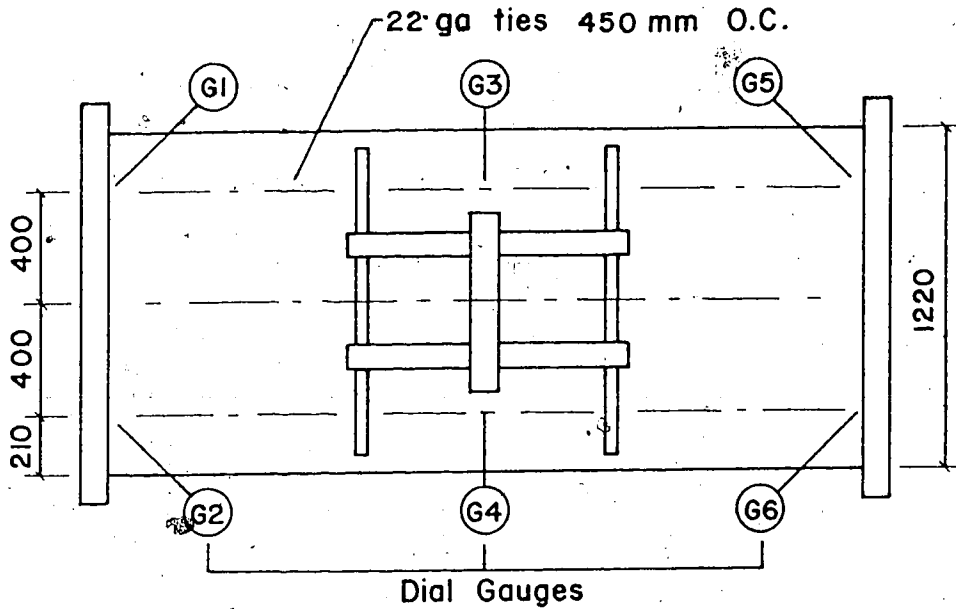
bridging were brazed to the studs at the centre service cut-outs. Each of the wall sections was 800 mm. wide and 2700 mm. long.

The third specimen was constructed to be a more exact model of the backing walls used for the full sized tests. Thus, there were three studs spaced at 400 mm. instead of two. Also, 22 gauge corrugated strip ties were fastened to the studs at a 400 mm. by 450 mm. staggered spacing. The wall section was 1220 mm. wide and 2700 mm. long. All other construction details were the same as those in the two-stud specimens. Figure 3.7 shows the details of the three-stud wall section in its testing frame.

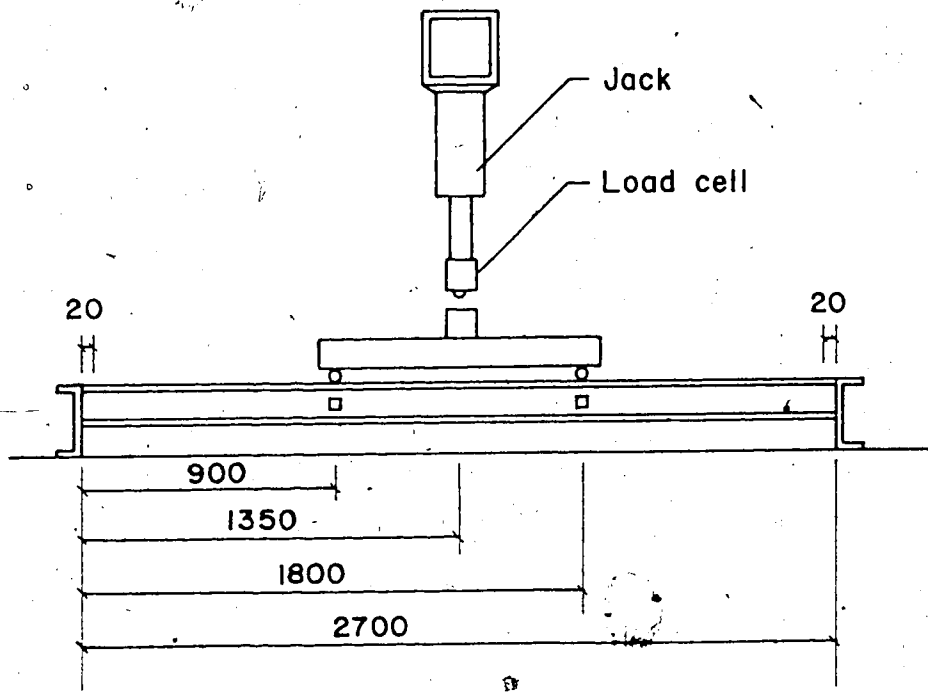
3.3.2.2 Testing Apparatus and Procedures

The specimens were fastened between two fixed channel supports using three 12 mm hex head bolts equally spaced along the centre of the track. After the wall sections were secured, the loading assembly was positioned so that the third points of the specimen were loaded. Figure 3.7 shows the apparatus used to test these wall sections. The load from the single-acting jack was transferred to rollers at the third points using a H.S.S. distributing beam. An extra distributing beam was used to limit the deflections of the rollers in the three-stud specimen's test.

A load cell was attached to the head of the jack and thus measured twice the load transferred to each of



PLAN



ELEVATION

Figure 3.7 Wall Section Testing Apparatus and Specimen

the rollers. Two metric dial gauges were placed at mid-span of each specimen. Each gauge was located on the centre of the outside stud lines. On the three stud section, gauges were also located 20 mm from the supports on each of the outside studs.

The jack was actuated using a hand pump. Readings of the static load and all deflections were recorded up to failure of the specimens.

3.4 Full Sized Wall Tests

In the final phase of the experimental program full height, masonry veneer, curtain wall sections were subjected to a positive pressure loading.

The purpose of this series of tests was to observe the load deflection behaviour of a typical section of veneer wall. The effects of tie type, tie arrangement and stud type on the deflection characteristics of this type of wall were investigated.

3.4.1 Specimen Description and Construction

A total of sixteen wall sections were tested in this part of the experimental program. These walls were fabricated and tested in four series with each series consisting of four walls.

Figures 3.8 and 3.9 show the construction details of a typical full sized wall specimen. Two concrete slabs served as the frame for each of the specimens. The concrete slabs

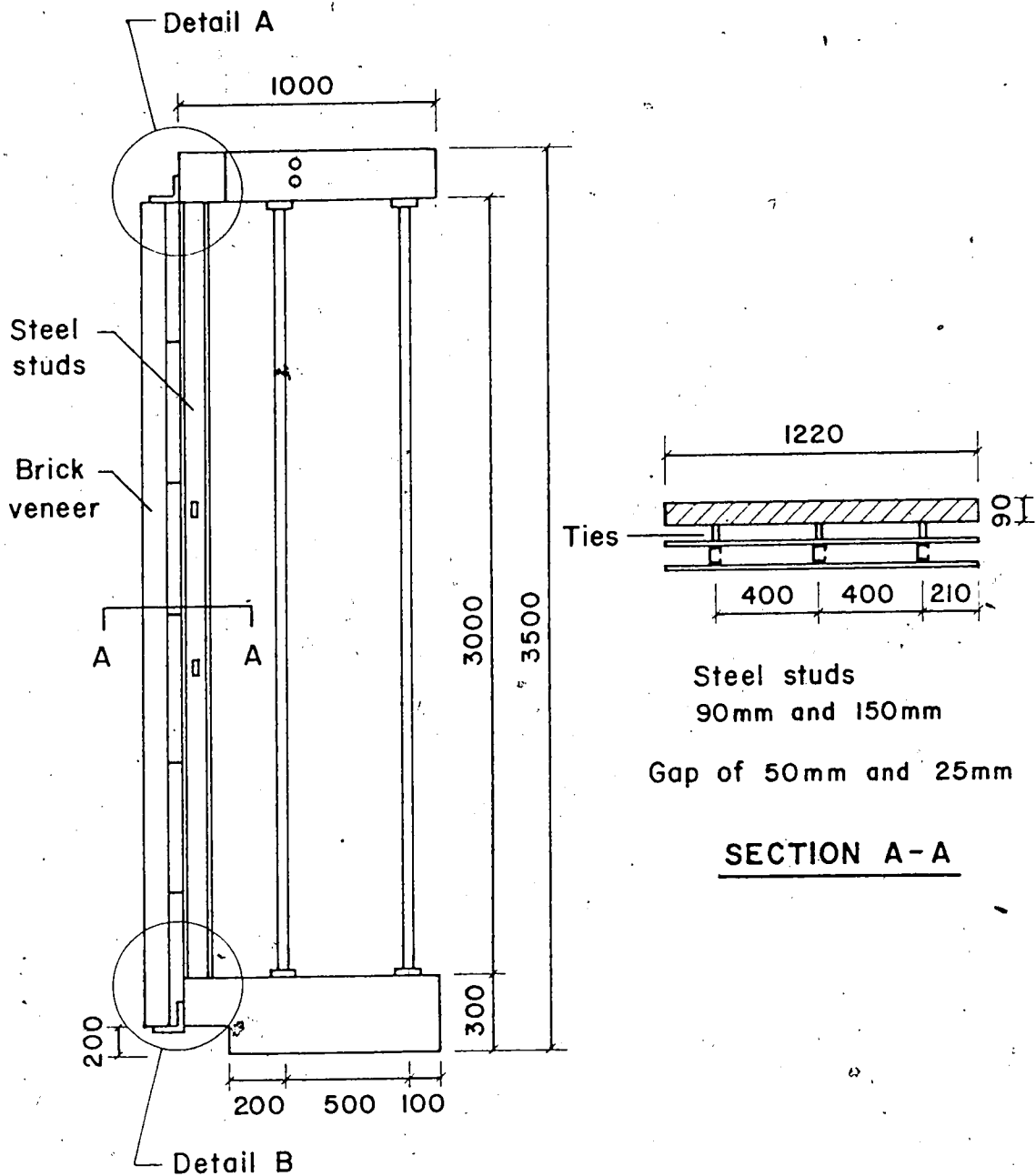
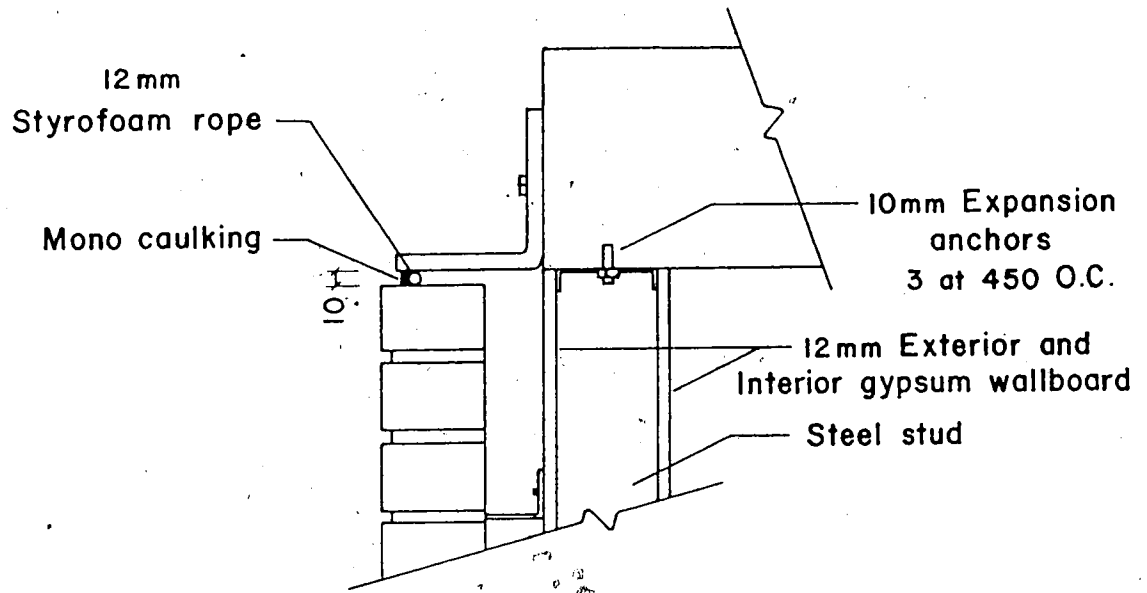
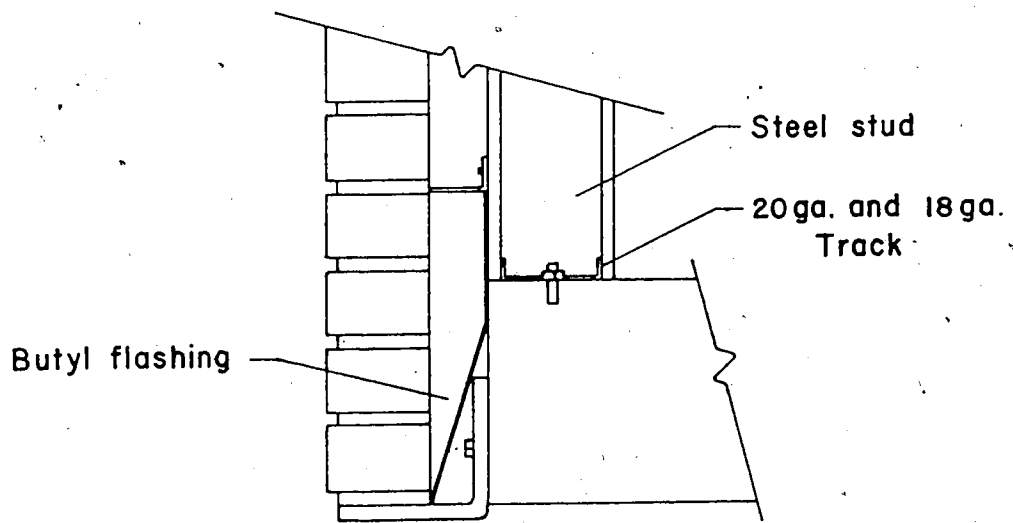


Figure 3.8 Full Sized Wall Specimen



DETAIL A



DETAIL B

Figure 3.9 Full Sized Wall Specimen Details

were separated by four 3.0 m. long, round H.S.S. columns. Attached to each slab was a 12 mm shelf angle used to support the brick veneer. These shelf angles were designed so that the maximum corbel of the brick veneer was 25 mm..

The construction of all the wall specimens followed the same sequence. The support track was fastened to the slabs using three expansion anchors on each track. Three steel studs were then attached to the track at a spacing of 400 mm on centre. The studs were held in position by number 14 self-tapping sheet metal screws, one to each end. Two lines of 12 mm. channel bridging were brazed to the steel studs. This bridging was run through the two centre service cutouts. Both of the 12 mm. gyproc panels were then fastened to the studs by 38 mm., self-drilling, "Teck" screws spaced at 600 mm. After the backing wall was completed, the butyl flashing and the brick ties were attached. The ties were fastened in the same manner as in the small tests. Finally, the brick veneer wall was built. Each wall was then cured for a minimum of 28 days. After twenty days of curing, the top expansion joint was filled with 12 mm. Styrofoam rope and Mono brand caulking. Figures 3.10 to 3.14 show a wall specimen at various stages its construction.

The brick veneer walls were built by a journeyman mason. A 5 mm. raking was performed on all the mortar joints. Special care was taken to ensure that the workmanship of the brickwork was comparable to a well-built wall in the field. The cavity was not cleaned.

>



Figure 3.10 Full Sized Wall Steel Track Secured



Figure 3.11 Full Sized Wall Studs and Bridging Assembled



Figure 3.12 Full Sized Wall Backing Wall Completed

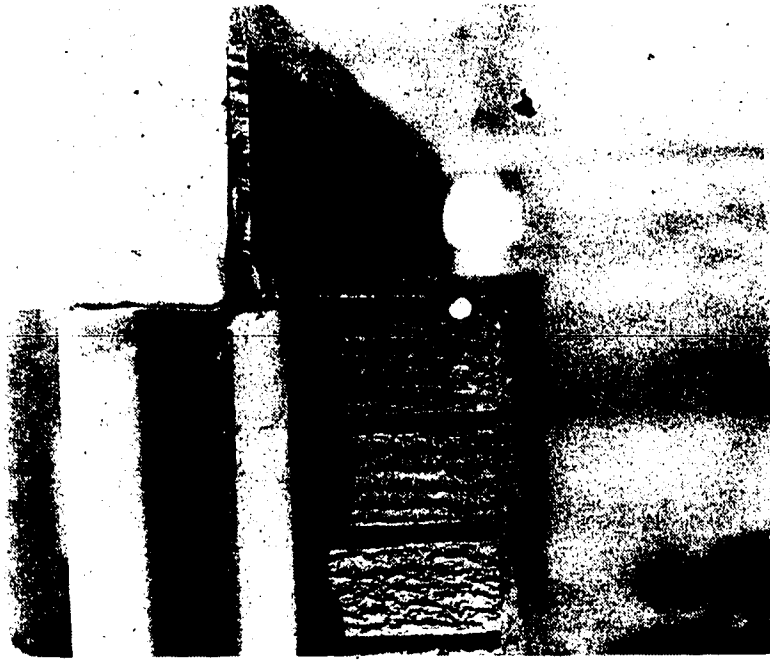


Figure 3.13 Full Sized Wall Top Expansion Joint Detail



Figure 3.14 Full Sized Wall Specimen Completed

All the mortar was mixed according to CSA A-179M⁶ specifications for type S mortar. Three mortar cubes were made from each mortar batch. Six prisms were made along with the walls in Series 1. For Series 2 to Series 4 a section of brick veneer was cut from each of the walls. The results of the tests conducted on these brick sections are reported in Appendix A.

Sixteen walls were built and tested. The tie type and arrangement and the type of steel stud used in the backing wall were varied. Figure 3.15 and Table 3.2 summarize the important parameters of each wall in the four series. The only walls duplicated were the two pairs of walls tested in Series 1.

3.4.2 Testing Apparatus and Procedures

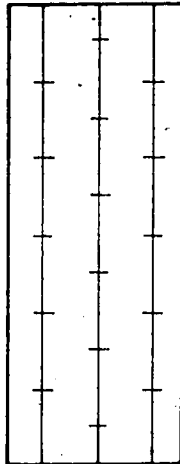
The full sized wall sections were tested in the apparatus shown in Figure 3.16. The testing frame consisted of four W shape columns, four connecting beams, a backing wall comprised of a fluted steel deck and 12 mm plywood, and an air bag.

The wall specimens were lifted into this frame by a crane. The specimens were transported using a cargo sling under the supporting angle and lifting hooks located at the rear of the bottom slab. By lifting in this way, the walls were not subjected to any stress due to the transporting procedure. After the wall section was positioned in the apparatus, the top slab was bolted to the column by a

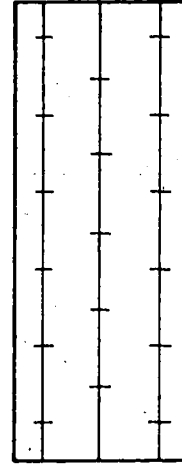
Table 3.2 A Summary of Full Sized Wall Specimens

Series	TEST VARIABLES					
	Wall	Tie Type	Stud Type	Tie Pattern	Gap	
1	1	22ga. Corr.	18 ga.	type A	50.	
1	2	22ga. Corr.	18 ga.	type A	50	
1	3	22ga. Corr.	18 ga.	type A	25	
1	4	22ga. Corr.	18 ga.	type A	25	
2	1	22ga. Corr.	18 ga.	type C	50	
2	2	22ga. Corr.	18 ga.	type B	50	
2	3	T	18 ga.	type B	50	
2	4	T	18 ga.	type C	50	
3	1	22ga. Corr.	20 ga.	type C	50	
3	2	22ga. Corr.	20 ga.	type B	50	
3	3	T	20 ga.	type B	50	
3	4	T	20 ga.	type C	50	
4	1	24ga. Corr.	20 ga.	type B	50	
4	2	16ga. Corr.	20 ga.	type B	50	
4	3	Ladder	20 ga.	type D	50	
4	4	V	20 ga.	type B	50	

Note: (1) 20 ga. = 20 ga. 6 in. steel stud
 (2) 18 ga. = 18 ga. 3 5/8 in. steel stud
 (3) Tie patterns are shown in Figure 3.11

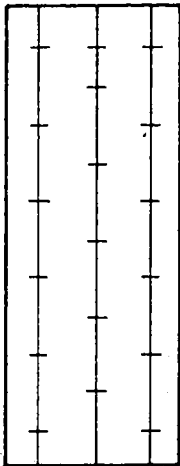


TYPE A

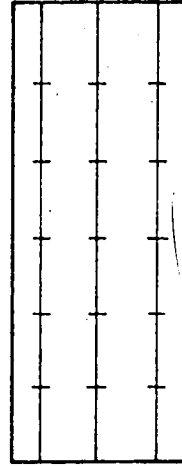


TYPE B

All tie spacing is 533 by 400mm
Ties staggered by 1/2 spacing



TYPE C



TYPE D

Figure 3.15 A Summary of Tie Patterns



Figure 3.16 Full Sized Wall Test Frame ,

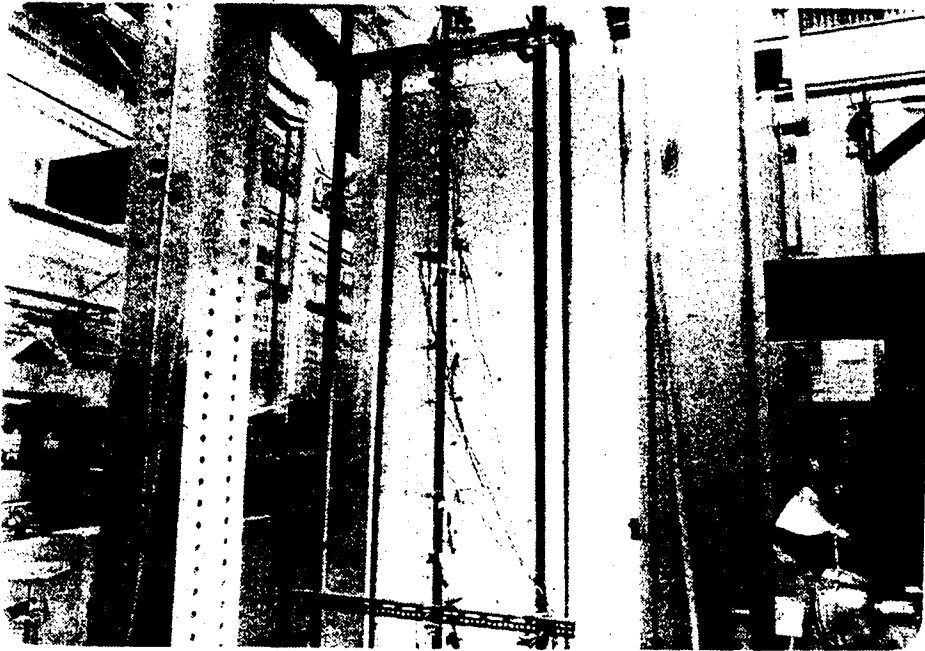


Figure 3.17 The L.V.D.T.s Assembly

connecting beam on each side. The bottom slab was brought to bear against a jack connected to the bottom of the columns.

A total of twelve linear variable differential transducers (LVDT) were used to measure the deflection of each wall section. Six monitored the deflection of the brick and six measured the deflection of the stud wall backing. The transducers were fastened to a common frame, which in turn was fastened to the two rear supporting pipes (see Figure 3.17). The locations of the transducers on the brick veneer and on the stud backing wall are shown in Figure 3.18. Wires connected the LVDT's to both the brick veneer and the backing wall. The wires were connected to the brick veneer using epoxy and extension rods. Screws were used to attach the wire to the stud backing wall. All the wires were tensioned using elastic bands.

The pressure in the air bag, and thus the load on the wall, was measured using a pressure transducer attached to the air bag. Air was supplied from the laboratory 690 KPa. air system using a series of pressure regulators.

All output from the measuring devices was monitored by a computerized data acquisition system.

After each wall specimen was fastened into the testing frame, a load of 0.30 KPa. (6.3 psf) was applied to the wall to ensure proper seating of the specimen. The load was then removed and the gauges were set to zero. The wall was subsequently loaded by slowly increasing pressure in the air bag. The wall loading was continued until either a peak load

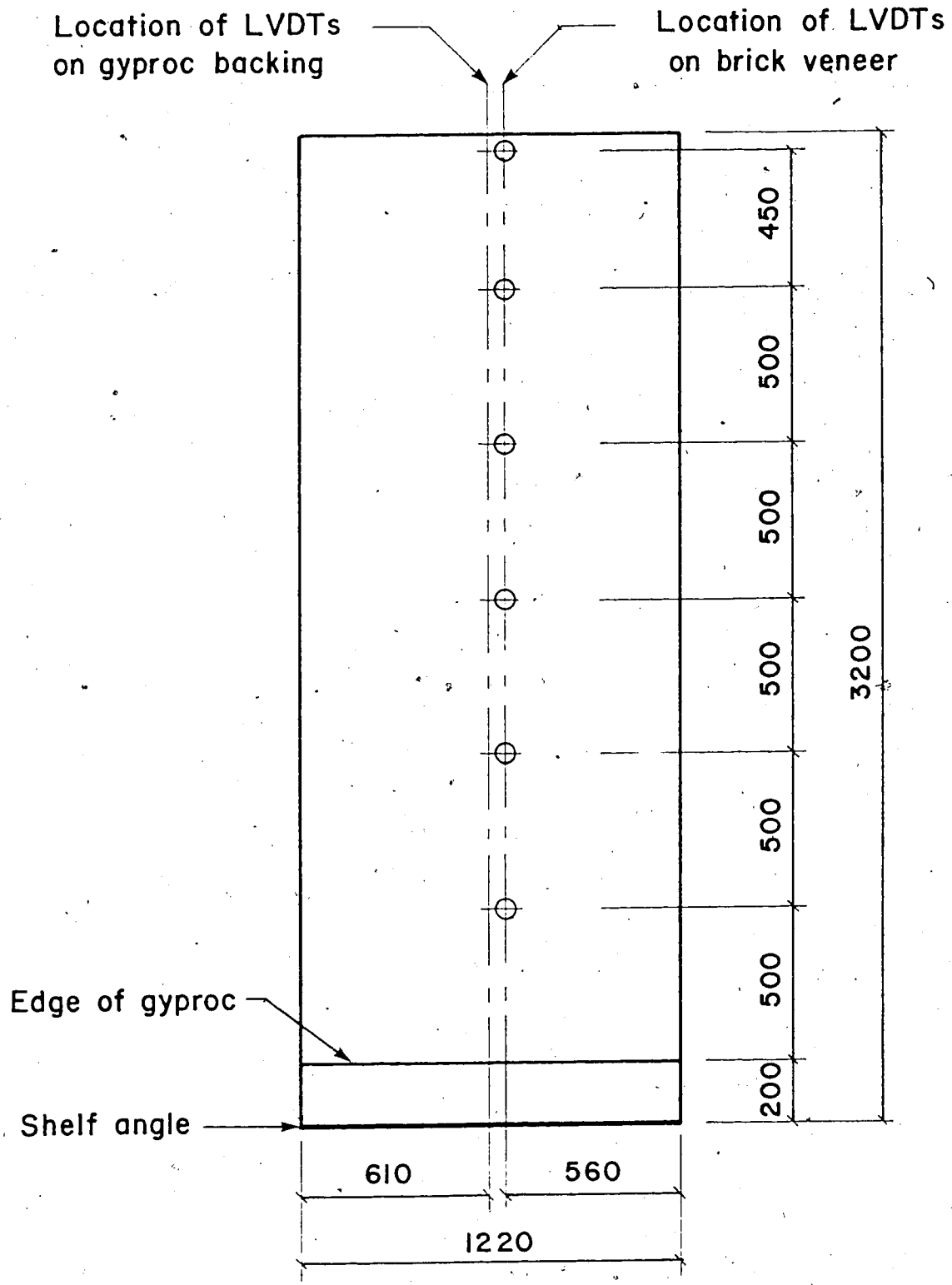


Figure 3.18 Location of the Measured Points of Deflection

was reached or the wall loading reached a value of 4.83 KPa. (100 psf). All sixteen walls were tested in this manner.

4. TEST RESULTS

4.1 Introduction

In this chapter, the results from all three phases of the experimental program are presented. The first section reports the findings of the tie tests. Subsequent sections present the results from the tests conducted on the stud backing walls and the full sized wall specimens.

4.2 Tie Test Results

The results of the stud and tie tests are presented in the following section. As previously outlined, five tie types were tested on the short studs (ie. 16, 22, and 24 gauge corrugated ties, "V" ties and ladder ties) and three tie types were tested on the wall sections (ie. 16 and 22 gauge corrugated ties and "T" ties). Two distinctive types of load deflection behaviour were observed, namely weak tie behaviour and strong tie behaviour. Weak tie behaviour was observed in tests using the 22 and 24 gauge corrugated ties. Strong tie behaviour was observed in tests using 16 gauge corrugated ties, "V" ties, "T" ties and ladder ties.

Four typical load deflection plots are presented. Two plots are presented for the short stud tests with either weak tie behaviour or strong tie behaviour. The two plots presented for the wall section tests demonstrate either weak tie behaviour or strong tie behaviour. The remaining data is summarized in Tables 4.1 to 4.5.

4.2.1 Short Stud and Tie Tests

4.2.1.1 Weak Tie Behaviour

Figure 4.1 shows the typical load deflection behaviour of the weak ties. Weak tie behaviour is differentiated from strong tie behaviour primarily by the low buckling load of the weak ties. The load deflection curve can be separated into two regions, a positively sloped linear region and a horizontal region.

The tie behaviour in the first region is described by a linear approximation. For each of the tie tests, a straight line was fitted to the initial portion of the load deflection curve. The slopes from each of the test curves are recorded in Tables 4.1 to 4.3. The straight line shown in Figure 4.1 is an example of such an approximation.

When a material behaves plastically, the load that it will resist remains constant while the material continues to deform. As shown in Figure 4.1, the weak ties behave in a plastic manner after the maximum load was exceeded.

All 24 and 22 gauge corrugated ties followed the load deflection pattern described above despite changes in the following four variables; the stud type, the tie type, the end offset and the wall gap. These variables only affected the slope of the linear portion of the curve and/or the maximum buckling load of the tie. The general shape of the load deflection curve did not

Table 4.1. Short Stud and Tie Test Results

SHORT STUD AND TIE TEST RESULTS							
Sp.No.	Tie Type	Gap (mm)	End Offset (mm)	Maximum Load (N)	Slope (N/mm)	Stud Type	
1	22ga. Corr.	25.0	0.0	890.	268.7	18 ga.	
2	22ga. Corr.	26.0	0.0	924.	269.4	18 ga.	
3	22ga. Corr.	26.0	0.0	979.	505.2	18 ga.	
4	22ga. Corr.	23.0	10.0	885.	412.6	18 ga.	
5	22ga. Corr.	24.0	10.0	835.	311.5	18 ga.	
6	22ga. Corr.	22.0	10.0	880.	311.5	18 ga.	
7	22ga. Corr.	49.0	0.0	593.	610.5	18 ga.	
8	22ga. Corr.	50.0	0.0	608.	648.3	18 ga.	
9	22ga. Corr.	53.0	0.0	499.	669.4	18 ga.	
10	22ga. Corr.	46.0	10.0	692.	690.4	18 ga.	
11	22ga. Corr.	49.0	10.0	578.	804.1	18 ga.	
12	22ga. Corr.	49.0	10.0	593.	661.0	18 ga.	
13	22ga. Corr.	50.0	18.0	613.	425.2	18 ga.	
14	22ga. Corr.	50.0	22.0	642.	479.9	18 ga.	
15	22ga. Corr.	50.0	24.0	628.	526.3	18 ga.	
16	22ga. Corr.	49.0	0.0	692.	513.6	18 ga.	
17	22ga. Corr.	53.0	1.0	643.	597.8	18 ga.	
18	22ga. Corr.	50.0	0.0	722.	675.0	18 ga.	
19	22ga. Corr.	45.0	9.0	811.	559.9	18 ga.	
20	22ga. Corr.	50.0	7.0	568.	623.1	18 ga.	

Table 4.2 Short Stud and Tie Test Results

SHORT STUD AND TIE TEST RESULTS						
Sp.No.	Tie Type	Gap (mm)	End Offset (mm)	Maximum Load (N)	Slope (N/mm)	Stud Type
21	22ga. Corr.	50.0	7.0	583.	1507.2	18 ga.
22	22ga. Corr.	50.0	22.0	623.	357.9	18 ga.
23	22ga. Corr.	50.0	21.0	672.	324.2	18 ga.
24	22ga. Corr.	49.0	22.0	717.	298.9	18 ga.
25	24ga. Corr.	53.0	0.0	400.	492.6	18 ga.
26	24ga. Corr.	49.0	0.0	578.	585.2	18 ga.
27	24ga. Corr.	50.0	0.0	435.	437.8	18 ga.
28	24ga. Corr.	50.0	11.0	465.	458.9	18 ga.
29	24ga. Corr.	50.0	10.0	450.	522.0	18 ga.
30	24ga. Corr.	46.0	12.0	568.	888.3	18 ga.
31	24ga. Corr.	49.0	0.0	519.	736.8	18 ga.
32	24ga. Corr.	50.0	0.0	623.	648.3	18 ga.
33	24ga. Corr.	49.0	0.0	519.	618.9	18 ga.
34	24ga. Corr.	50.0	9.0	539.	665.2	18 ga.
35	24ga. Corr.	50.0	11.0	425.	345.2	18 ga.
36	24ga. Corr.	51.0	10.0	455.	669.4	18 ga.
37	16ga. Corr.	49.0	2.0	816. 1631.	316.6 65.3	18 ga.
38	16ga. Corr.	50.0	0.0	1110. 1705.	257.9 53.0	18 ga.

Table 4.3 Short Stud and Tie Test Results

SHORT STUD AND TIE TEST RESULTS						
Sp. No.	Tie Type	Gap (mm)	End Offset (mm)	Maximum Load (N)	Slope (N/mm)	Stud Type
39	16ga. Corr.	52.0	2.0	1170. 1720.	261.0 71.6	18 ga.
40	16ga. Corr.	50.0	10.0	880. 1582.	387.3 130.5	18 ga.
41	16ga. Corr.	48.0	11.0	1650.	353.6	18 ga.
42	16ga. Corr.	49.0	10.0	1255. 1631.	311.5 84.1	18 ga.
43	V.	43.0	0.0	1850. 3351.	395.7 202.1	18 ga.
44	V.	43.0	0.0	1990. 3559.	437.8 197.9	18 ga.
45	V.	42.0	0.0	1900. 2867.	404.2 101.0	18 ga.
46	ladder	60.0	0.0	1490. 2155.	496.8 164.9	18 ga.
47	ladder	61.0	0.0	1577. 2199.	433.6 190.2	18 ga.
48	ladder	60.0	0.0	1383. 1829.	564.1 191.1	18 ga.
49	22ga. Corr.	51.0	0.0	657.	144.8	20 ga.
50	22ga. Corr.	50.0	0.0	642.	138.9	20 ga.
51	22ga. Corr.	50.0	0.0	751.	437.8	20 ga.
52	16ga. Corr.	51.0	0.0	1160. 1880.	198.0 116.1	20 ga.
53	16ga. Corr.	50.0	0.0	1120. 1630.	211.6 118.0	20 ga.

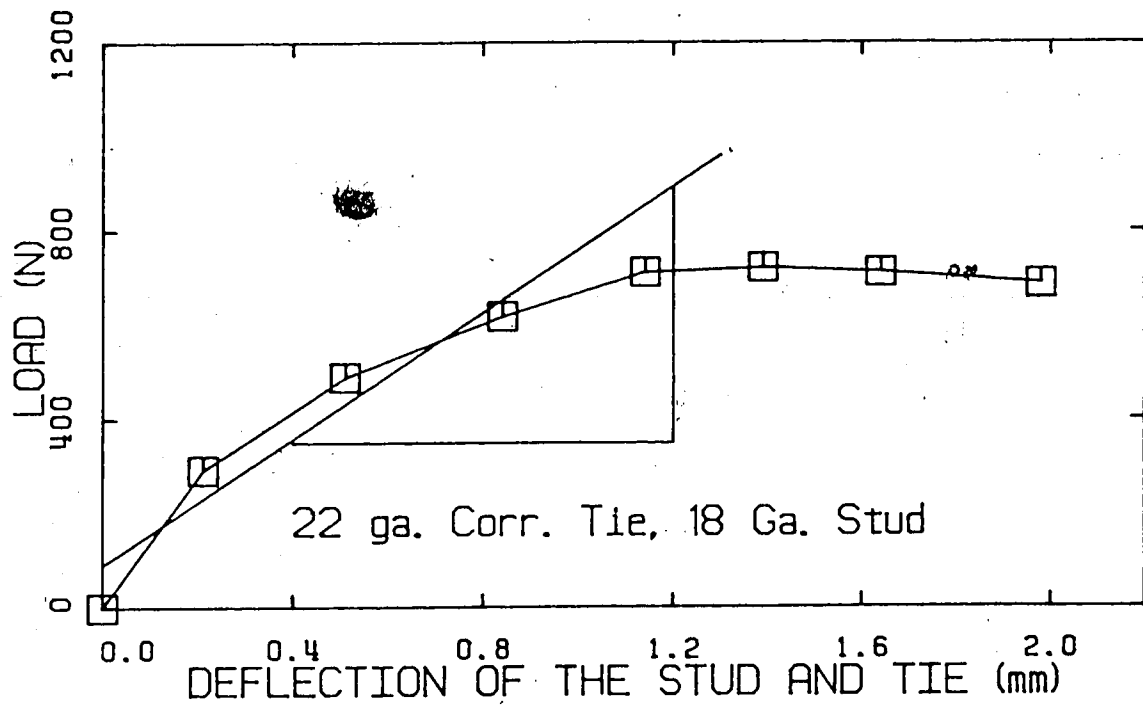


Figure 4.1 Typical Weak Tie Behaviour (Short Stud Tests)

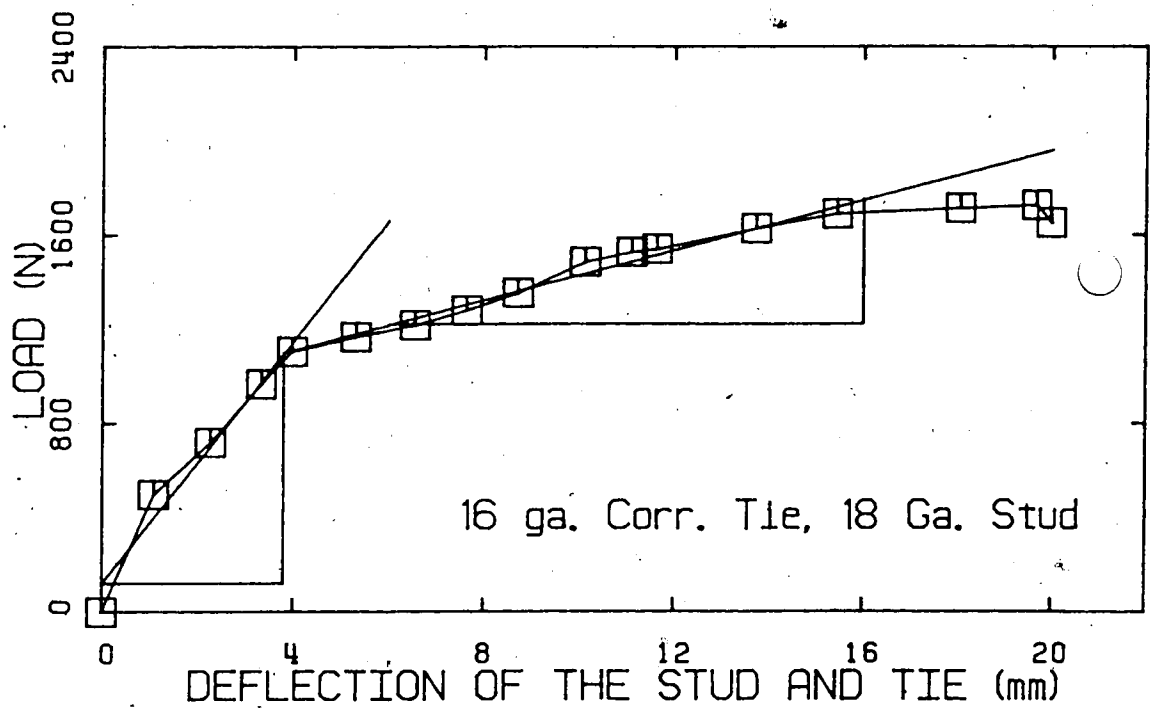


Figure 4.2 Typical Strong Tie Behaviour (Short Stud Tests)

change.

The 90 mm 18 gauge and 150 mm. 20 gauge studs showed no signs of distress during the testing of the weak ties. The gyproc pads, however, showed a small amount of permanent deformation upon completion of the tests.

4.2.1.2 Strong Tie Behaviour

Figure 4.2 shows the typical load deflection behaviour of the 16 gauge corrugated ties, "V" ties, and ladder ties. These ties demonstrate strong tie behaviour. The initial region of the strong tie load deflection curve is bilinear. There is a change in slope of the curve in the higher load range of this region. Ultimately, the load deflection curve flattens to form the plastic region. The slopes of the two linear approximations and their respective maximum loads are also tabulated in Tables 4.1 to 4.3.

As with the weak ties, changes in the four experimental variables affect only the slopes of the linear portion of the curve and/or the maximum load that the tie-stud junction resisted.

Specimen No. 41 was an 16 gauge corrugated tie and as such should have followed a trilinear load deflection curve. In Table 4.3, only one slope is shown for this specimen because the second slope was so flat that it could be approximated as horizontal.

During the testing of the strong ties, the flange of the backing stud bent significantly at the higher loads. Before the maximum load was reached, the flange and a portion of the stud web began to twist laterally away from the line of the applied load. The failure of the strong tie-stud junction was due to the tie buckling, or to the twisting failure of the stud flange and web.

All the ties tested on the 18 gauge stud, except for the "V" ties, failed by the buckling of the tie. In the "V" tie tests, the 18 gauge stud failed. The 16 gauge corrugated tie was the only strong tie tested on the 20 gauge stud and failure in these tests was also due to the twisting failure of the stud. In all the strong tie tests, the flange of the backing stud was permanently deformed and the gyproc pad severely crushed.

4.2.2 Tie and Wall Section Tests

The load deflection behaviour of the ties tested against the backing wall sections can also be divided into ties demonstrating weak tie behaviour and strong tie behaviour. As before, the 22 gauge corrugated ties behave as weak ties, while the 16 gauge corrugated ties and the "T" ties exhibit strong tie behaviour.

4.2.2.1 Weak Tie Behaviour

Figure 4.3 shows the typical load deflection behaviour of the weak ties tested on the stud wall section. The general shape of the curve is similar to that obtained for the weak ties, in the short stud and tie tests. Thus, as with the short stud tests, straight lines were fitted to the initial portion of the load deflection curves. The slopes of these lines are tabulated in Tables 4.4 and 4.5.

Figure 4.3 also shows the beam deflection of the backing stud wall. The slopes obtained from the beam deflection curve and the difference between the tie slope and the beam slope, for each tie test, are recorded in Tables 4.4 and 4.5. This net slope was calculated by taking the difference of the reciprocals of two slopes.

Failure of the tie stud junction is again due to the buckling of the weak ties. The gyproc immediately behind the tie crushed during the testing but the studs were not damaged.

4.2.2.2 Strong Tie Behaviour

When the strong ties were tested against the wall sections, the load deflection curves generated resembled the curves obtained for the short stud tests for the same tie type. Figure 4.4 shows a typical load deflection plot of a strong tie tested against the wall section. Again, the lower section of the curve can be

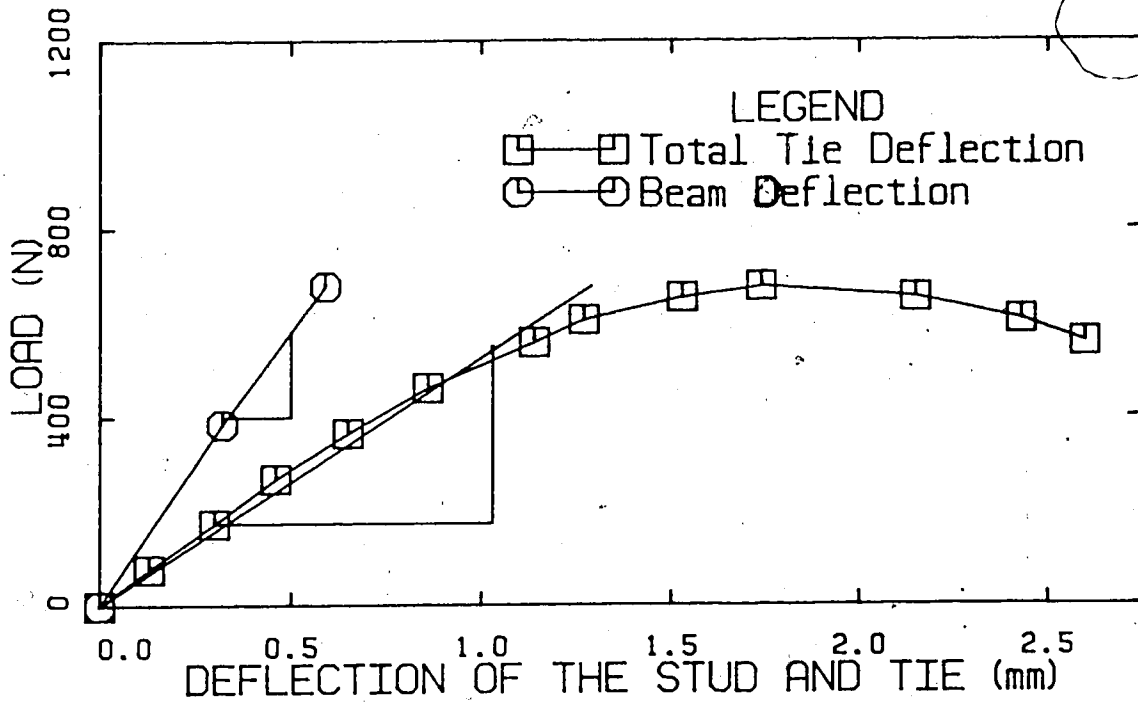


Figure 4.3 Typical Weak Tie Behaviour (Wall Section Tests)

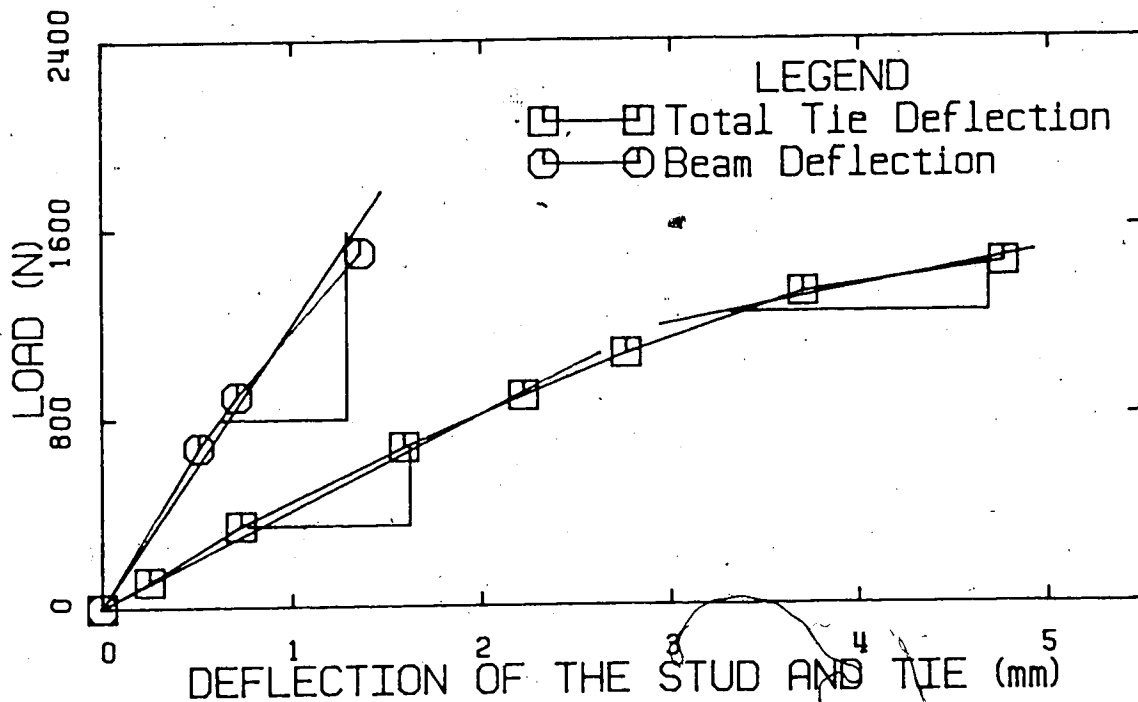


Figure 4.4 Typical Strong Tie Behaviour (Wall Section Tests)

approximated by a bilinear relationship. The slopes of the linear approximations and their respective maximum loads are listed in Tables 4.4 and 4.5. Also reported in these tables are the slopes of the load deflection curves resulting from the beam deflection of the stud wall. Due to the limitations of the testing apparatus, the load plateau for many of the tests was not reached. The tests where this occurred have their maximum loads designated with a "+" sign indicating that the actual maximum load is higher.

While the weak tie tests only resulted in the crushing failure of the gyproc in a very localized area, the strong tie tests caused severe damage to the stud and gyproc backing wall. In both the "T" tie tests and the 16 gauge tie tests, the ties punched through the gyproc sheet and resulted in permanent deformation to the stud flange.

4.3 Backing Wall Test Results

4.3.1 Stud and Track Interaction

The load deflection curves obtained from the track and stud interaction tests are shown in Figures 4.5 and 4.6. Figure 4.5 defines the load deflection behaviour of the 90 mm. 18 gauge stud and track specimens, and Figure 4.6 defines the behaviour of the 150 mm. 20 gauge stud and track specimens. The right hand side (R.H.S) and left hand side

Table 4.4 Wall Section and Tie Test Results

Sp.No.	Tie Type	Gap (mm)	Stud Type	Flg. D. (mm)	Max. Load (N)	Curve Slopes (N/mm)		
						Tie	Beam	Net
1	22ga. Corr.	50.0	18 ga.	25.0	689.	565.3	1095.3	1186.3
2	22ga. Corr.	50.0	18 ga.	23.0	678.	557.1	1024.6	1221.0
3	22ga. Corr.	50.0	18 ga.	28.0	718.	381.7	1227.0	554.1
4	22ga. Corr.	50.0	18 ga.	26.0	706.	442.5	1288.7	673.9
5	22ga. Corr.	50.0	18 ga.	32.0	694.	427.4	1292.0	638.7
6	22ga. Corr.	50.0	18 ga.	21.0	765.	914.1	2298.9	1517.5
7	22ga. Corr.	50.0	18 ga.	30.0	745.	389.7	1968.5	485.9
8	22ga. Corr.	50.0	18 ga.	36.0	724.	339.7	6410.3	358.7
9	22ga. Corr.	50.0	18 ga.	26.0	894.	602.8	1424.5	1045.0
10	22ga. Corr.	50.0	18 ga.	6.0	811.	1285.4	2222.2	3049.1
11	22ga. Corr.	25.0	18 ga.	20.0	1149.	684.9	1748.3	1126.0
12	22ga. Corr.	25.0	18 ga.	18.0	1114.	679.3	2008.0	1026.6
13	22ga. Corr.	25.0	18 ga.	20.0	1160.	2	1113.6	994.0
14	22ga. Corr.	50.0	20 ga.	17.0	783.	554.3	1631.3	839.6
15	22ga. Corr.	50.0	20 ga.	16.0	794.	539.4	1763.7	777.0
16	22ga. Corr.	50.0	20 ga.	17.0	800.	476.0	2083.3	617.0
17	22ga. Corr.	50.0	20 ga.	28.0	695.	376.7	2066.1	460.7
18	22ga. Corr.	50.0	20 ga.	7.0	765.	727.8	1607.7	1329.8

Note: (1) flg. D. is the location of the tie in relation to the stud web

Table 4.5 Wall Section and Tie Test Results

Sp.No.	Tie Type	Gap (mm)	Stud Type	Fig. D. (mm)	Max. Load (N)	Curve Slopes/ (N/mm)		
						Tie	Beam	Net
19	16ga. Corr.	50.0	20 ga.	18.0	945. 1390.+	531.3 87.8	1703.6	772.1 92.6
20	16ga. Corr.	50.0	20 ga.	16.0	1128. 1545.+	644.3 87.3	1642.0	1060.4 92.2
21	16ga. Corr.	50.0	20 ga.	18.0	1140. 1560.+	463.2 136.9	747.4	1218.1 167.6
22	16ga. Corr.	50.0	18 ga.	27.0	1180. 1635.	394.2 158.0	1149.4	600.0 183.2
23	16ga. Corr.	50.0	18 ga.	30.0	1054. 1446.	339.0 74.5	1203.4	471.9 79.4
24	16ga. Corr.	50.0	18 ga.	10.0	1275. 1600.+	607.2 110.5	955.1	1667.0 125.0
25	T.	50.0	18 ga.	22.0	1412. 1973.+	388.3 184.7	778.8	774.4 242.2
26	T.	50.0	18 ga.	21.0	861. 1847.+	471.0 244.5	881.1	1011.9 338.4
27	T.	50.	18 ga.	20.0	889. 1790.	381.5 165.5	1222.5	554.6 191.4

Note: (1) Fig. D. is the location of the tie with respect to the stud web.

(L.H.S) support load and settlement were plotted for each specimen.

The 18 gauge track and stud load deflection behaviour is approximately linear in the lower load levels (below 2.0 KN.). An average of the slopes of the linear portion of each of the curves is shown on the plot in Figure 4.5. Each curve varies somewhat, possibly due to a difference in where the load was applied. The load may have been slightly off centre resulting in in one side being loaded more than the other. The abrupt change of slope on the load deflection curve of specimen 2 (R.H.S) is due to the track slipping in the testing frame supports.

Failure of the 18 gauge specimens occurred at the centre of each of the studs. A plastic hinge formed at this point at a load of 4997 N. for specimen 1 and at a load of 5264 N. for specimen 2.

The 20 gauge track and stud specimens load deflection behaviour is also linear at the lower load levels. Unlike the 18 gauge specimens, however, the 20 gauge specimens exhibit definite signs of yielding after a load of 1.0 KN.. Ignoring the yielding portion of the four load deflection curves, an average of the slopes of each curve results in the straight line shown in Figure 4.6.

Each of the specimens failed by a buckling of the stud web at one of the supports. For specimen 1, this failure occurred on the left hand side at a load of 1520 KN.. Specimen 2 also failed on the left hand side but at a load

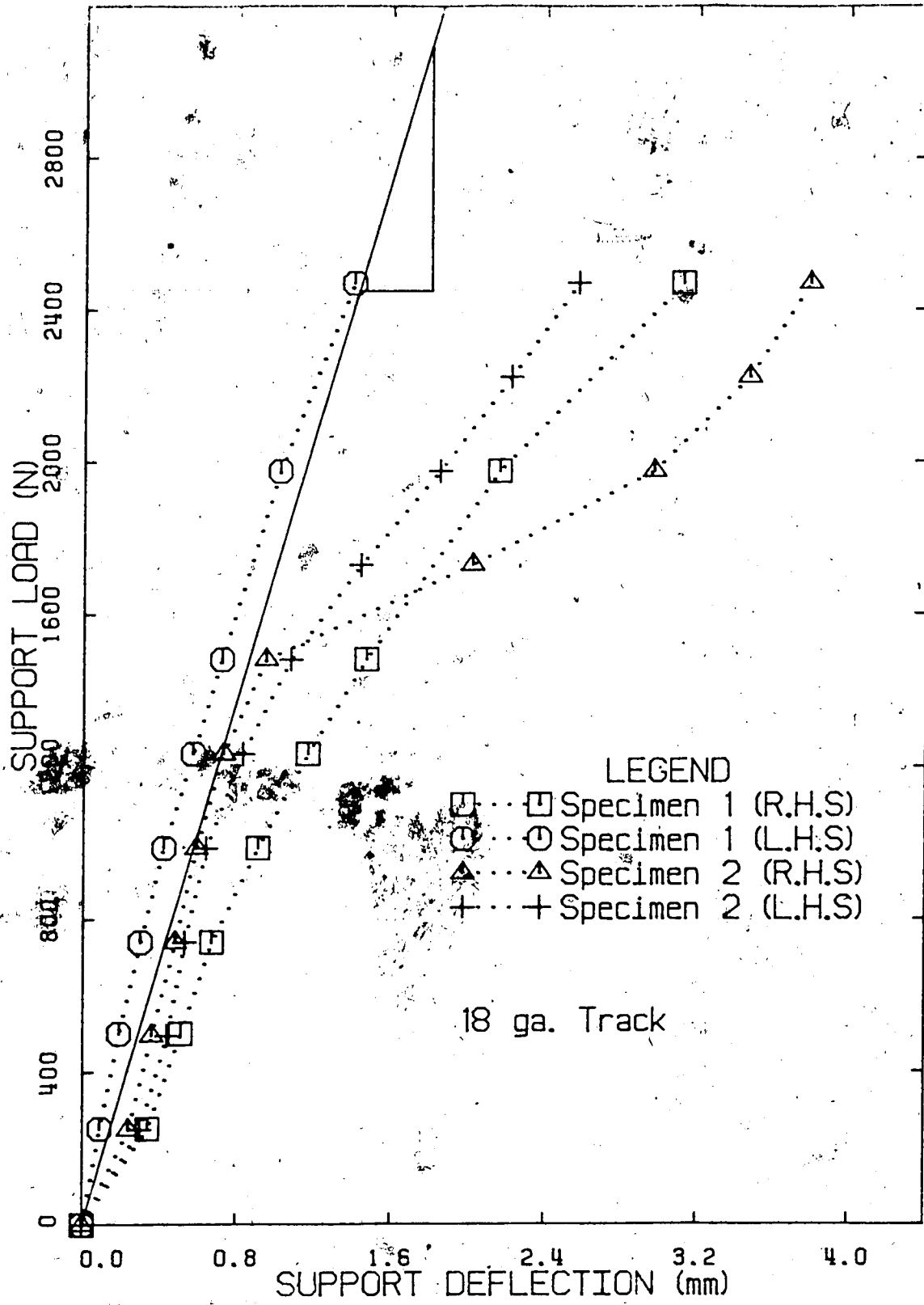


Figure 4.5 Track and Stud Interaction (18 gauge)

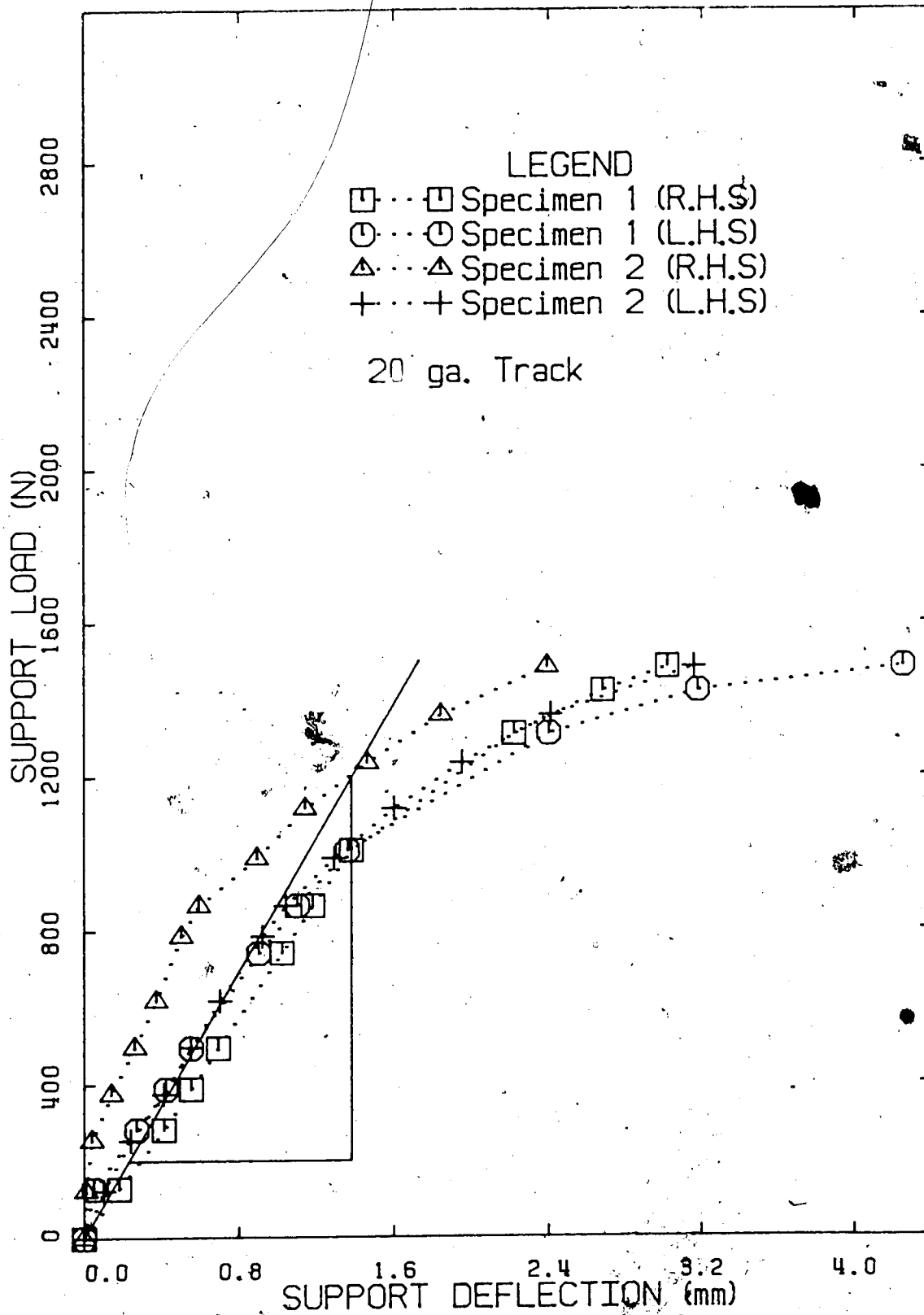


Figure 4.6 Track and Stud Interaction (20 gauge)

of 1557 KN.. After the 20 gauge tests were completed, it was observed that the 20 gauge track flange sustained permanent deformation as a result of the testing.

4.3.2 Gyproc and Stud Interaction

Figure 4.7 shows the load deflection behaviour of the gyproc and stud specimens tested under a third point loading. Specimens 1 and 2 are two-stud wall specimens and specimen 3 is a three-stud wall specimen. Also shown on the plot, is the average support settlement for specimen 3.

The load deflection curves for all three specimens are predominantly linear, especially at the lower loads. Specimens 1, 2 and 3 failed at maximum third point loads of 4393 N, 4349 N and 6499 N respectively. The failure of all three specimens was due to a plastic hinge forming at the third point of the span on each of the wall specimens.

4.4 Results of the Full Sized Wall Tests

The subsequent sections present the results of the load deflection behaviour of the sixteen full sized wall specimens subjected to positive pressure loading. The tie type, tie pattern and wall gap will be described for each wall specimen. The stud type changed only once during the testing and therefore will be reported here. Series No.1 and No.2 tests used 90 mm. 18 gauge studs and Series No.3 and No.4 tests used 150 mm. 20 gauge studs.

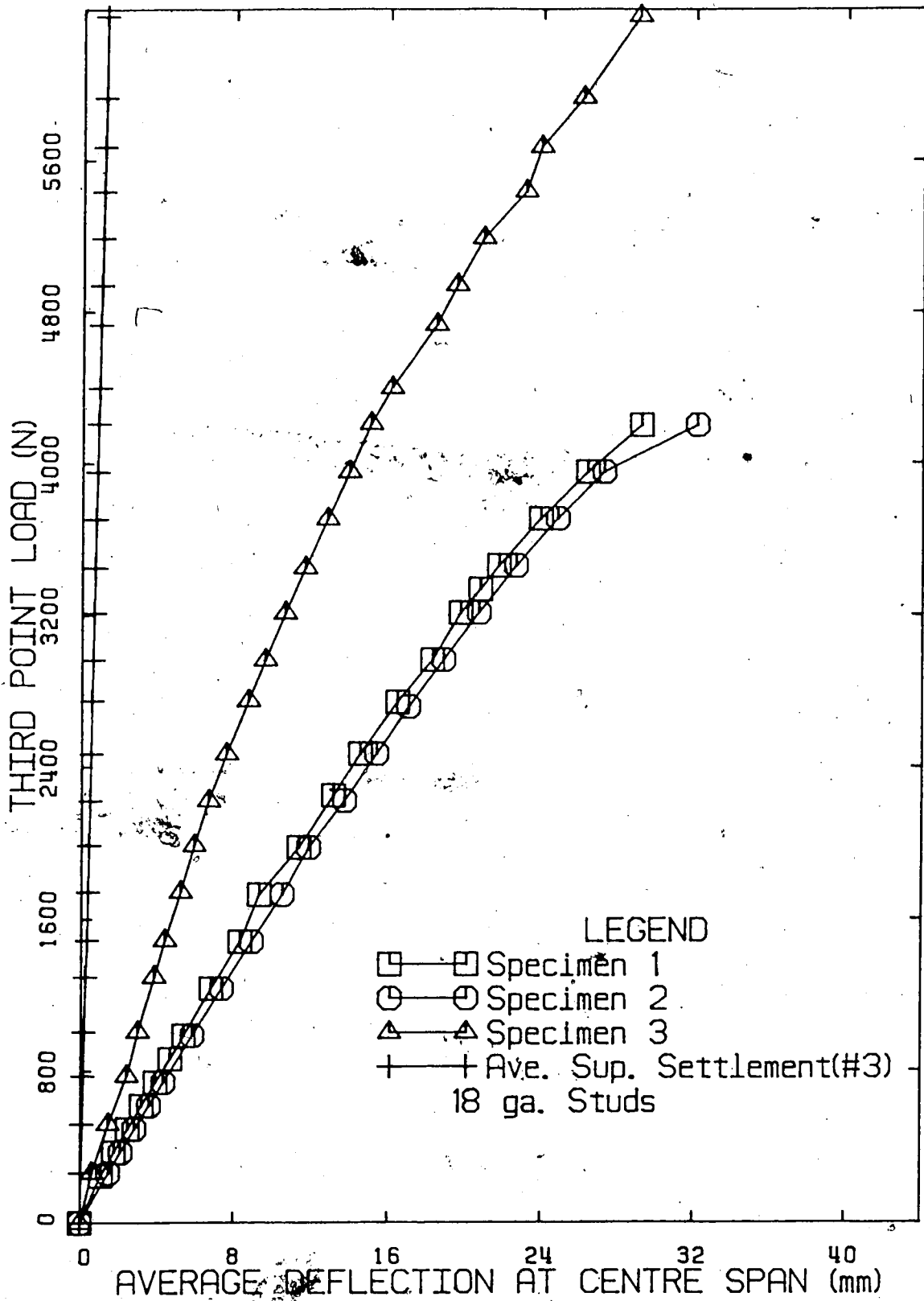


Figure 4.7. The Stud and Gyproc Wall Section Test Results

Appendix B contains all the load deflection plots for the brick veneer and stud backing of each wall specimen. The maximum load shown on each plot is either the maximum load resisted by the wall specimen or, in the case of walls that were loaded to 4.83 KPa. (100.8 psf.), an arbitrarily assigned load determined by the plots scale restrictions and by the load at which a repeating pattern was observed.

4.4.1 Series No.1

4.4.1.1 Series No.1 Wall No.1

The first wall in series No.1 consisted of 22 gauge corrugated ties, arranged in tie pattern A, with a gap of 50 mm.. Figures B-1 and B-2 show the load deflection behaviour of the stud backing wall and the brick veneer, up to the wall's maximum load. The curves in Figure B-1 show that the deflection of the brick veneer remained proportional to the load below a load of approximately 1.50 KPa. (31.4 psf.). When this load was exceeded, the uppermost tie, located on the middle stud line, buckled and the brick veneer wall rotated about its base. This rotation resulted in a "zipper-like" buckling of the remaining ties. Figure 4.8 shows the appearance of the wall cavity after the buckling of the ties.

The large deflection of the top of the brick veneer showed that the expansion joint, located between the veneer and the top angle, did not significantly restrain the brick veneer's movement. When the maximum load of



Figure 438 Buckled Ties in Wall Cavity

1.53 KPa. (31.7 psf) was reached the brick veneer simply rotated about its base and eventually came into contact with the stud backing wall.

The deflections of the stud backing wall remained proportional to the applied load over the full load range. Deflections of the stud backing wall, at the top stud and track junction, confirmed the flexibility of this type of support connection.

4.4.1.2 Series No.1 Wall No.2

Wall No.2 was identical in construction to Wall No.1. The two walls had similar load deflection behaviour. The tests results indicate that below a load of 1.40 KPa. (29.2 psf) there was little difference in their load deflection curves (see Figures B-3 and B-4). Both the brick veneer and stud wall deflections were approximately equal for a given load. The ties in Wall No.2 began to buckle at a load of 1.52 KPa. which is slightly higher than the buckling load of Wall No.1. The maximum load that this wall was able to resist was 1.75 KPa. (36.6 psf.).

4.4.1.3 Series No.1 Wall No.3

Wall No.3 of Series No.1 consisted of 22 gauge corrugated ties arranged in tie pattern A, with a gap of 25 mm.. The load deflection behaviour for both the backing wall and the brick veneer is shown in Figures B-5 and B-6. While this wall was able to resist a load

of 4.83 KPa. (100.8 psf.), the load deflection behaviour of the wall was plotted only to a load of 3.00 KPa. (62.7 psf.). Above this load, the wall continued the deflection pattern shown in the load deflection curves for loads between 2.00 KPa. (41.5 psf.) and 3.00 KPa..

The deflections of Wall No.3 were proportional to the load, up to a load of approximately 1.65 KPa. (34.6 psf.). When this load was exceeded, a crack formed in a mortar joint of the brick veneer at an elevation of 1340 mm.. The crack acted as a hinge so that the brick veneer effectively became two members. Subsequent loading of the wall resulted in the brick veneer rotating about this hinge and transferring a larger portion of the load to the centre of the backing wall. While no failure of the ties was observed, the large differential movement between the studs and brick veneer indicated that the top row of ties must have failed at some point during the test.

4.4.1.4 Series No.1 Wall No.4

Wall No.4 was identical to Wall No.3 and its load deflection behaviour closely resembled that of Wall No.3. Wall No.4 cracked at a load of 1.25 KPa. (26.1 psf.). The crack formed in a mortar joint at an elevation of 1735 mm.. Figures B-7 and B-8 show that after the brick veneer cracked, it behaved as two members joined by a hinge. Subsequent loading of this wall widened the crack as the stud backing wall

deflected. No significant failure of the ties was observed but the load deflection plots indicate that the uppermost ties on each of the stud lines must have buckled.

As with Wall No.3, Wall No.4 was able to resist a maximum load of 4.83 KPa.. Subsequent load deflection data repeated preceding patterns, therefore the load deflection response of this wall was only plotted to a load of 3.00 KPa. (62.7 psf.).

4.4.2 Series No.2

4.4.2.1 Series No.2 Wall No.1

The first wall of Series No.2 was built using 22 gauge corrugated ties, arranged in tie pattern C, with a 50 mm. gap.

The load deflection behaviour of Wall No.1 is shown in Figures B-9 and B-10. The deflections of the brick veneer and the stud wall increased proportionally to the load until the brick cracked at an elevation of 1935 mm., with a load of 1.46 KPa. (30.6 psf.). When the brick veneer cracked, there was an increase in the deflections of the brick veneer and the steel stud backing wall. The ties, at elevation 1866 mm. and 2400 mm. on the outside stud lines, showed signs of buckling at a load of 2.62 KPa. (54.7 psf.). Subsequent loading of Wall No. 1 resulted in the brick veneer rotating about the crack as the stud wall deflected. The middle

ties eventually collapsed at a load of 3.31 KPa. (69.1 psf.). Wall No.1 resisted a maximum load of 3.35 KPa. (70.1 psf.).

4.4.2.2 Series No.2 Wall No.2

Wall No.2 was constructed identically to Wall No.1 except tie pattern B was used.

The load deflection behaviour of this wall is shown in Figures B-11 and B-12. The deflections of the brick veneer and the stud backing wall remained proportional to the load until a load of 1.75 KPa. (36.5 psf.) was reached. At this load, the brick veneer cracked at an elevation of 1610 mm.. The load deflection plots show a large increase in the deflection of both the brick veneer and the stud backing wall after the brick cracked. Subsequent loading of Wall No.2 resulted in those ties, at mid-height, buckling when a load of 2.96 KPa. (60.5 psf.) was reached. After the maximum load of 3.46 KPa. (72.2 psf.) was reached, the top ties buckled and the upper section of brick veneer rotated into the backing wall.

4.4.2.3 Series No.2 Wall No.3

Wall No.3 was constructed using "T" ties, arranged in tie pattern B, with a 50 mm. gap.

The load deflection behaviour of Wall No.3 is presented in Figures B-13 and B-14. The brick veneer and stud backing exhibited deflections proportional to the

applied load. At a load of 2.07 KPa. (43.2 psf.), the brick veneer cracked in a mortar joint located at an elevation of 1550 mm..

The plots show a large increase in the deflections, above a load of 2.07 KPa. (43.2 psf.). Further loading of Wall No.3 resulted in the brick veneer rotating about the cracked joint, as the stud backing wall deflected.

Wall No.3 was loaded up to 4.83 KPa. and no tie failure was observed over this entire load range.

4.4.2.4 Series No.2 Wall No.4

Wall No.4 used "T" ties, arranged in tie pattern C, with a gap of 50 mm. Figures B-15 and B-16 show the load deflection behaviour of this wall. The brick veneer and stud wall deflections are proportional to the applied load. At a load of 2.76 KPa. (58.0 psf.), a crack formed in the brick veneer at an elevation of 1930 mm.. A large increase in the deflections of the brick veneer and stud backing wall was observed after the brick cracked. Subsequent loading of Wall No.4 caused the brick veneer to rotate about the mortar joint as it followed the deflections of the stud backing wall.

Wall No.4 resisted a maximum load of 4.83 KPa.. During the full range of loading, no failure of the ties was observed.

4.4.3 Series No.3

The walls in Series No.3 were constructed using 150 mm. 20 gauge steel studs.

4.4.3.1 Series No.3 Wall No.1

The ties in Wall No.1 were 22 gauge corrugated ties, arranged in tie pattern C, with a gap of 50 mm..

The load deflection plots for this wall specimen are shown in Figures B-17 and B-18. The deflection of the wall appears to be proportional to the applied load, up to a load of 2.97 KPa. (62 psf.). At 2.97 KPa., the top ties began to buckle and subsequent loading caused the brick veneer to rotate about its base. The maximum load was 3.16 KPa. (66.0 psf.). After the maximum load was reached, the brick veneer rotated into the stud backing wall.

4.4.3.2 Series No.3 Wall No.2

The 22 gauge corrugated ties used in the construction of Wall No.2 were arranged in pattern B, with a 50 mm. gap.

Figures B-19 and B-20 show the load deflection behaviour for wall No.2. Up to a load of 2.20 KPa. (46.0 psf.), the deflections of the brick veneer and stud backing were proportional to the load. When the 2.20 KPa. load was exceeded, the top row of the ties began to buckle. Subsequent loading of this wall resulted in the brick veneer rotating about its base and a sequential

buckling of the remaining ties. The maximum load was 2.32 KPa. (48.4 psf.). Loading of Wall No.2 was stopped when the brick veneer came into contact with the backing wall. Over the full load range, no cracking of the brick veneer was observed.

4.4.3.3 Series No.3 Wall No.3

Wall No.3 included "T" ties, arranged in tie pattern B, with a gap 50 mm..

Figures B-21 and B-22 show the load deflection behaviour of Wall No.3. Up to a load of 2.00 KPa. (41.8 psf.), the deflections of the brick veneer and stud backing increased proportionally to the applied load. When the 2.00 KPa. load was exceeded, a crack formed in the brick veneer at an elevation of 1540 mm.. Further loading of Wall No.3 resulted in a widening of the crack as the stud backing wall continued to deflect. At a load of 3.10 KPa. (67.8 psf.), the webs of the studs began to buckle at the top stud and track junction. Figure 4.9 shows this junction after it failed. Wall No.3 resisted the full 4.83 KPa. loading without any noticeable failure of the "T" ties.

4.4.3.4 Series No.3 Wall No.4

"T" ties and a gap of 50 mm were also used for Wall No.4. The "T" ties, however, were arranged in the tie pattern C.

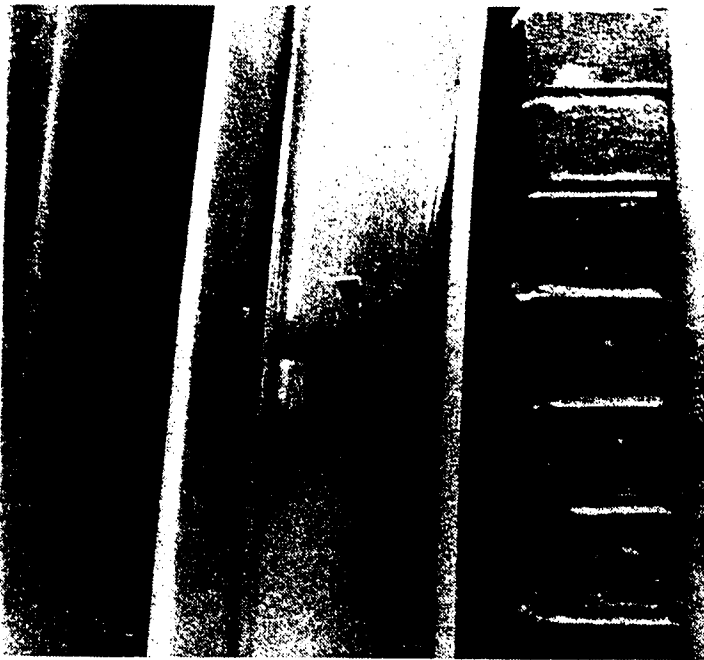


Figure 4.9. Failure of Stud Web

The load deflection behaviour of this wall specimen is shown in Figures B-23 and B-24. The wall's deflection behaviour was proportional to the load up to a load of 2.14 KPa. (44.6 psf.). When this load was exceeded, the brick veneer cracked at an elevation of 1265 mm, resulting in much greater deflections of the stud backing wall. The brick veneer rotated about the hinge formed at the cracked mortar joint. As with Wall No.3., the top of the steel studs failed at a load of 3.40 KPa. (67.8 psf.). No tie failure was observed up to the maximum test load of 4.83 KPa..

4.4.4 Series No.4

4.4.4.1 Series No.1 Wall No.1

Wall No.1 was constructed using 24 gauge corrugated ties. These ties were arranged in tie pattern B, with a gap of 50 mm.

Figures B-25 and B-26 show the load deflection behaviour of the brick veneer and stud backing. The load deflection curves show that after the top ties began to buckle, at a load of 0.90 KPa. (19.2 psf), the brick began to rotate about its base. Subsequent loading of this wall resulted in the sequential buckling of the remaining ties and a further rotation of the brick veneer. Up to the maximum load of 1.35 KPa. (28.3 psf.), no cracking of the brick veneer or failure of the studs was observed.

The LVDT, at an elevation of 1700 mm., stuck during testing. Therefore, data from this LVDT was disregarded and is not included in the plot.

4.4.4.2 Series No.4 Wall No.2

Wall No.2 was comprised of 16 gauge corrugated ties, arranged in pattern B, with a gap of 50 mm..

The load deflection behaviour of this wall specimen is shown in Figures B-27 and B-28. The brick veneer and stud backing deflected proportionally to the applied load up to a load of 2.50 KPa. (52.2 psf.). When this load was exceeded, the brick veneer cracked at an elevation of 1065 mm.. A large increase in the deflections of both the brick veneer and stud backing wall was observed after the brick cracked. Further loading of Wall No.2 caused widening of the crack as the stud backing wall deflected. Between 2.75 KPa. (57.6 psf.) and 3.00 KPa. (62.7 psf.) the ties, at the 1333 mm. elevation, punched through the gyproc and began to buckle the stud flange as shown in Figure 4.10. The stud web, at the top of the stud backing wall, failed at a load of 3.45 KPa. (72.0 psf.). Loading of the wall to a maximum load of 4.83 KPa. also resulted in failure of the stud at the lower track and stud junct.

The load deflection of the stud backing wall, at an elevation of 2700 mm., is not included on the load deflection plots because of a malfunction of the LVDT in this location.



Figure 4.10-Typical Stud-Flange Failure

4.4.4.3 Series No.4 Wall No.3

Wall No.3 was constructed using ladder ties, arranged in tie pattern D, with a gap of 50 mm.

Figures B-29 and B-30 show the load deflection plots for Wall No.3. The deflection of this wall specimen was proportional to the load, up to a load of 1.33 KPa. (27.8 psf.). At this load, the brick veneer cracked at an elevation of 1270 mm.. Deflections of the brick veneer and the stud backing increased rapidly between 2.41 KPa. (50.4 psf.) and 2.75 KPa. (57.6 psf.). The stud web, at the top stud and track junction, failed in this load range. Further loading caused the top row of ties to punch through the gyproc and bend the stud flange. The stud flange was bent to a shape similar to that shown in Figure 4.10, after the 4.83 KPa. maximum load was reached.

4.4.4.4 Series No.4 Wall No.4

The final wall of the full size wall section tests was built using "V" ties. These ties were arranged in the tie pattern B, with a gap of 50 mm..

The load deflection behaviour of Wall No.4 is shown in Figures B-31 and B-32. Deflections of the brick veneer and the stud backing wall were proportional to the applied load up to a load of 2.07 KPa. (43.0 psf.). When this load was exceeded, the brick veneer cracked at an elevation of 935 mm.. The failure of the stud web occurred at the top of the backing wall at a load of

approximately 2.40 KPa. (50.0 psf.). Additional loading caused local buckling of the stud flange at the top tie locations. Wall No.4 achieved a maximum load of 4.83 KPa..

5. ANALYSIS AND DISCUSSION

5.1 Introduction

The test results for all three phases of the experimental program are analysed and discussed in this chapter. The first section examines the tie tests and the effects of the five experimental variables. Subsequent sections evaluate the results of the backing wall tests and full sized wall tests. The analytical models developed to simulate tie behaviour and full-sized brick veneer and steel stud curtain wall behaviour are examined. Finally, this chapter will present a review of the adequacy of the design methods outlined in Chapter Two.

5.2 Evaluation of the Tie Tests

This section presents a qualitative evaluation of the load deflection behaviour of the metal veneer ties. The results of the tie testing program were sufficient to establish trends in the load deflection behaviour of a number of different ties, under a variety of conditions. However, further testing is required to accurately quantify the effects of the variables on the behaviour of the ties.

Two parameters are used to define the behaviour of the tie and stud junction. These are the overall junction stiffness and the maximum load of the ties. The stiffness of the tie junction is defined as the slope of the linear portion of the load deflection curve obtained from each of

the tie tests.

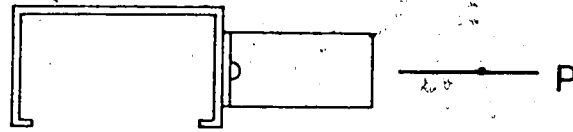
The effects of the tie type, stud type, end offset, gap, and location of the tie on the slope of the curve and on the maximum load of the tie are discussed. The difference in the behaviour of the ties on the short stud tests and on the wall section tests is also examined.

5.2.1 The Effects of the Tie Type

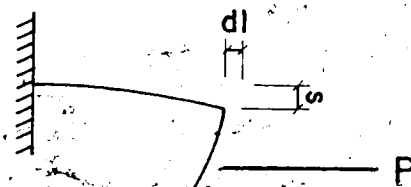
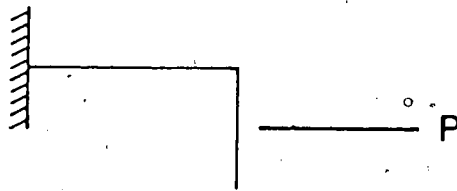
5.2.1.1 Junction Stiffness

The effect of the tie type on the junction stiffness is explained by examining the action of the junction under load. Figure 5.1 shows the assumed action of the stud web and flange. The end of the stud web is assumed to be fixed and the web and remaining flange form a cantilevered frame. Upon loading, the stud flange and web are free to rotate and deflect as shown in Figure 5.1. Connecting a tie to the stud's flange, adds another member to the frame. The screw connection between tie and flange, allows significant rotation and is therefore, assumed to behave as a pin. The clamped end of the tie (brick end) is assumed to be fixed, with respect to rotation but free to translate axially.

When the tie and stud junction is loaded, the lateral stiffness of the tie acts to restrain the sway (S) of the web and flange frame. As the lateral stiffness of the tie is increased the sway (S) and its resulting deflection (δ_1) are decreased. When similar



TYPICAL TIE AND STUD JUNCTION



ACTION OF JUNCTION UNDER LOAD

Figure 5.1 Tie and Stud Junction

ties are compared, a laterally stiff tie has a greater overall junction stiffness than a laterally weak tie.

A two dimensional analysis was conducted on the frame formed by the tie and stud. This analysis found that there was little difference in the load deflection behaviour of the corrugated ties. There was a large variation in the lateral stiffness, but all the corrugated ties were sufficiently stiff to reduce the sway to an insignificant value. The analysis also indicated that the axial compression of the tie accounted for less than one percent of the total tie deflection.

The 18 gauge short stud tests for 22 and 24 gauge corrugated ties demonstrated weak tie behaviour. Their load deflection curves exhibited a linear region followed by a region at constant load for increasing deflection. These two ties demonstrated approximately the same junction stiffness. The average slope for the 22 gauge tie was 619 N/mm and the average slope for the 24 gauge tie was 587 N/mm. The difference was only five percent.

The 16 gauge corrugated ties, V ties, and ladder ties demonstrated strong tie behaviour. They exhibited bilinear behaviour in the lower portion of their load deflection curves. The change in slope is probably caused by the second order loading effects and the crushing of the gyproc. These two mechanisms increase

the junction deflection and thus reduce the slope.

As there was permanent deformation of the strong tie junction in the second linear region of their load deflection curves, the strong ties are assumed to fail at the load at which a significant slope change is observed. Therefore the following discussion of the strong behaviour ignores the second slope of the load deflection curve.

The 16 gauge corrugated ties, tested on the short 18 gauge studs, exhibited a weaker junction stiffness than was expected. The average slope for the 16 gauge ties was 278 N/mm which was fifty percent less than the average slope for the 22 gauge ties. This large a variation cannot be explained entirely by experimental variability. Examination of the failed test specimens provides a possible explanation. The 16 gauge corrugated ties are 1.5 mm. thick. The 22 gauge corrugated ties are 0.78 mm. thick. Therefore, the 90 degree bend for the 16 gauge ties has a larger radius. This larger radius combined with large amplitude corrugations produces an eccentricity of loading of up to 4 mm. with respect to the gyproc and tie contact. This eccentricity of the tie load results in a prying action which increases the load at the gyproc and tie contact point. The corrugations and bend reduce the effective contact area. Thus the stress on the gyproc is larger than expected and the gyproc undergoes significant deformation. As the gyproc

crushes, the eccentricity of the load is increased and the prying force effect is also increased.

The deformation of the gyproc is also increased by the lateral stiffness of the 16 gauge ties. As the flange of the stud deflects, the very stiff 16 gauge tie remains rigid. Thus there is an increasing angle formed between the tie and stud flange. The tie load is, therefore, concentrated in an increasingly small area. As with the prying mechanism, increased stress results in increased gyproc deformations.

The crushing pattern of the gyproc behind the 16 gauge corrugated ties supports the hypothesis outlined above.

The 16 gauge corrugated ties were included in the testing program to increase the range of tie stiffness tested. This gauge of tie is not normally used in steel stud and brick veneer curtain walls. In fact, the 16 gauge corrugated ties used were modified dovetail anchors normally used to fasten brick veneer to concrete walls. The poor performance of this tie is, therefore, not significant for most applications of steel stud and brick veneer curtain walls. This tie should not be used where it will bear directly on gyproc sheathing. For such applications the use of a steel backing platform is recommended.

Crushing of the gyproc was not significant for 22 and 24 gauge corrugated ties or ladder ties. As a

backing platform was used to connect the tie directly to the stud flange, the deformation of the gyproc was not significant for the "V" ties.

Ladder ties are weak laterally when compared to corrugated ties. The 22 gauge corrugated tie is two orders of magnitude stiffer than a ladder tie. The decrease in lateral stiffness causes the stud web to sway more resulting in greater overall tie deflections. Therefore the junction stiffness of a ladder tie and stud combination is weaker than a corrugated tie and stud combination. Results of the short tie tests revealed that the ladder ties were less stiff axially than the 22 and 24 gauge corrugated ties. This confirms the assumed frame action of the stud flange and web.

Results of the short stud and "V" tie tests indicate that the "V" tie junction is also weaker than the 22 and 24 gauge corrugated tie junctions. The "V" ties are also weaker than the ladder ties. The results for the "V" tie tests are contrary to the expected behaviour for these stiff ties. However, although the rod portion of the "V" tie is very stiff laterally, the clip connection allows a significant amount of slip between the rod and backing platform. This slip significantly reduces the lateral restraint that the "V" tie provides the stud. Therefore, although the "V" tie is very stiff by itself, its overall junction stiffness is less than the junction stiffness of the other less

substantial ties.

The "T" ties also exhibited a tie stiffness that was less than expected. The "T" ties were tested only on the wall sections. Their load deflection slopes were substantially lower than the slopes for the 22 gauge corrugated ties tested in the same manner. The frame analysis for the "T" ties predicted a stiffer tie and stud junction. The cause of the poor performance of the "T" ties is the substantial deformation of the gyproc backing. Because the cross-section of this tie results in a small contact area and high stress levels in the gyproc, the deformation of the gyproc becomes a significant part of the deflection of the "T" ties.

The lateral stiffness of the metal veneer ties appears to be the tie characteristic that has the greatest impact on the overall junction stiffness. A greater lateral tie stiffness results in a greater junction stiffness.

The magnitude of stress applied to the gyproc sheathing is also important. The backing of the ties should ensure that the stress applied to the gyproc is low enough to preclude significant deformation of the gyproc at service load levels.

5.2.1.2 Maximum Load

The maximum load of the tie junction is greatly affected by the type of tie. Where the maximum load of the junction is governed by the buckling load of the

tie, the ties with the greater radius of gyration have the greater maximum load. This applies to the weak 22 and 24 gauge corrugated ties, and to the 16 gauge corrugated and ladder ties. The 24 gauge corrugated tie has the smallest radius of gyration and an average maximum load of 512 N. The ladder tie has the largest radius of gyration and the largest average ultimate load of 2060 N.

The mode of junction failure changes at a particular value of the radius of gyration. For sufficiently stiff ties the failure of the junction is due to a failure of the stud's flange and web. This type of junction failure is demonstrated in the "V" tests.

The results indicate that the use of very stiff ties in conjunction with steel strapping is a waste of material because the maximum junction load is governed by the stud failure load.

Two maximum load values are shown for each of the 16 gauge corrugated ties, ladder ties, and "V" ties in Tables 4.2 to 4.5. The first value is the load at which a significant change in the slope of the tie load deflection curve is observed. Second order loading effects and deformation of the gyproc become significant factors in the load deflection behaviour of the junction above this load. As most load deflection curves did not possess a sharp slope change, the value of this first maximum was subject to a large interpretation error. The

ladder and "V" ties exhibited the highest first loads. The 16 gauge corrugated tie exhibited first maximum loads that were much lower. It appears that the ties which restrain the sway of the stud the most and deform the gyproc the least have the highest first maximum loads. In general, the stiffer the tie the higher the maximum loads resisted by the tie and stud junction. However, there is an upper limit on the ultimate load of the junction defined by the strength of the stud.

5.2.2 The Effect Of Stud Type

5.2.2.1 Junction Stiffness

As discussed in the previous section, the stud flange and web behave as a cantilevered frame (see Figure 5.1). Analysis indicates that any change in the stud gauge will drastically affect the stiffness of the standard tie junction.

In the short stud tests, the 22 gauge corrugated ties tested on 20 gauge studs exhibited an overall junction stiffness that was less than when they were tested on 18 gauge studs. The thirty five percent decrease in stud thickness for the 20 gauge studs as compared to the 18 gauge studs, resulted in slopes that were two thirds smaller.

The action of the weaker 20 gauge studs alleviates several problems associated with the 16 gauge corrugated ties. Increased deflection of the stud flange and web

decreases the deformation of the gyproc to a less significant portion of the total deflection. The junction stiffness for the 16 gauge ties is approximately 15 percent less than for the 22 gauge corrugated ties when both are tested on 20 gauge studs.

Reducing the thickness of the stud can drastically reduce the stiffness of the stud and tie junction because of the frame action of the flange and web of the steel stud. In fact, the thickness of the stud has a far greater effect on the junction stiffness than the tie type.

5.2.2.2 Maximum Load

The type of stud does not significantly affect the ultimate load of the tie junction, except where the failure load of the stud falls below that of the tie used. The failure loads for the 22 gauge ties, tested on 20 gauge studs, are not significantly different from the failure loads of 22 gauge ties tested on 18 gauge studs. A similar statement can be made for the 16 gauge corrugated tie tests. However, in this case the maximum loads are approximately the same because the failure load of the 20 gauge stud appears to be approximately the same as the buckling load of the 16 gauge tie.

5.2.3 The Effect Of The Tie End Offset

5.2.3.1 Junction Stiffness

The tie end offset has little effect on the stiffness of the tie and stud junction. An examination of the forces acting on the stud flange indicates that offsetting the ends of the tie does not affect the value of the horizontal load applied to the centre of the flange. The deflection of the stud flange and consequently the junction deflection, are not changed.

Figure 5.2 shows the slopes of the load deflection curves for the 22 and 24 gauge corrugated ties obtained for various end offsets. While there is a high degree of variation in the test results, a least squares curve fitting analysis indicates that there is little change in the junction stiffness below an offset of 15 mm.

The reduction in the junction stiffness for offsets greater than 15 mm is probably caused by an increase in the deformation of the gyproc. As the offset was increased, the 90 bend rotated about the screw connection. This rotation reduced the contact area and resulted in an increased deformation of the gyproc.

Increasing the end offset for the 16 gauge tie did not reduce the overall stiffness of the tie and stud junction. In fact, there appeared to be a small increase in the junction stiffness. However, because there was a high degree of variability in the tests conducted, it is sufficient to conclude that the end offset does not

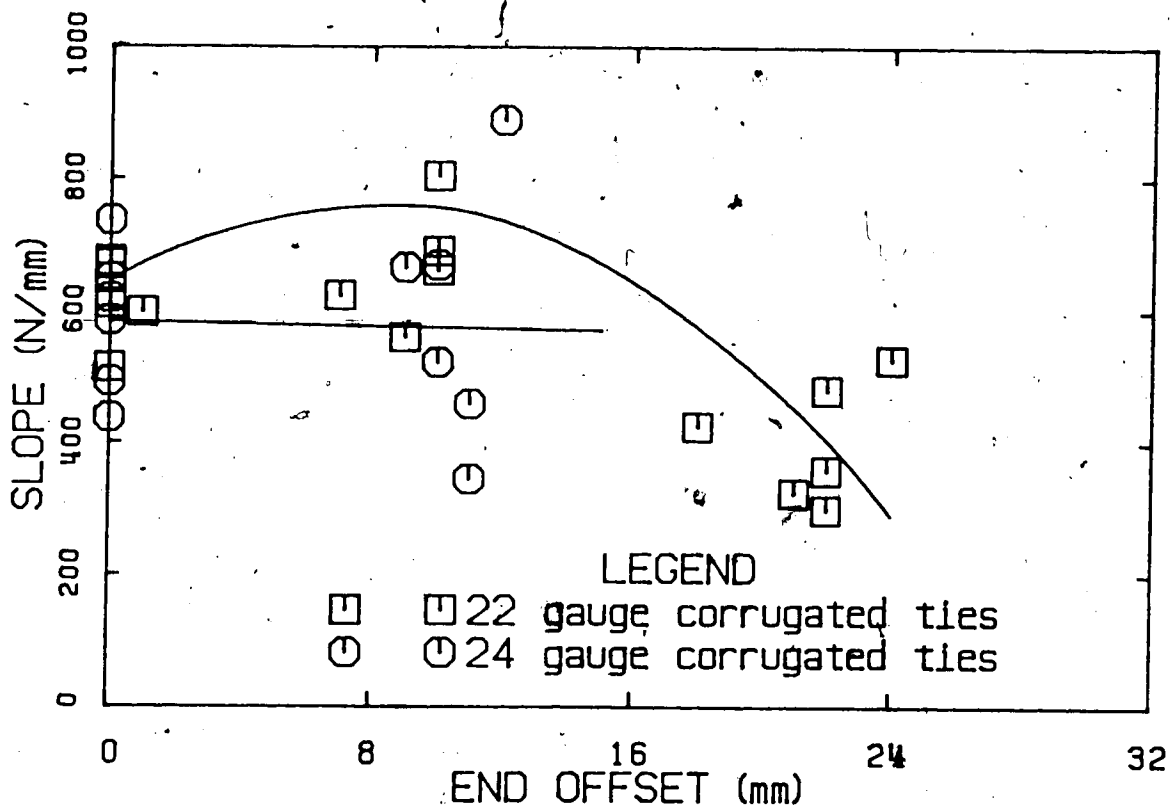


Figure 5.2 Variation of Slope With End Offset

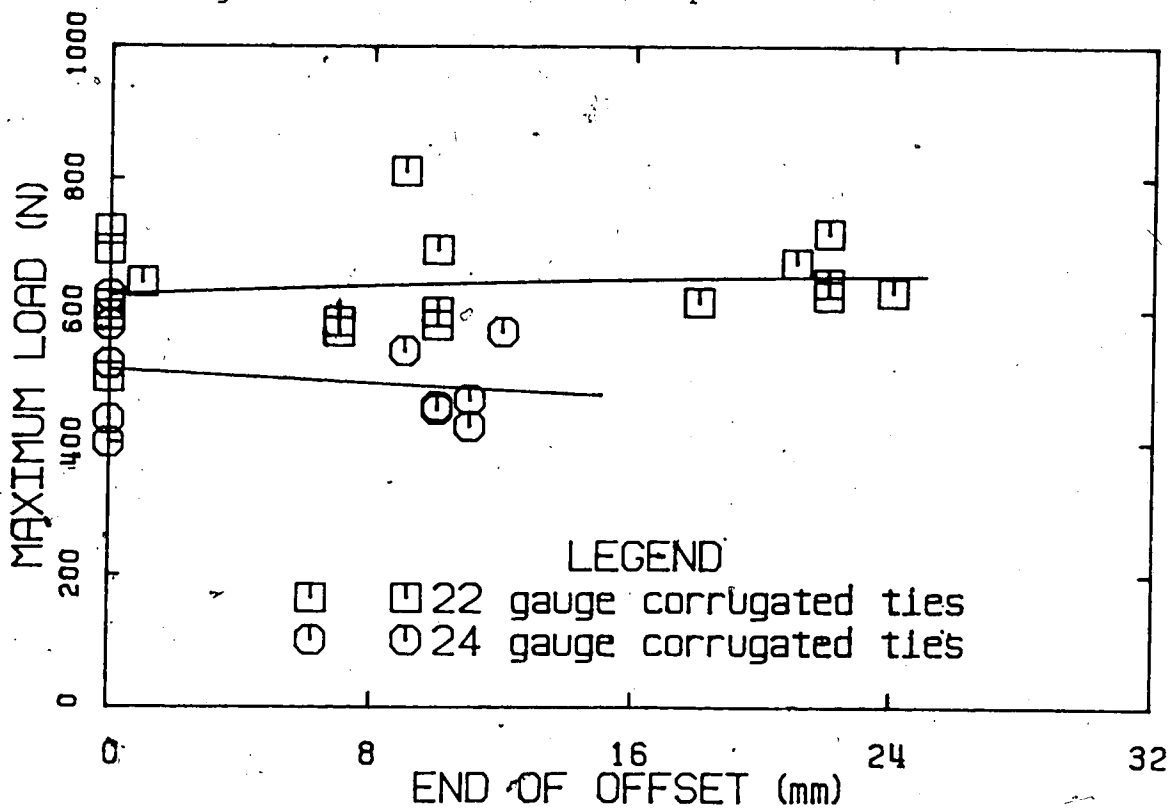


Figure 5.3 Variation of Maximum Load With End Offset

effect the stiffness of the 16 gauge corrugated tie and stud junction.

In most applications of metal veneer ties, the end offset will be less than 15 mm.. Therefore, the offset of tie ends can be ignored when analysing load deflection behaviour of the tie and stud junction.

5.2.3.2 Maximum Load

The offset of the tie ends does not appear to affect the maximum load of the 22, 24 and 16 gauge corrugated ties. Figure 5.3 shows the maximum loads of the 22 and 24 gauge corrugated ties for a range of offset values. A least squares analysis shows little change in the maximum loads of these ties over the entire range of offsets. The 16 gauge ties exhibit much the same behaviour as the 24 gauge corrugated ties.

The analysis of a tie with an increasing end offset indicates that the maximum buckling load of the tie should decrease as the end offset increases. However, the observed shape of the displaced tie was not the same as that illustrated in Figure 3.4. As the ends of the tie were displaced the 90 degree bend simply widened and a bend was formed at the clamped end. The tie itself remained approximately straight. A tie in this configuration will fail at a higher load than a tie deformed as illustrated in Figure 3.4, although not at as high a load as a concentrically loaded tie.

Variation of the end conditions of the ties could account for the remaining increase in the stability of the offset ties. However, further testing in this area is required before an adequate hypothesis can be formulated.

5.2.4 The Effect Of Gap Size

5.2.4.1 Junction Stiffness

A two dimensional frame analysis indicates that gap size should not significantly affect the load deflection behaviour of the stud and tie junction. However, the results of the tie tests indicate that the 20 mm gap corrugated ties underwent significantly more deflection with a gap of 25 mm. than with a gap of 50 mm. The gyproc behind the ties with a 25 mm. gap was severely deformed over a much smaller area than the gyproc behind the ties with a 50 mm. gap.

The increased lateral restraint of the shorter tie prevents the tie from following the deflection of the stud flange. Due to the difference in the rotations of the tie and flange, an increasingly smaller area is loaded. The resulting increase in stress causes a greater deformation of the gyproc. Again, the gyproc sheathing plays a major role in the load deflection behaviour of the stud and tie junction.

5.2.4.2 Maximum Load

According to simple column theory, a decrease in the effective length of a concentrically loaded column results in an increase in its buckling load. The maximum load of the 22 gauge corrugated ties should increase with a decrease in the gap length. Test results support this and show an average increase in the maximum tie load of 60 percent for a 50 percent decrease in the length of 22 gauge corrugated ties tested.

5.2.5 Location Of Tie

5.2.5.1 Junction Stiffness

The location of the tie with respect to the stud web has a significant effect on the stiffness of the tie and stud junction. As the distance between the stud web and the location of the screw in the tie increases, the deflection of the stud and tie junction increases. Results of the wall section and tie tests are plotted in Figure 5.4. While the gyproc sheathing restrains the deflection of the stud flange, a definite decrease in junction stiffness occurs as the distance from the stud web increases. All combinations of studs and ties tested on the wall sections showed sharp declines in junction stiffness with an increase in web distance.

The above discussion applies to the initial slopes of the load deflection curves of the strong and weak ties only. For the second slope of the strong ties, no

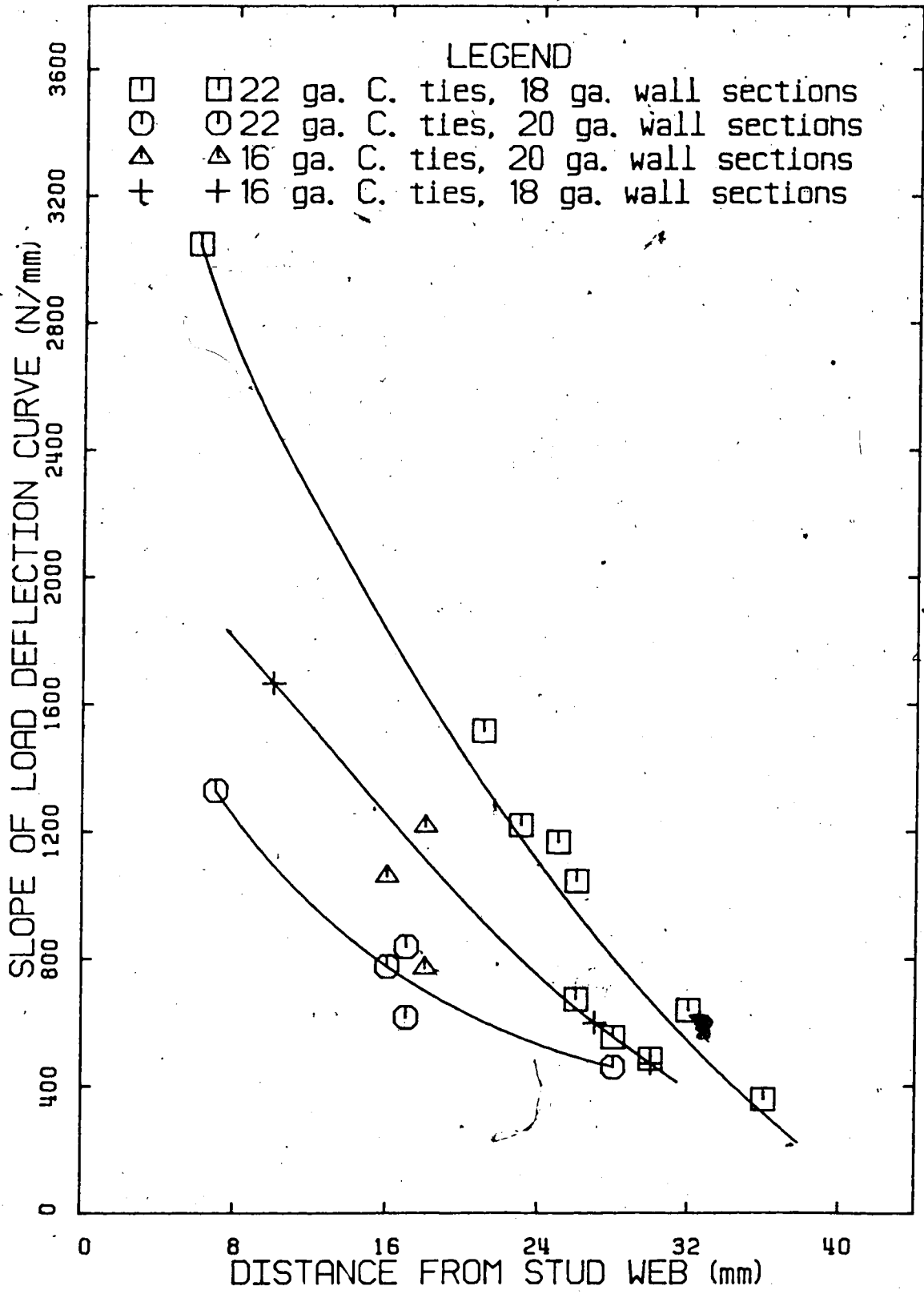


Figure 5.4 Variation of the Junction Stiffness with Web Distance

relation between tie location and slope value was evident. The distance from the stud web to the tie location does not significantly change the amount of gyproc deformation or the magnitude of the second order effects.

In most wall construction, the location of the tie is highly variable. Thus the stiffness of any particular tie and stud junction in a wall, can vary widely.

5.2.5.2 Maximum Load

The maximum load resisted by the tie and stud junction is not affected by the location of the tie. Test results indicate that the maximum loads for all the ties, both weak and strong, do not vary with the distance from the stud web.

It should be noted that for most of the strong ties, the ultimate load of the tie was not reached, due to the limitations of the testing apparatus. Failure to define the ultimate load of the strong ties is not detrimental to the value of this investigation as the magnitude of the maximum applied loads, even when limited by the apparatus, is significantly greater than the loads experienced by ties in actual construction.

5.2.6 Wall Section Tests Versus Short Stud Tests

5.2.6.1 Junction Stiffness

Values of the junction stiffness obtained in the wall section tests were greater than in corresponding short stud tests. For the 22 and 24 gauge corrugated ties the effective junction stiffness approximately doubled. The two slopes for the load deflection curve of the 16 gauge corrugated tie load deflection curve also increased.

The gyproc sheathing significantly restrained the deflection of the stud flange and web. The gyproc was assumed to span continuously across all three studs of the wall section and a frame analysis of the resulting structure indicated that the stud and junction stiffness theoretically increased by approximately 80 percent, due to the presence of the gyproc. The properties for the gyproc used in this analysis were obtained from the tests reported in Appendix B. Both tests and analysis show that the presence of exterior gyproc sheathing can greatly increase the stiffness of the tie and stud junction. Replacement of this exterior gyproc by more flexible sheathing will probably cause a significant reduction in the effective stiffness of the tie and stud junction.

5.2.6.2 Maximum Load

The maximum loads for both the weak and strong ties were not affected by whether or not they were tested on short studs or on wall sections.

5.3 The Evaluation of Gyproc, Track and Stud Interaction

In brick veneer and steel stud curtain walls, the stud backing wall is comprised of studs, supporting track, and gyproc sheathing. The interaction of these three components is the subject of the following discussion.

Results of the stud and track tests indicate that the flanges of the 90 mm., 18 gauge and 150 mm., 20 gauge steel track deflect significantly under load. The load deflection behaviour of the 18 gauge track remains approximately linear to a load of 2500 N.. Up to a load of approximately 1000 N, the load deflection behaviour of the 20 gauge track is also linear. Figures 4.5 and 4.6 show average slopes of the linear regions of the 18 and 20 gauge track load deflection curves. The average slope of the 18 gauge track is 1720 N/mm. and the average slope of the 20 gauge track is 867 N/mm..

As expected the 20 gauge track is significantly weaker than the 18 gauge track. However, for both the 18 gauge and 20 gauge track specimens a screw was used to fasten the stud to the track flange on the load side. Thus, the load was resisted by both flanges. If the studs are held in place by crimps or just by the gyproc sheathing, there will be only one track flange resisting load resulting in considerably more support settlement of both the 18 and 20 gauge stud and track connection.

The support settlement of each of the two stud backing wall specimens was calculated using the 867 N/mm. slope

obtained from the 18 gauge track tests and assuming that each stud and track connection supported one quarter of the total specimen load. The resulting support settlements were then subtracted from the centre span deflections to produce the load deflection curves shown in Figure 5.5.

Figure 5.5 also shows the load deflection curve of the three stud backing wall specimen (No.3). The true centre span deflections, for this specimen, were calculated by taking the difference between the average measured centre span settlements and the average measured support settlements.

The linear portion of each of the load deflection curves yields an average slope of 185 N./mm., for the two stud wall specimens (No.1 and No.2), and a slope of 320 N/mm., for the three stud specimen (No.3).

The effective moment of inertia (I), for each wall specimen, was calculated using the classic elastic beam formula:

$$\Delta = \frac{23 P L^3}{648 E I} \quad (1)$$

For each calculation, the slope of the load deflection curve was set equal to P/Δ and the value of Young's Modulus (E), as obtained from tension coupon tests reported in Appendix A, was taken as 210500 MPa..

The above calculations yield an effective moment of inertia of $6.14 \times 10^5 \text{ mm}^4$, for specimens No.1 and No.2, and an effective moment of inertia of $10.31 \times 10^5 \text{ mm}^4$ for specimen No.3. These values equate to an effective moment of

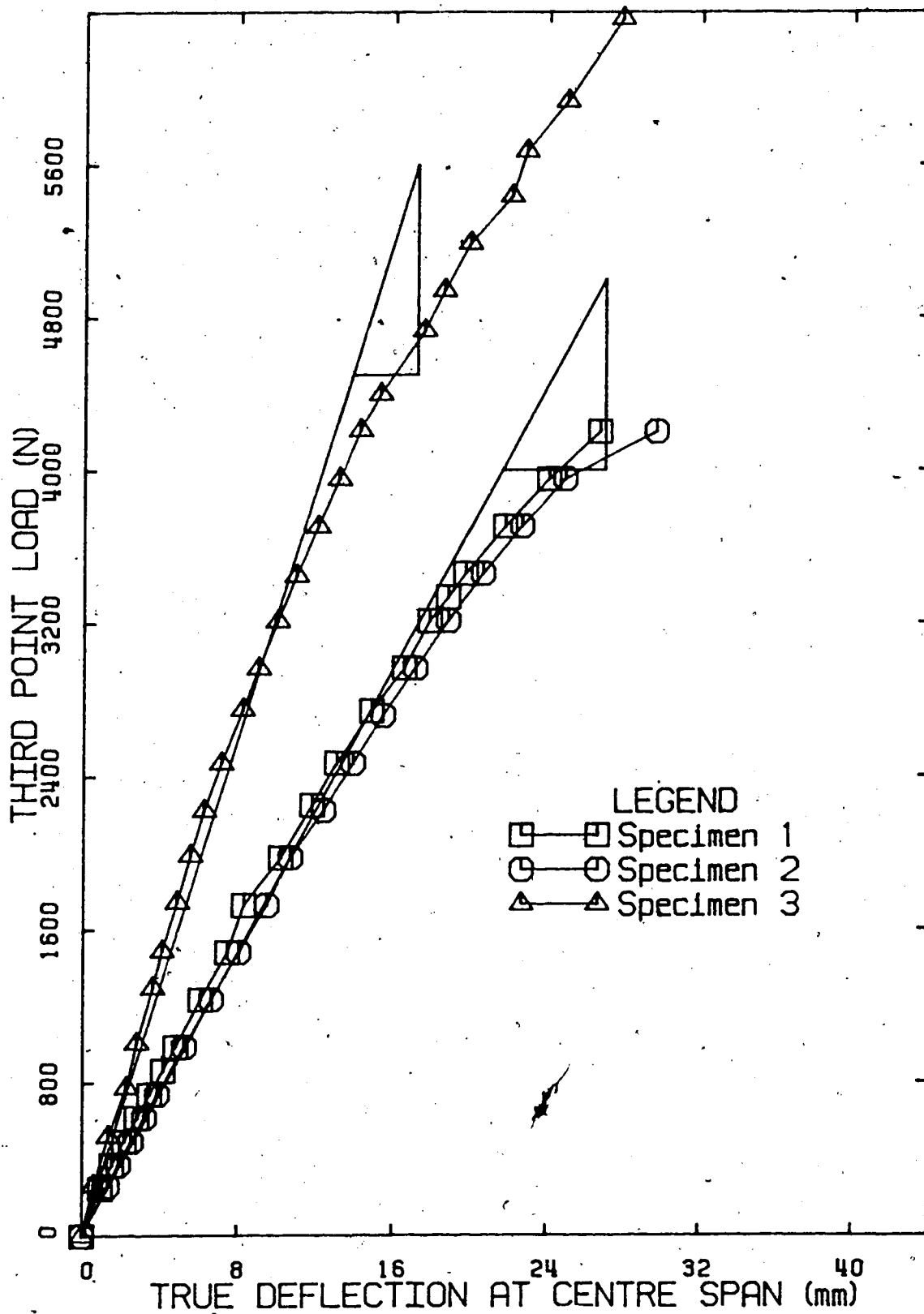


Figure 5.5 True Load Deflection Curves for the Backing Walls

inertia per stud of 3.07×10^5 mm⁴., for the two stud wall specimens, and an effective moment of inertia of 3.44×10^5 mm⁴. per stud, for the three stud wall sections.

An average measured moment of inertia was calculated using the measured dimensions of the studs. Comparing effective moment of inertia to the average measured moment of inertia of the stud shows that there is little difference between the two values. In the case of the two stud specimen, the effective moment of inertia (3.07×10^5) is 93 percent of the average measured value (3.3×10^5). The effective moment of inertia of the three stud wall specimen (3.44×10^5), is 10 percent larger than the average measured moment of inertia (3.14×10^5).

All three tests indicate that there is no significant composite action between the gyproc sheathing and the 90 mm., 18 gauge steel studs. The only significant structural benefit of the gyproc sheathing is its restraint of the stud's flange and web. This restraint stabilizes the stud against lateral torsional buckling and, as mentioned earlier, increases the effective stiffness of the ties.

5.4 Evaluation of Full Sized Wall Tests

This section evaluates the performance of the sixteen full sized wall specimens. The objective of this research is to evaluate the performance of brick veneer and steel stud curtain walls designed close to the limit of current CSA specifications. Each wall specimen was 3200 mm. high. The

code limit is 3600 mm.. The height of the specimens was greater than the height of most curtain walls used in construction.

To properly evaluate the performance of the full sized wall sections a comparison must be made between the failure load and the design load of each wall specimens. According to the steel stud manufacturer's load table, the wall specimens using 90 mm., 18 gauge studs have a design load of 1.21 KPa. (25.2 psf.), and the specimens using the 150 mm., 20 gauge steel studs have a design load of 2.70 KPa. (56.4 psf.). For the purposes of this report, the failure load of the wall sections is defined as the load at which the brick veneer cracked or the load at which the ties buckled. 150 mm., 20 gauge studs were used to evaluate the performance of the brick veneer and steel stud curtain walls over a wide range of backing wall stiffnesses.

5.4.1 Wall Performance

The failure loads of the sixteen wall specimens are summarized in Table 5.1. The table also includes the mode of failure and the design load of the walls. The sixteen wall specimens can be separated into two groups; walls constructed using the 90 mm. 18 gauge steel studs and walls constructed using 150 mm. 20 gauge steel studs.

5.4.1.1 90 mm. 18 Gauge Walls

Table 5.1 shows that all walls constructed using the 90 mm., 18 gauge steel studs attained their design

load. The factors of safety ranged from 1.03 to 2.3. For this height of wall, the procedures used for the design of brick veneer and steel stud curtain walls result in walls with factors of safety lower than what is generally acceptable for masonry design.

Wall No.4 in Series No.1 exhibited the most unsatisfactory performance. This wall barely reached the design load. While the gap on this wall was sufficiently small to preclude tie buckling as the initial mode of failure, the structural support was flexible enough to cause cracking of the brick veneer.

The load deflection curves in Appendix B show that the walls constructed using tie pattern A underwent the greatest deflections of all the wall specimens resulting in the cracking of the brick veneer at lower loads. The use of tie pattern A also increased the tributary area of the top ties, thus lowering the wall load at which the top ties buckled. Consequently, construction practices resulting in tie pattern A should be avoided. This patterning of ties is most commonly seen at the corners of walls and around openings.

Tie pattern B is the tie pattern most commonly found in curtain wall construction. The two walls constructed using this tie pattern and 18 gauge studs deflected less when compared to walls constructed using pattern A, but deflected more than identical walls using tie pattern C.

Table 5.1 Summary of Wall Failure Loads

WALL FAILURE LOADS							
Series	Wall	Tile Type	Stud Type	Tie Pattern	Gap	D.Load (KPa)	F.Load (KPa)
1	1	22ga. Corr.	18 ga.	type A	50	1.21	1.50*
1	2	22ga. Corr.	18 ga.	type A	50	1.21	1.52*
1	3	22ga. Corr.	18 ga.	type A	25	1.21	1.66
1	4	22ga. Corr.	18 ga.	type A	25	1.21	1.25
2	1	22ga. Corr.	18 ga.	type C	50	1.21	1.47
2	2	22ga. Cor	18 ga.	type B	50	1.21	1.72
2	3	T	18 ga.	type B	50	1.21	2.14
2	4	-	18 ga.	type C	50	1.21	2.78
3	1	22ga. Corr.	20 ga.	type C	50	2.70	2.97*
3	2	22ga. Corr.	20 ga.	type B	50	2.70	2.20*
3	3	T	20 ga.	type B	50	2.70	2.00
3	4	T	20 ga.	type C	50	2.70	2.14
4	1	24ga. Corr.	20 ga.	type B	50	2.70	0.92*
4	2	16ga. Corr.	20 ga.	type B	50	2.70	2.49
4	3	Ladder	20 ga.	type D	50	2.70	1.33
4	4	V	20 ga.	type B	50	2.70	2.06

Note: (1) 20 ga. = 20 ga., 6 in. steel stud
 (2) 18 ga. = 18 ga., 3 5/8 in. steel stud
 (3) Tie patterns are shown in Figure 3.11
 (4) D.Load is the design load of the wall
 (5) F.Load is the failure load of the wall
 (6) * indicates the walls that failed initially by tie buckling

Tie pattern C utilizes an extra tie at the top of the center stud line. This extra tie reduces the deflection of the wall slightly by reducing the load on each of the top ties. The reduction of the tie load also increases the wall load at which the 22 gauge corrugated ties buckled. Although the cracking load of the brick veneer for 22 gauge ties and tie pattern C is lower than that of a similar wall employing tie pattern B., the brick veneer of the wall employing tie pattern C with the "T" ties cracked at a higher load than a similar wall employing tie pattern B. The premature cracking of the wall employing 22 gauge corrugated ties with tie pattern C is probably due to the low modulus of rupture for the brick veneer. Thus, tie pattern C improves the performance of the brick veneer and steel stud curtain walls and its use is recommended.

As indicated by the performance of Wall No.2 and Wall No.3 of Series No.2, the type of tie used in the 90 mm, 18 gauge stud walls has little effect on the load deflection behaviour at low load levels. Figures 5.6 and 5.7 show little difference in the deflections of these walls up to a loading of 1.50 KPa. (31.3 psf.). As service level loads are below this load, it can be concluded that the 22 gauge corrugated ties and "T" ties perform equally well under service load conditions.

A comparison of Wall No.1 and Wall No.4 of Series No.2 indicates that the load deflection behaviour of the

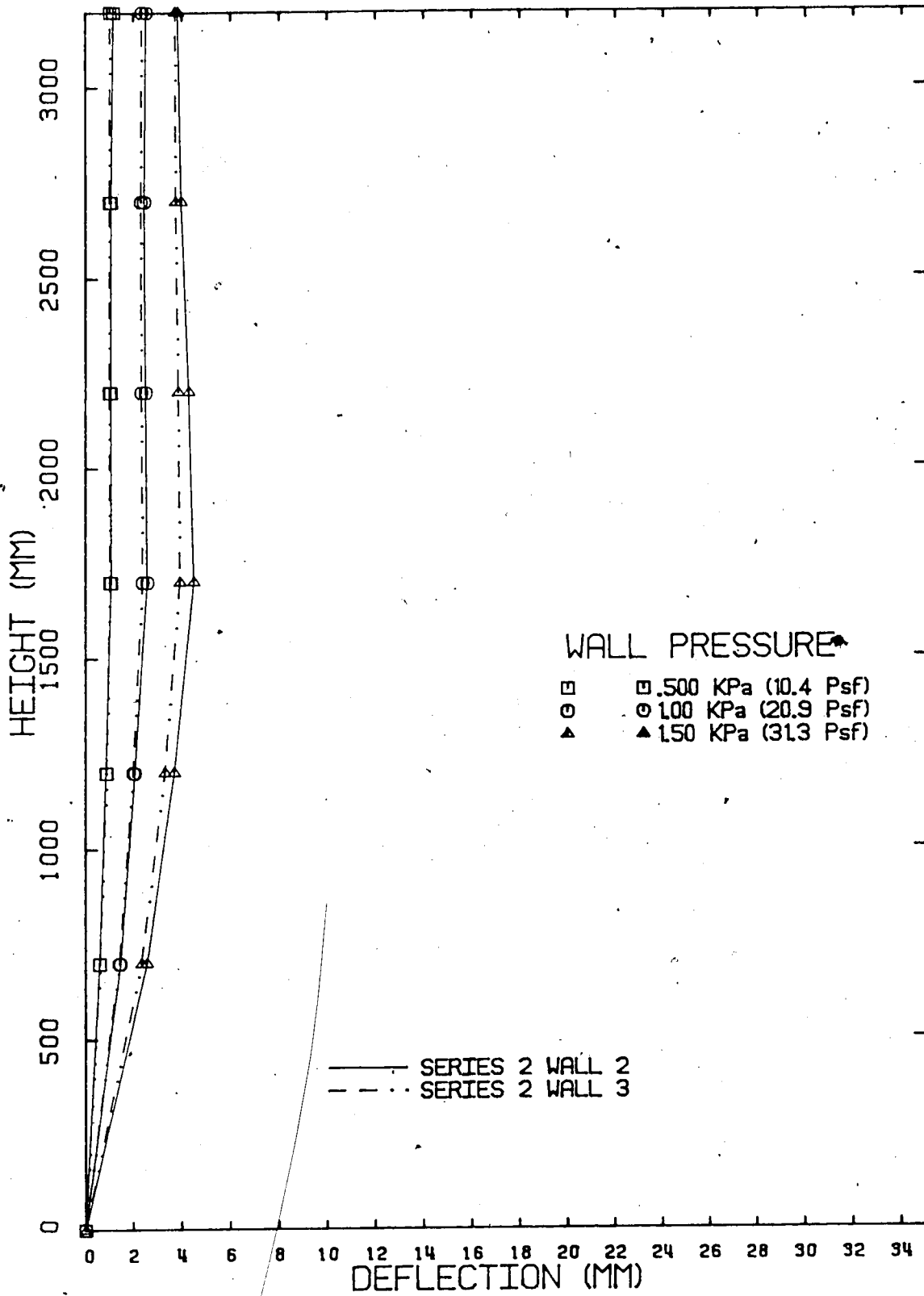


Figure 5.6 A Comparison of Brick Veneer Deflections

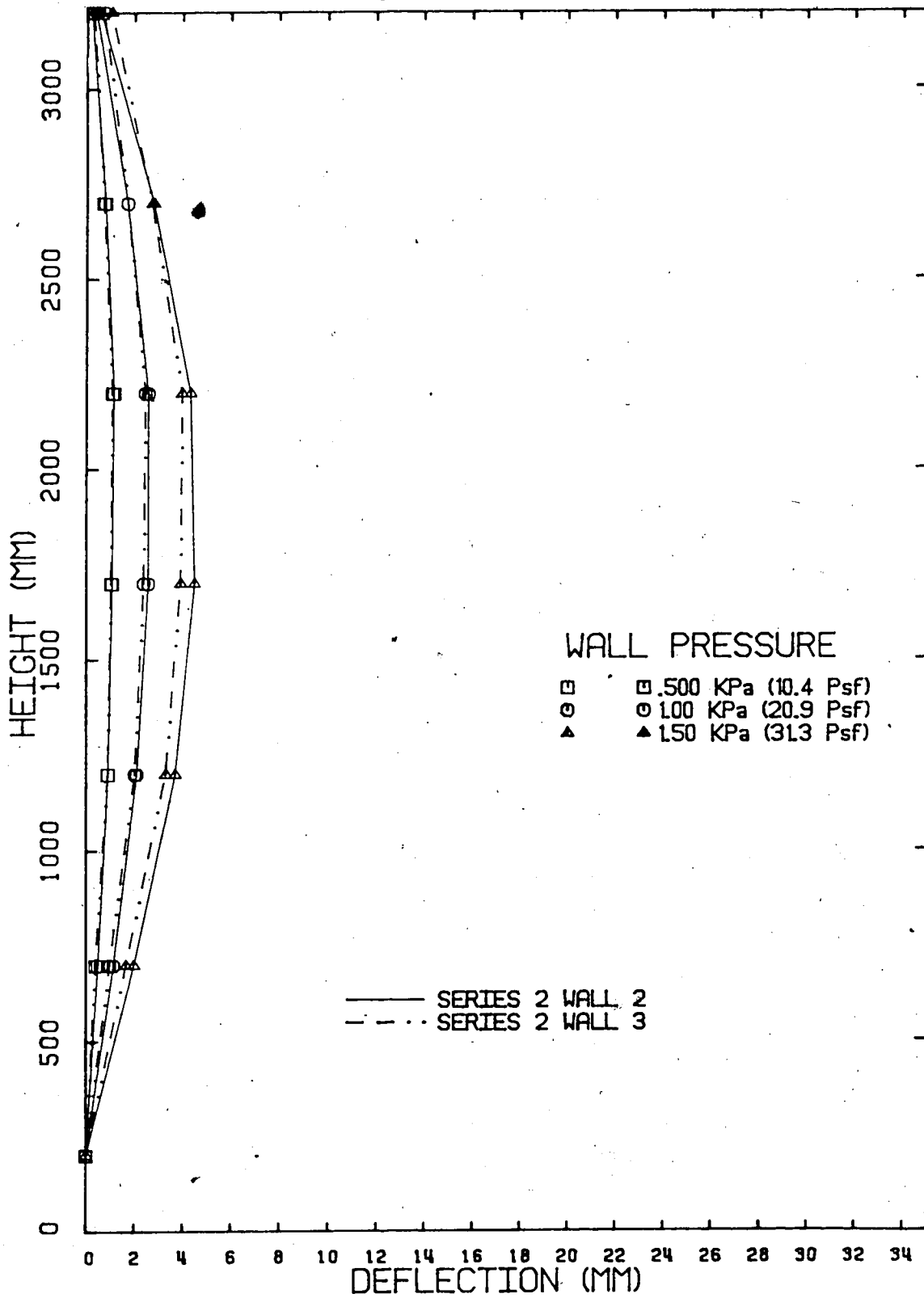


Figure 5.7 A Comparison of Steel Stud Deflections

"T" ties and 22 gauge ties are also the same for tie pattern C. below the cracking load of Wall No.1.

The evaluation of the tie tests indicates that there should be a difference between the load deflection behaviour of walls using 22 gauge corrugated ties and those using "T" ties. However, the tie tests also show that the location of the tie, with respect to the stud web, has a dramatic effect on the tie and stud stiffness. Therefore, the variation of the tie location in each wall was probably sufficient to hide any effect of the "T" ties' reduced tie and stud junction stiffness.

Tie type primarily affects the ultimate failure mode of the walls. If the ties are sufficiently weak, the mode of failure will be tie buckling which is undesirable. The ties should be arranged in patterns that will guarantee that the load on each tie does not exceed the buckling load of this particular type of tie, before cracking of the brick veneer.

5.4.1.2 150 mm 20 Gauge Walls

Table 5.1 indicates that only one wall constructed using 150 mm., 20 gauge studs reached the design load before failing (Wall No.1 in Series 3). The current procedures used to design brick veneer curtain walls appear to be inadequate.

As for the 18 gauge steel stud curtain walls, tie pattern C performed the best with the least deflection

and the highest failure loads.

The type of tie had a greater effect on the load deflection behaviour of the brick veneer and 150 mm., 20 gauge steel stud curtain walls than for the walls utilizing the 18 gauge studs. The total deflection of the backing wall was so small that the deflection of the stud and tie junction became significant. For the same load, the stud and tie junction for the 20 gauge walls deflected much more than the junction for the 18 gauge walls. At the lower load levels the tie type did not change the load deflection behaviour severely. The 16 gauge corrugated ties exhibited the most deflection. There was very little difference observed between the load deflection behaviour of the "T" ties and the 22 gauge corrugated ties before the ties buckled. Again, it is likely that the varied location of the ties masked some of the effects of the different tie types. As with the 18 gauge stud walls, the type of tie primarily affected the mode of failure of the walls.

A comparison of the deflections of Wall No.2 of Series No.2 and Wall No.2 of Series No.3 indicates that, at a load of 1.50 KPa. (31.3 psf.), the maximum deflection of the brick veneer of the two walls differed by only 15 percent. As the stiffness of the studs in the backing walls changed by a factor of 2.1, a much greater difference in the deflections of the two walls was expected. However, increased tie and stud junction

deflections increased the deflections of the brick veneer and thus counteracted the effect of the increased stud backing wall stiffness. The effective stiffness of the stud backing was also reduced by significant deflection of the stud supports.

The performance of the ladder ties and the 24 gauge corrugated ties in the 20 gauge stud walls was very poor. The 24 gauge ties buckled at a load that was one third of the design load. The buckling of this tie at such a low load makes it unsatisfactory for curtain walls with 50 mm gaps and tie arrangement B. If the 24 gauge ties had been arranged in tie pattern C they may not have buckled as soon but it is doubtful whether they would have been able to reach the design load of 2.70 KPa. (56.4 psf.).

The ladder ties had cross wires spaced at 381 mm. on center. The tie load was, therefore, transferred to the stud flanges at distances greater than one half of the flange width from the stud web. This resulted in weak stud and tie junctions and subsequently large brick veneer deflections which caused early cracking of the veneer. If the cross wires had been spaced at 400 mm. there would have been a considerable improvement in the performance of the ladder ties.

The 150 mm., 20 gauge steel stud backing walls, unlike the 90 mm., 18 gauge backing walls, failed at load levels exceeding 3.10 KPa. (64.8 psf.). There were

two forms of stud failure; the first form was a shear buckling of the stud web at the top stud and track junction, and the second form was a buckling of the stud flange at the stud and tie junctions. Thus, even if the brick veneer did not crack, the 20 gauge studs would fail at loads barely exceeding their design load.

Rotation of the brick veneer concentrates the wind load at the top of the supporting structure. This concentration of load at the top of the backing wall probably caused the premature buckling of the stud.

All the wall specimens performed poorly in relation to their design loads. The brick veneer and 90 mm., 18 gauge stud wall specimens were able to reach their design loads, but they had very low factors of safety. The type of tie used did not significantly affect the stiffness of the wall. However, the mode of wall failure was governed by both the type of tie and the pattern of the ties. Tie pattern C improved the performance of the walls particularly in regards to post cracking behaviour. The performance of the 150 mm., 20 gauge studs questions the reliability of using this type and height of wall for load levels exceeding 1.21 KPa..

5.5 Analytical Models

This section presents the analytical techniques used to model the load deflection behaviour of the brick veneer and steel stud curtain walls.

A two dimensional stiffness method was used to analyse the frame action of the brick veneer, the ties, and the steel studs. This method used the basic matrix equation:

$$\{F_i\} = [K_{ij}] \{\Delta_j\} \quad (2)$$

Where F_i are the forces at each node of the frame, Δ_j is the nodal degrees of freedom, and K_{ij} is the elastic formulas relating to each nodal force. The unknown displacements (degrees of freedom) are calculated using Equation No.2 and the applied nodal forces. Therefore, any unknown forces can be solved using Equation No.2.

A computerized version of the direct stiffness method was used for the analysis of the brick veneer and steel stud wall section. The wall model used for this plane-frame-truss program is shown in Figure 5.8. Each member, its nodes, and the nodal degrees of freedom are shown in this figure. The plane frame analysis assumes that each stud acts independently with a 400 mm. wide section of brick veneer.

The flexibility of the track and stud connection is modeled using a "dummy" member at each end of the stud. These dummy members have an axial stiffness but no flexural stiffness. The axial stiffness was defined by an effective area (A_e) using the equation:

$$A_e = \frac{P L}{\Delta E} \quad (3)$$

An effective area was calculated by setting P/Δ equal to the average slope obtained from tests on each of the track types, L equal to 50 mm. and the Young's Modulus (E) equal to 210,500 MPa. The effective area used for the dummy

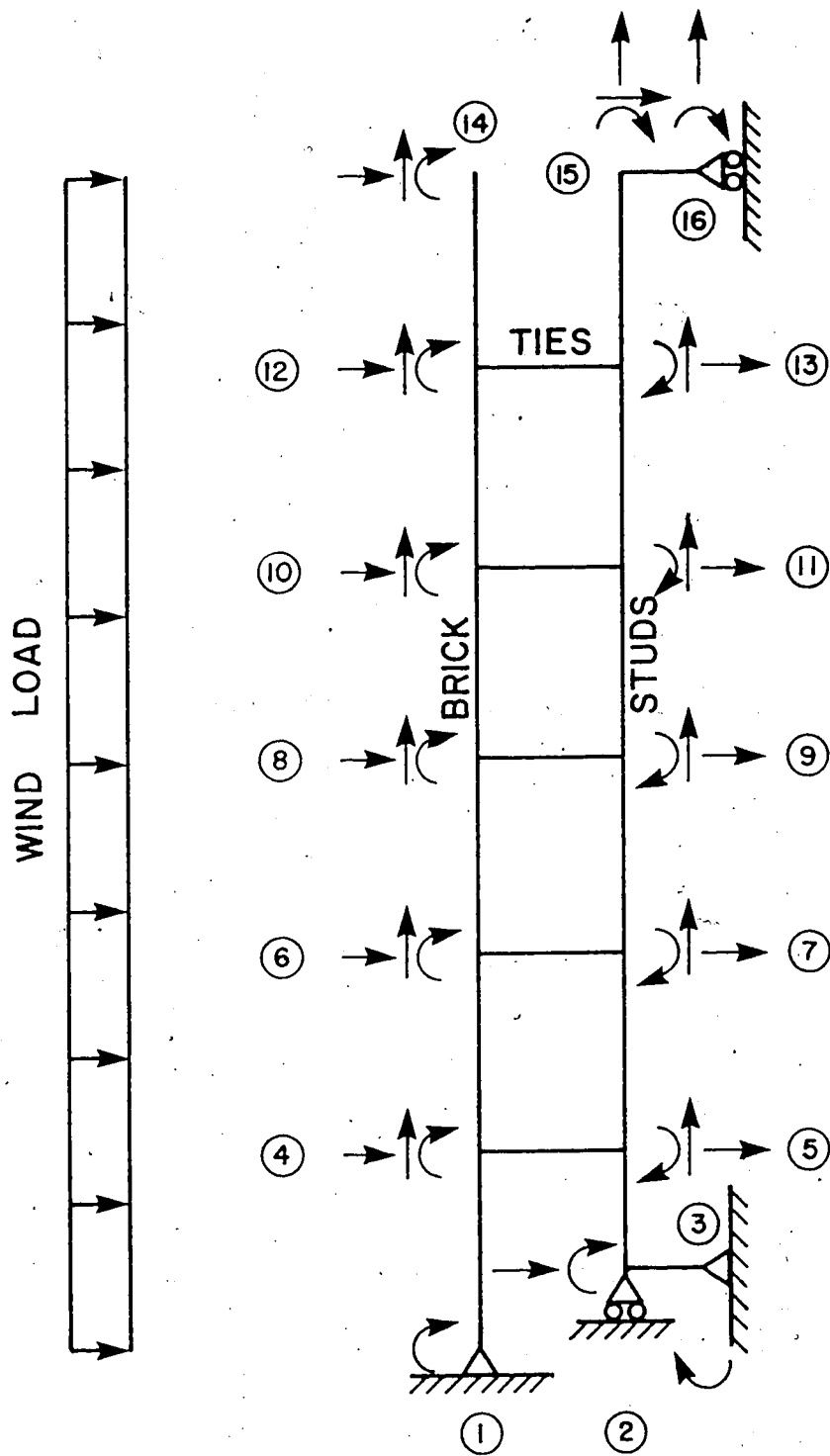


Figure 5.8 Curtain Wall Direct Stiffness Model

members was 0.409 mm^2 , for the 18 gauge track and 0.200 mm^2 , for the 20 gauge track.

The load deflection behaviour of the tie members was modeled in a similar fashion. Each tie member was given an effective area based on Equation No.3. The value of E was taken as 210500 MPa and P/Δ was set equal to the slope of the load deflection curve for the tie junction.

The behaviour of the curtain walls was analysed for increasing positive wind load. After each incremental increase in the wind load, the axial loads on each tie were checked. If the tie loads exceeded the maximum load for that tie then the tie was removed and resisting joint loads were applied at each of the ties' nodes. The value of this joint load was equal to the maximum load of the tie. For the "V", "T", ladder, and 16 gauge corrugated ties a weaker tie member was also inserted. This weaker member had an effective area calculated from the second slope of the load deflection curves of these ties.

5.6 Evaluation of the Analytical Model

This section of the report compares the results of the analysis to the results of the wall tests. This comparison determines the accuracy of the model in describing the behaviour of the walls. The results of the analysis for four wall specimens are discussed. The four walls included in the following discussion represent a variety of tie types and stud types with which to evaluate the analysis techniques

and models. The analytical results for the other twelve walls agree with their test results to an equal or better degree than the four walls chosen.

The modulus of Elasticity (E) of the brick veneer walls was obtained from the tests reported in Appendix A. The values of E used for the analysis ranged from 8000 MPa to 10,000 MPa. Results of the brick prism tests indicated that the values of E for the brick veneer range from 670 MPa. to 20,000 MPa.

The actual value of E for the brick veneer walls does not significantly effect the results of the analysis. Results for Wall No.2 of Series No. 2, are shown in Figure 5.9 and 5.10 for a load of 1.0 KPa. (20.9 psf.). When the E is doubled, there is a maximum change in the defection of the brick veneer of 18 percent. This is not considered to be a significant change relative to the large increase in the value of E.

The values of the effective areas for the two different stud types were based on the tie test results. For purposes of the analysis it was assumed that the ties could have been placed as far as 3 mm. from the centre of each stud. Two slopes were chosen and the effective areas were calculated using Equation No.3. The effective area of the ties used on the 18 gauge stud walls was 0.14 mm². (for a 600 N/mm. slope). The effective area of the ties used on the 20 gauge stud walls was 0.10 mm². (for a 420 N/mm. slope). Figures 5.11 and 5.12 show the deflections generated by the analysis

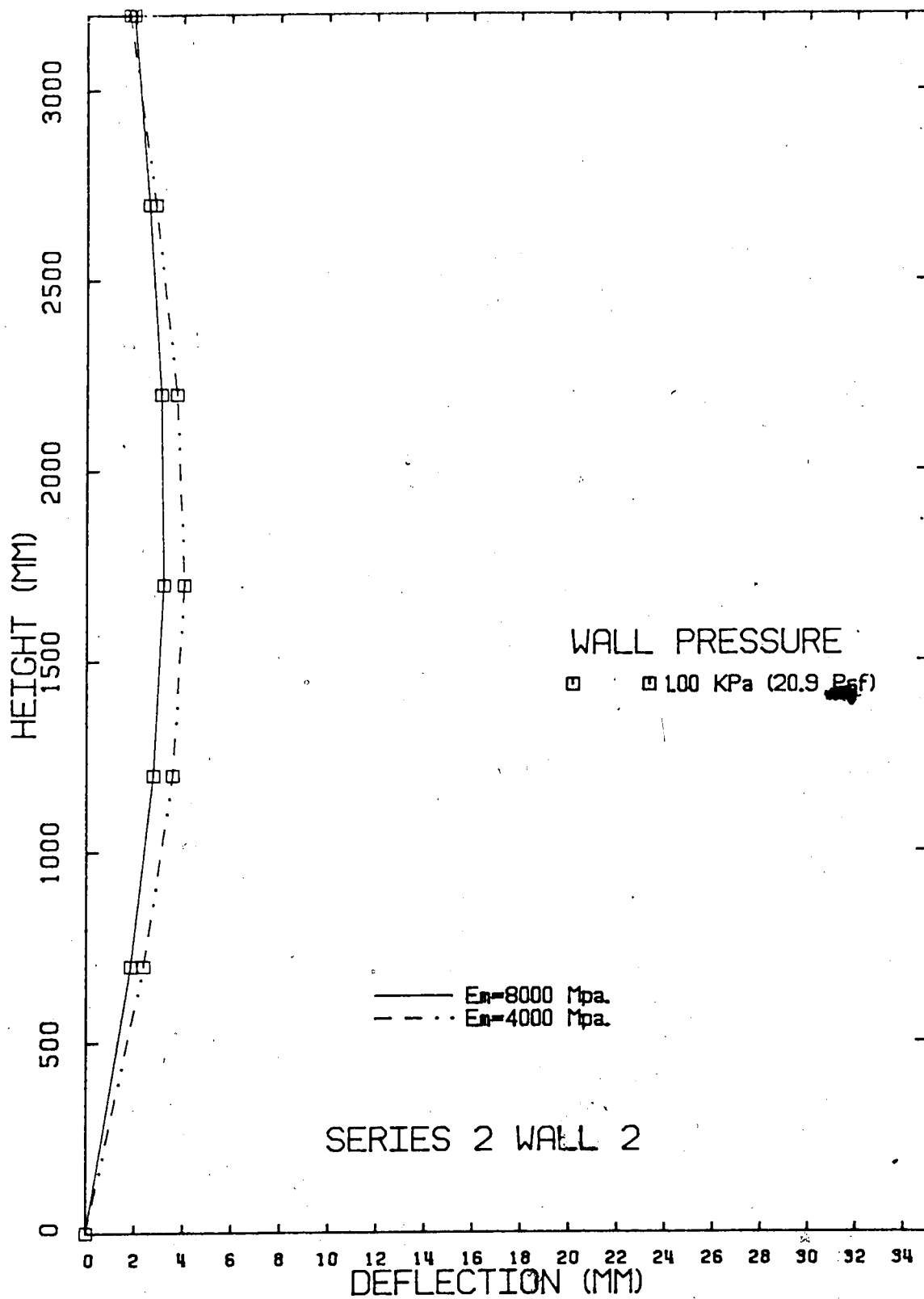


Figure 5.9 A Comparison of Brick Veneer Deflections

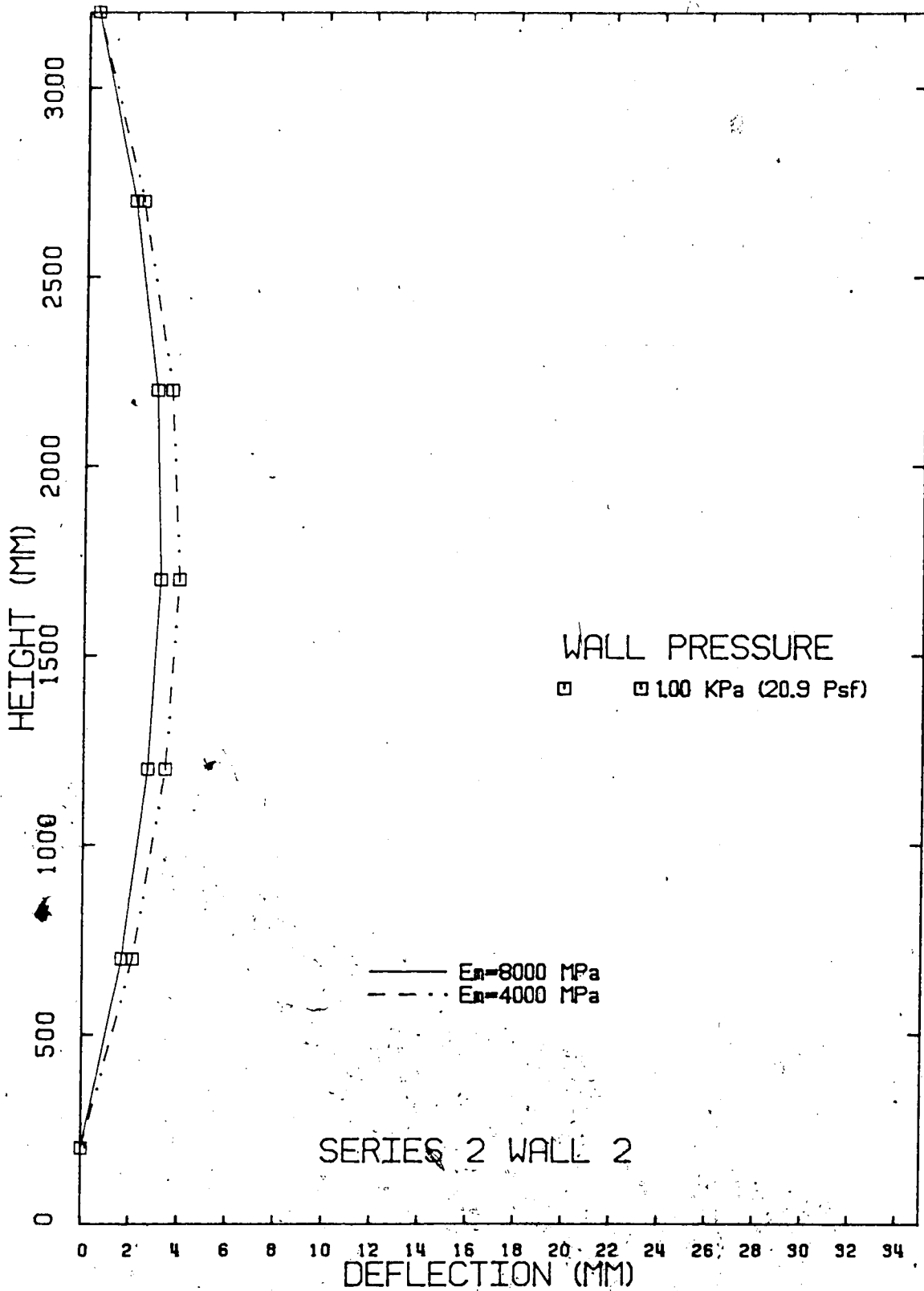


Figure 5.10 A Comparison of Stud Wall Deflections

at a load of 1.00 KPa. (20.9 psf.) for Wall No.2 of Series No.2 with different effective areas. As was the case with the Modulus of Elasticity of the brick veneer, doubling the effective area of the ties did not significantly affect the deflections of the brick veneer or the steel stud backing wall. The 150 mm., 20 gauge studs were affected by a change in the effective area of the ties to a greater degree than the 90 mm., 18 gauge studs but over the possible range of tie areas the effect was still not considered to be significant.

For the analysis the following maximum loads were used; 700 N. for the 22 gauge studs, 1100 N. for the "T" ties, and 1900 N. for the "V" ties.

The value of the moment of inertia used for the analysis was obtained from the backing wall tests, for the 90 mm., 18 gauge studs; and from measurements, for the 150 mm., 20 gauge studs. The 90 mm. studs were assumed to have a moment of inertia of $3.44 \times 10^5 \text{ mm}^4$. and the 150 mm. studs were assumed to have a moment of inertia of $7.2 \times 10^5 \text{ mm}^4$.

Wall No.1 of Series No.1, Wall No.2 of Series No.2, Wall No.2 of Series No.3, Wall No.4 of Series No.4 were analysed and the results of the analysis were plotted against the test results. These plots appear as Figures B-33 to B-40 in Appendix B. The figures show that the analysis models the behaviour of the walls reasonably well up to the cracking load of the brick veneer. After the brick veneer cracks, the analytical model is no longer valid.

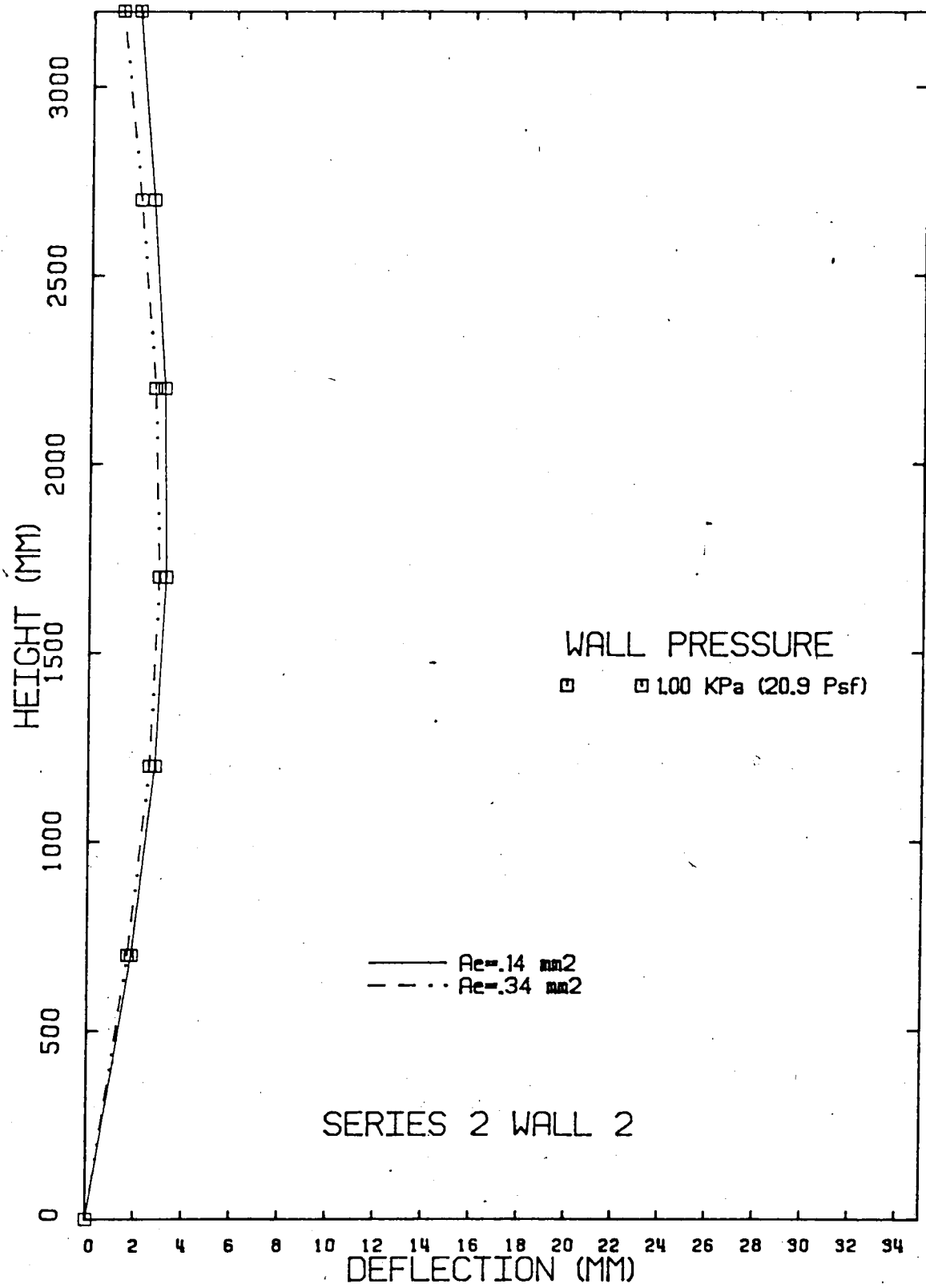


Figure 5.11 A Comparison of Brick Veneer Deflections

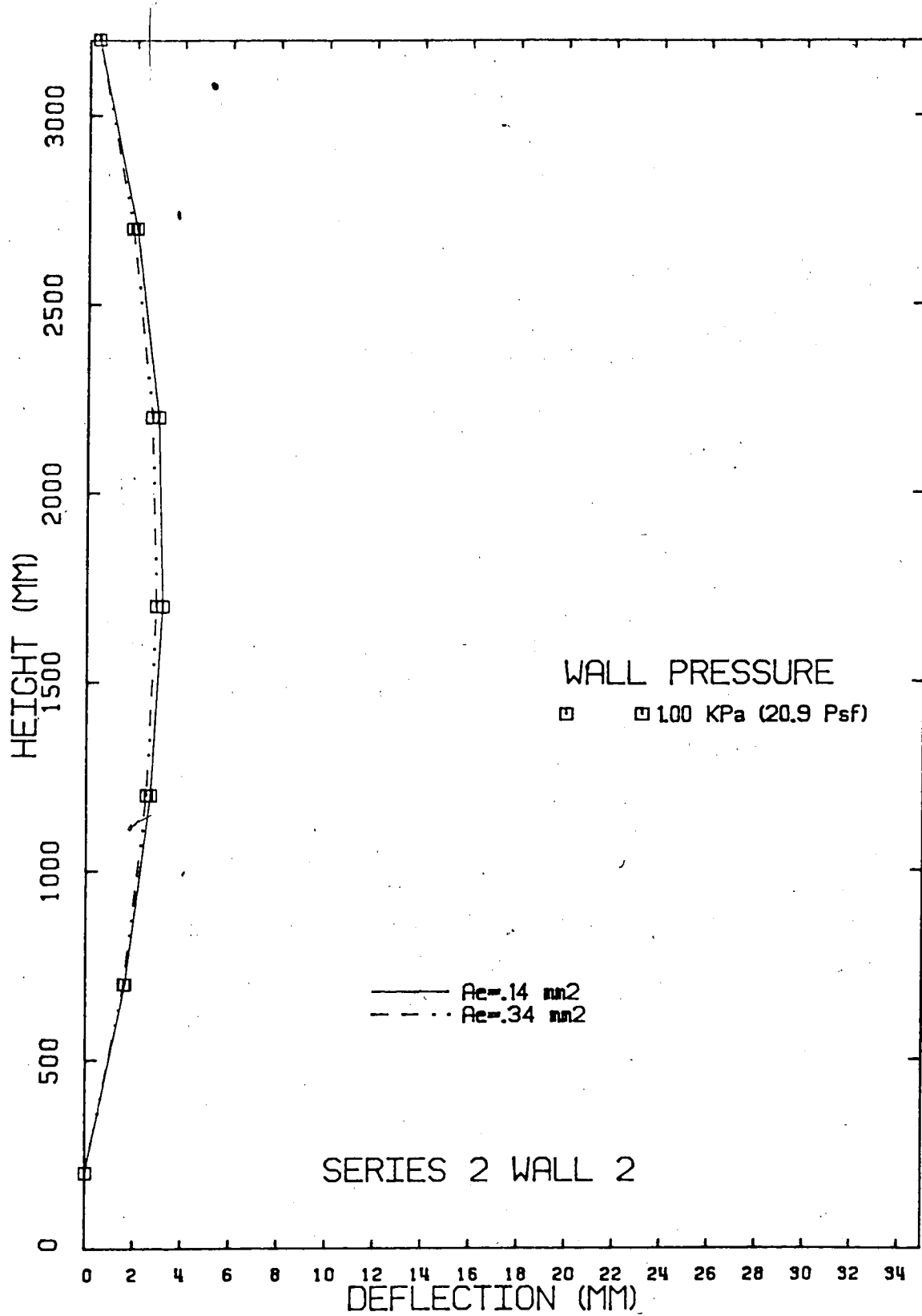


Figure 5.12 A Comparison of Stud Wall Deflections

The maximum error between the analysis and the test results occurs on the deflection of the brick veneer of Wall No.4, Series No.4. The analysis overestimated the deflection of the brick veneer by 30 percent. All other analyses predicted the behaviour of the walls to a greater accuracy than for Wall No.4 of Series No.4.

For the walls using tie pattern B, the analysis indicated that the exterior stud line dominated the load deflection behaviour of the wall specimens. For the walls using tie pattern A, the analysis indicated that the interior stud line dominated the load deflection behaviour.

Wall No.2 of Series No.2 and Wall No.4 of Series No.4 failed by cracking of the brick veneer. For both these walls, the analysis showed that the moment at the crack location was within 10 percent of the maximum moment veneer moment. The moment at the crack was 0.40 KN.m. for Wall No.2 and 0.144 KN.m. for Wall No.4. A maximum tensile stress at the crack was calculated by taking the difference between the maximum flexural stress and the compressive stress due to the weight of the brick above the crack. Wall No.2 of Series No.2 cracked at a calculated tensile stress of 1.06 MPa.. This value is within 13 percent of the Modulus of Rupture of the brick prism cut from this wall (0.92 MPa.). Wall No.4 of Series No.4 cracked at a calculated tensile stress of 0.40 MPa., which is within 24 percent of the Modulus of Rupture of the brick prism cut from this wall (.51 MPa.).

A direct stiffness analysis using the model outlined in Section 5.4 can be used to predict the load deflection behaviour of brick veneer and steel stud curtain walls with a reasonable degree of accuracy. This analysis can also indicate the mode and load of wall failure.

5.7 Evaluation of Current Design Procedures

Chapter 2 of this report outlined the currently accepted procedures for the design of brick veneer and steel stud curtain walls. This section discusses the adequacy of these methods.

The design of brick veneer and steel stud curtain walls using methods which ignore the brick veneer and simply design the steel studs to resist a uniformly distributed wind load can result in unsafe wall designs. These methods ignore three important factors in the behaviour of the curtain walls; the increased load at the top of the stud due to the action of the brick veneer, the interaction of the tie and stud and the behaviour of the brick veneer. The brick veneer is assumed to follow the deflected shape of the steel stud backing. Results of the full sized wall tests show that this assumption is not true.

Another inadequacy of these design methods is the maximum stud deflection limit of $L/360$. This limit was imposed on the stud deflection to preclude cracking of the brick veneer. Most of the wall specimens, in the present investigation, cracked at maximum stud deflections of $L/500$

to $L/750$. Therefore, the deflections of the steel studs should be limited to a value below $L/1400$ to provide an adequate factor of safety for curtain walls of the height used in this investigation.

Current design methods have resulted in walls being constructed that perform adequately in the field. However, applying the same design procedures to curtain walls which are of a greater height than usual and/or are subjected to larger wind loads, quickly illustrates the inadequacy of this method. The average factor of safety for the walls designed for a load of 1.21 KPa. was 1.46 and the average factor of safety for the walls designed for a load of 2.70 KPa. was 0.75. Both of these factors of safety are far too low.

The 400 mm. by 600 mm. maximum tie spacing recommended by 'CAN3-A37-M84' assumes equal loading of the each of the ties. As mentioned previously, the action of the brick veneer loads the top portion of the structural backing far more than the lower portion. Thus, the ties in the upper region of the wall are heavily loaded and consequently will buckle before the others. The arrangement of the ties should compensate for this extra loading. Using tie pattern C would accomplish the reduction of the tributary area of the more heavily loaded top ties.

The performance of the 22 and 24 gauge corrugated ties, illustrates the need for a minimum thickness of 22 gauge for corrugated ties, arranged in tie pattern C, for curtain

walls with a cavity (gap) of 50 mm.. The maximum tie spacing of 600 mm. by 400 mm. of appears to be adequate if tie pattern C is used.

When tie and wall section details are of a non-standard nature, the performance of the tie and stud junction must be evaluated by load tests. The behaviour of the resulting brick veneer and steel stud backing wall can then be approximated using the models and analysis techniques outlined in this chapter.

6. CONCLUSIONS AND RECOMMENDATIONS

6.1 Conclusions

The experimental investigation evaluated the load deflection behaviour of masonry veneer and steel stud curtain walls. As part of this investigation, the interaction of the metal tie and steel stud and the load deflection behaviour of the stud backing wall were studied. An analytical procedure was developed to model the behaviour of this wall system. Finally, the adequacy of the currently accepted design methods were evaluated.

The results of this investigation lead to the following conclusions:

1. The effective axial stiffness of the metal ties depends on the interaction of the tie, steel stud and gyproc sheathing. The open section of the stud causes the flange and web of the steel stud to act as a cantilevered frame.
2. Important factors in the load deflection behaviour of the tie and stud junction are: the location of the tie in relation to the web of stud, the type of stud, the restraint provided by the gyproc sheathings, and the magnitude of the stress applied to the gyproc by the tie contact.
3. The type of tie has only a minor effect on the stiffness of the tie and stud junction. Laterally stiff ties have stiffer junctions than laterally weak ties.

4. The results of the tie tests indicate that a difference in the elevation of the ends of the corrugated ties does not significantly affect the load deflection behaviour of the tie and stud junction.
5. At low load levels, there is little difference in the load deflection behaviour of the full sized brick veneer and steel stud walls with changes in the tie type.
6. The primary effect of tie type on full sized wall behaviour is on the mode of failure of the wall. If the maximum tie load exceeds the buckling load of the tie before the brick veneer can crack, the wall will fail by a sequential buckling of the ties.
7. Tie arrangement can dramatically affect the behaviour of brick veneer and steel stud curtain walls. The arrangement governs the load on the ties and, thus the mode of wall failure.
8. The present limits on tie spacing do not recognize the unequal loading of the ties due to the action of the brick veneer.
9. There is a significant deflection of the support track and stud connection under service level loading. The lighter the gauge of track used, the greater the significance of this track and stud deflection.
10. There is no significant composite action between the steel studs and the gyproc sheathing.
11. The stud type affects the load deflection behaviour of brick veneer and the steel stud curtain walls. However,

an increase in the moment of inertia of the steel stud will not cause a proportional decrease in wall deflections.

12. The application of a direct stiffness analysis modelled the behaviour of the brick veneer and steel stud wall specimens with a reasonable degree of accuracy. The stiffness of the tie and stud junction, and the stud and track junction were successfully modelled by a semi-empirical "effective area" approach.
13. In current design procedures, the steel studs are designed to resist the total uniformly distributed wind load while limiting the maximum stud deflection to a value of $L/360$. The 3000 mm. high test specimens, thus designed, performed unsatisfactorily. The 90 mm. stud wall specimens had an average safety factor of 1.46, and the 150 mm. stud wall specimens had an average safety factor of 0.75. A stud deflection limit of $L/360$ also proved inadequate as most of the brick veneer cracked at maximum stud deflections between $L/500$ and $L/750$.

6.2 Recommendations

The results of the investigation lead to the following recommendations:

1. The arrangement of the metal ties must compensate for the unequal loading of the ties. For the tie spacing limits of 400 mm. by 600 mm., it is recommended that the ties be arranged so that there is a tie located on each

stud line one half spacing from the top of the wall.

2. Further testing is needed to evaluate the behaviour of the tie and stud junction. In particular, the effects of tie end offset and sheathing deformation on the junction's load deflection behaviour requires further investigation.
3. An experimental evaluation of the effect of different exterior sheathings on the load deflection behaviour of the steel stud backing wall is also required.
4. Further testing is needed to evaluate the influence of wall height and gap on the load deflection behaviour of the brick veneer and steel stud curtain walls. After these investigations, an accurate evaluation and modification of the current design procedures can be performed.

LEAF 122 OMITTED IN PAGE NUMBERING.

References

1. CAN3-A370-M84, "Connectors for Masonry", Canadian Standards Association., Rexdale, Ontario, 1984.
2. CAN3-S304-M78, "Masonry Design and Construction for Buildings", Canadian Standards Association., Rexdale, Ontario, 1984.
3. "Brick Veneer Panel and Curtain Walls", Brick Institute of America Technical Note 28B, Maclean, Virginia, 1980.
4. J. Arumala and R. H. Brown, "Performance Evaluation of Brick Veneer and Steel Stud Backup", Department of Civil Engineering Clemson University, Clemson, South Carolina, 1982
5. M. Hatzinikolas, J. Longworth, J. Warwaruk, "Strength and Behaviour of Metal Ties in 2-Wythe Masonry Walls", Alberta Masonry Institute, Edmonton , Alberta, 1981.
6. CSA Standard A179M, "Mortar and Grout for Unit Masonry", Canadian Standards Association., Rexdale, Ontario, 1976.

APPENDIX A - MATERIAL TESTS

A-1 Masonry Tests

The results of the tests conducted on the mortar cubes and brick prisms are summarized in Table A-1.

All the mortar cubes were made and tested according to CSA Standard A-179 M-76.

Each of the brick prisms was tested under a third point loading. The load deflection curves resulting from this testing are shown in Figures A-1 to A-3. A slope was fitted to the most linear portion of each curve and an Elastic Modulus calculated for each prism.

The Modulus of Rupture for each prism was calculated using the maximum moment at the location of the crack. Included in this calculation was the self weight of the brick.

Five brick units were tested in accordance to CSA Standard CAN3-A82.2-M78. The average compressive failure stress of these brick units was 52.4 MPa., with a standard deviation of 4.6 MPa.. Using the equation outlined in clause 4.3.3.3 of CSA Standard CAN3-S304-M-78, the compressive strength of the brick units is 45.6 MPa.. For this strength of brick and type S mortar, this standard also suggests that a value of 14000 Mpa. be used for the Elastic Modulus of the brick and mortar composite.

A-2 Steel Coupon Tests

Table A-1 Summary of the Masonry Material Tests

MASONRY MATERIAL TESTS						
Series	Wall No.	Mortar Cubes		Prism Tests		
		A. St. (MPa.)	Sdev. (MPa.)	E (MPa.)	M. R. (Mpa.)	
1	1	16.68	1.48	---	---	.254*
1	2	13.35	2.60	---	---	.135*
1	3	15.13	2.39	---	---	.453*
1	4	13.24	3.68	---	---	.430*
2	1	12.36	1.90	---	---	---
2	2	11.79	2.24	670.	---	.410
2	3	11.72	2.04	---	---	---
2	4	9.93	1.92	1730.	---	.910
3	1	12.63	2.95	8367.	---	.905
3	2	9.86	1.95	---	---	---
3	3	11.77	1.05	11495.	---	.998
3	4	8.97	2.55	5125.	---	.891
4	1	10.10	2.71	4200.	---	.830
4	2	7.80	1.40	13049.	---	.910
4	3	8.40	1.70	20460.	---	.590
4	4	10.18	1.79	18740.	---	.509

Note: (1) A. St. is the average maximum compressive stress for the mortar cubes of each wall
 (2) Sdev. is the standard deviation of the cube tests
 (3) M. R. is the Modulus of Rupture
 (4) * denotes the separate prism tests

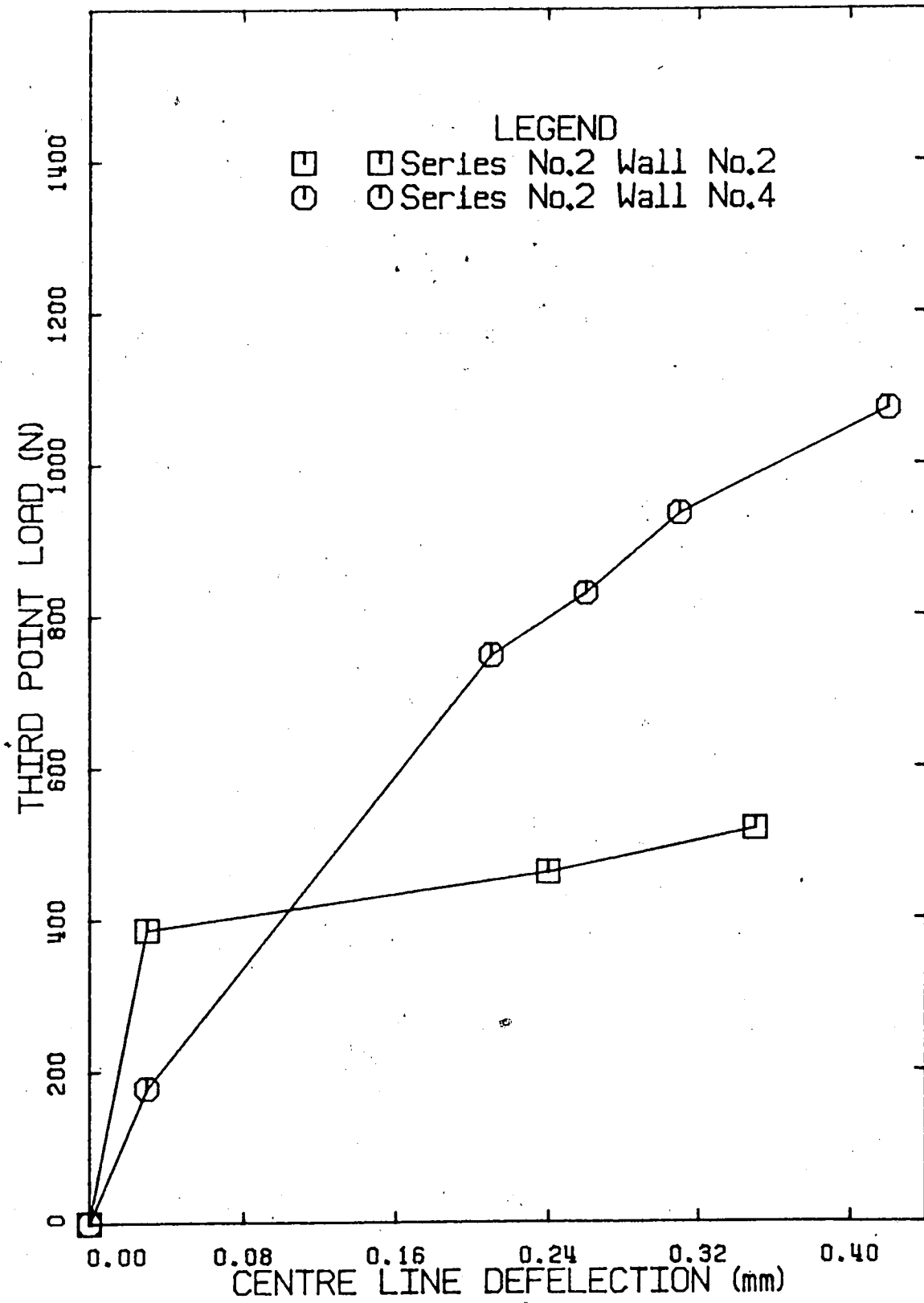


Figure A-1 Brick Prism Deflections - Series No.2

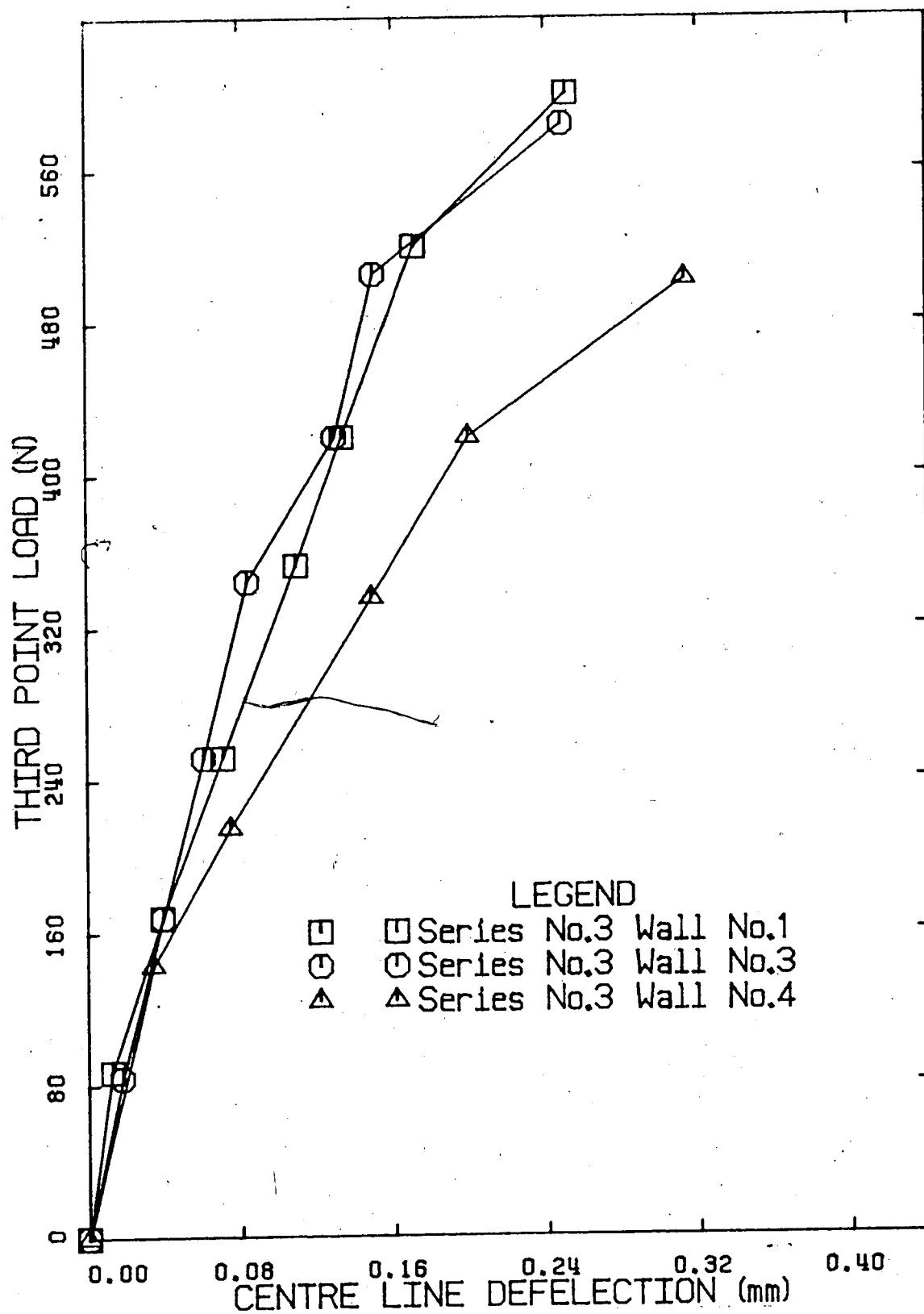


Figure A-2 Brick Prism Deflections - Series No.3

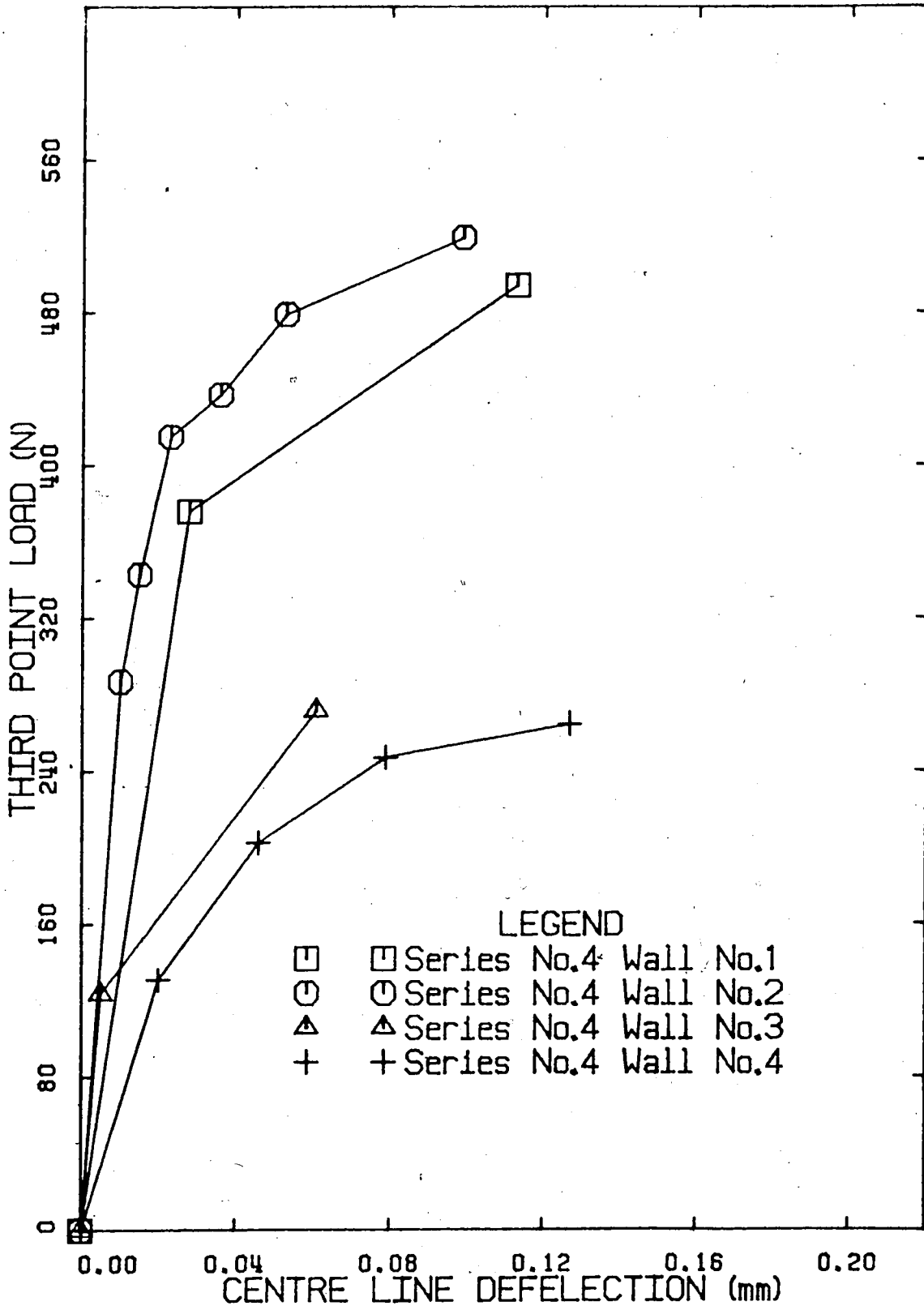


Figure A-3 Brick Prism Deflections - Series No.4

Four tension coupons were cut out of the steel studs, two coupons from the 18 gauge studs and two coupons from the 20 gauge studs. These coupons were tested according to ASTM Standard A370-M77 and the results are plotted in Figure A-4. Both the 18 gauge and 20 gauge steel coupons exhibit an Elastic Modulus of 210500 MPa.. The 20 gauge steel coupons have a yield stress of approximately 325 MPa. and the 18 gauge coupons have a yeild stress of approximately 280 MPa..

A-3 Gyproc Tests

Ten, 12 mm. by 100 mm. by 1000 mm. long, strips of gyproc were tested to obtain a value of Elastic Modulus for this material. Each strip was placed over supports and a weight was hung from the centre of the 780 mm. span. The resulting deflections were measured after the gyproc strip was allowed to creep for 15 seconds. A summary of the test results is presented in Table A-2.

The Elastic Modulus (E) of the gyproc strips was calculated using the elastic beam formula for the maximum deflection of a centrally loaded beam. The average E value obtain from the tests is 2568 MPa. .

Table A-2 Gyproc Tests

GYPROC TEST RESULTS		
Load (N)	C.Defl.(mm)	E (MPa)
11.50	3.89	2075
11.50	4.10	1983
11.50	3.26	2427
11.50	3.23	2488
11.50	2.84	2817
11.50	3.37	2408
11.50	2.83	2799
11.50	2.76	2889
11.50	2.84	2837
11.50	2.69	2950

NOTE: (1) C.Defl. is the centre deflection after 15 sec.

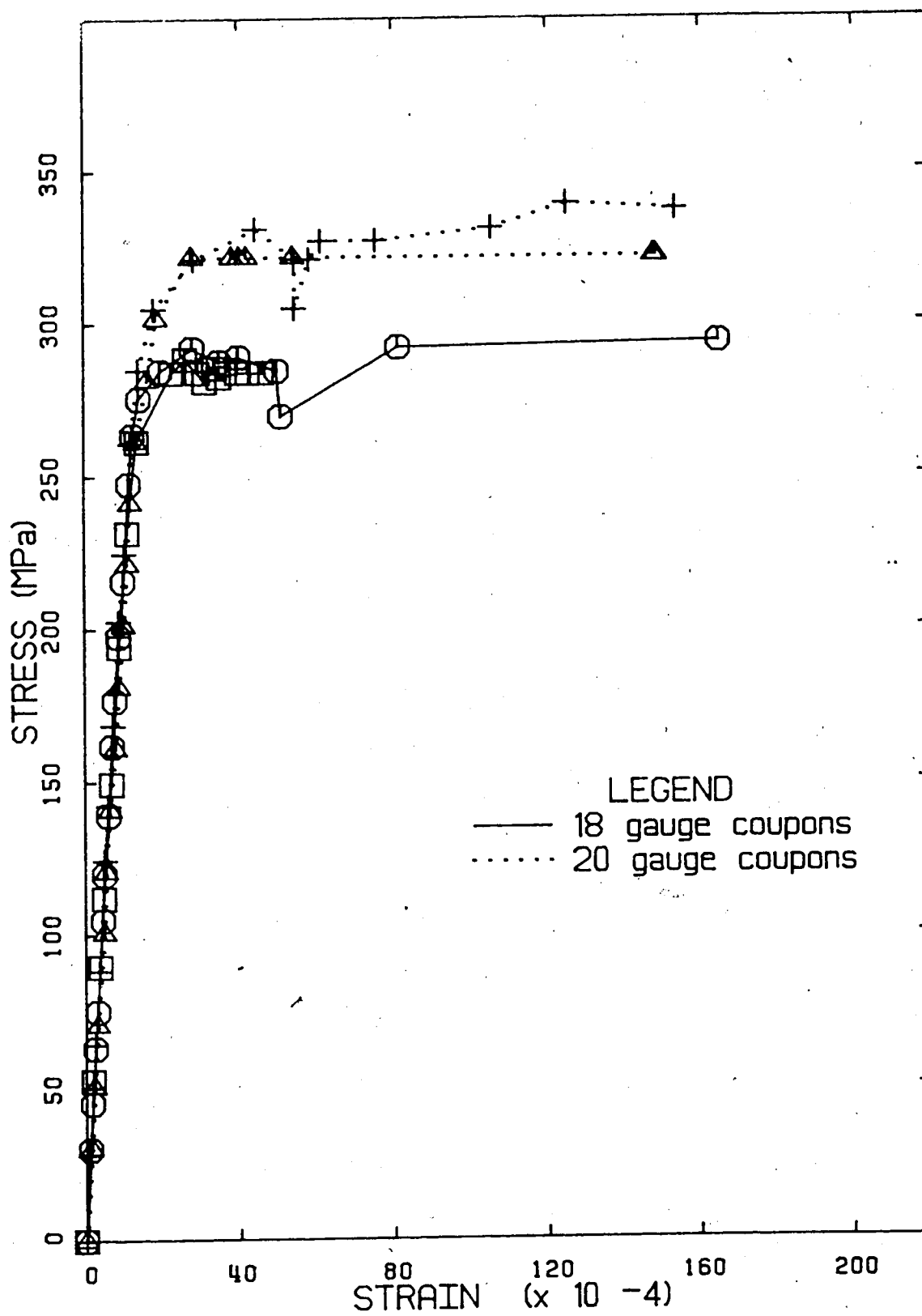


Figure A-4 Steel Tension Coupon Tests

APPENDIX B - LOAD DEFLECTION CURVES

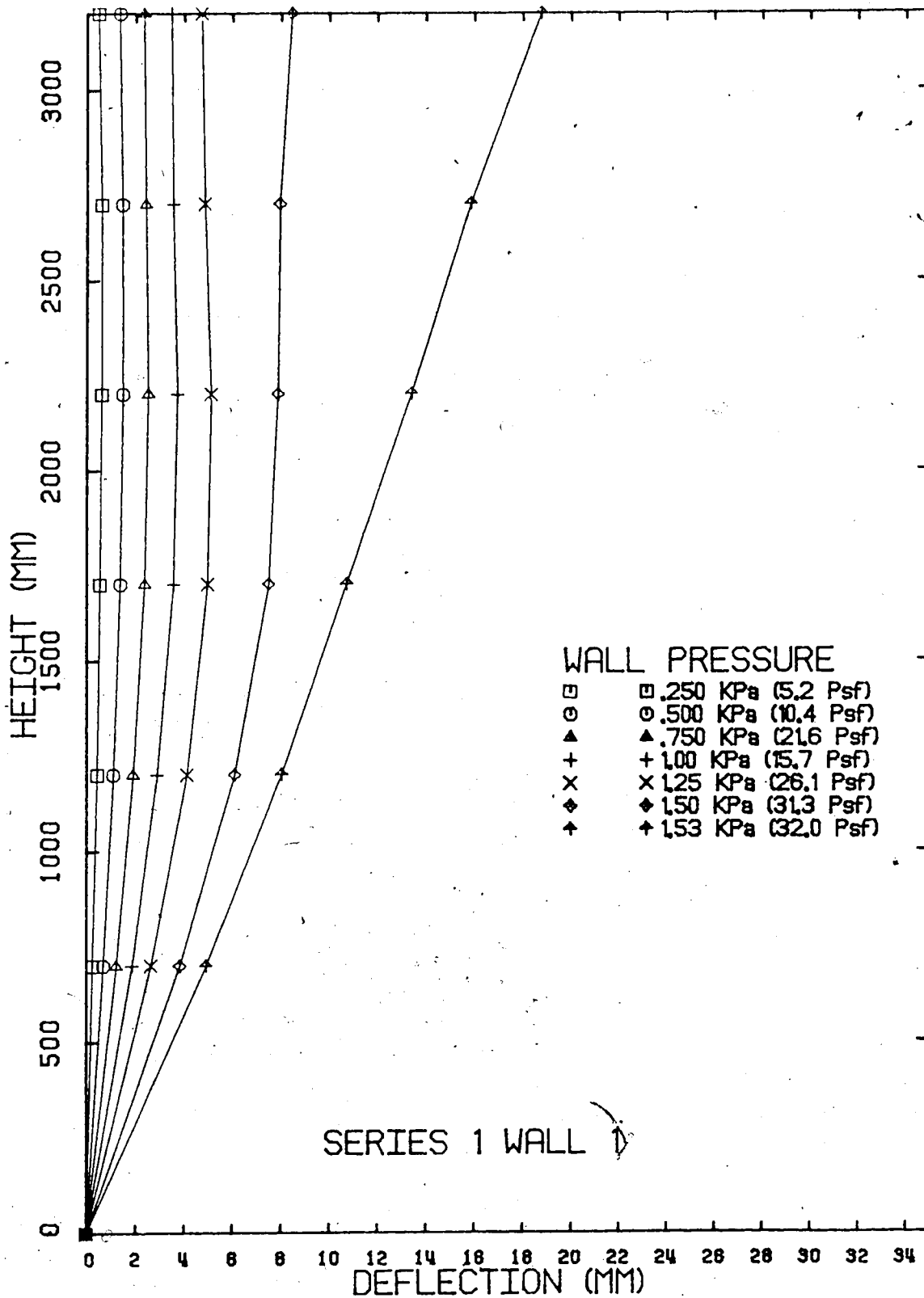


Figure B-1 Brick Veneer Deflections - Series No.1 Wall No.1

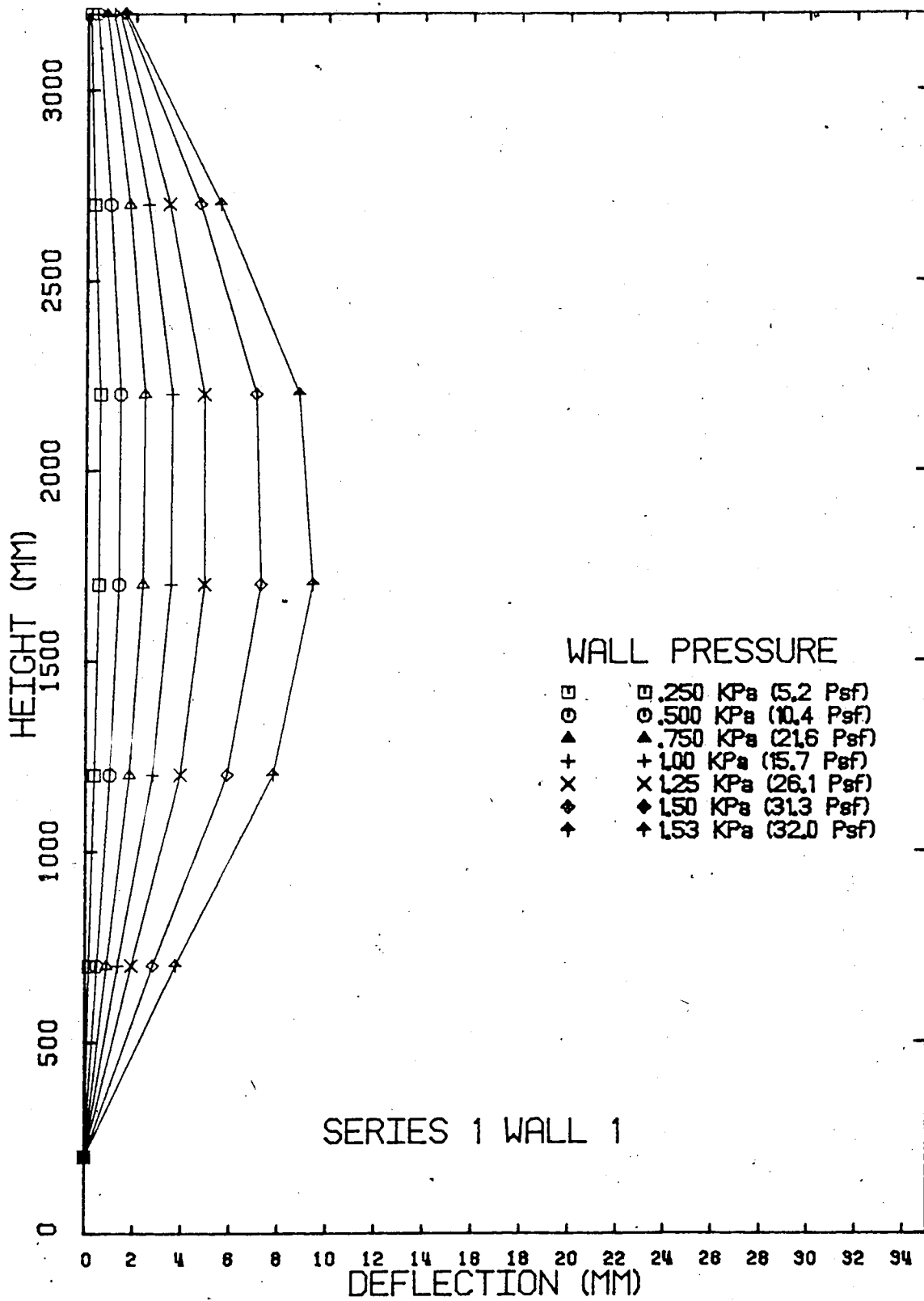


Figure B-2 Stud Wall Deflections - Series No.1 Wall No.1

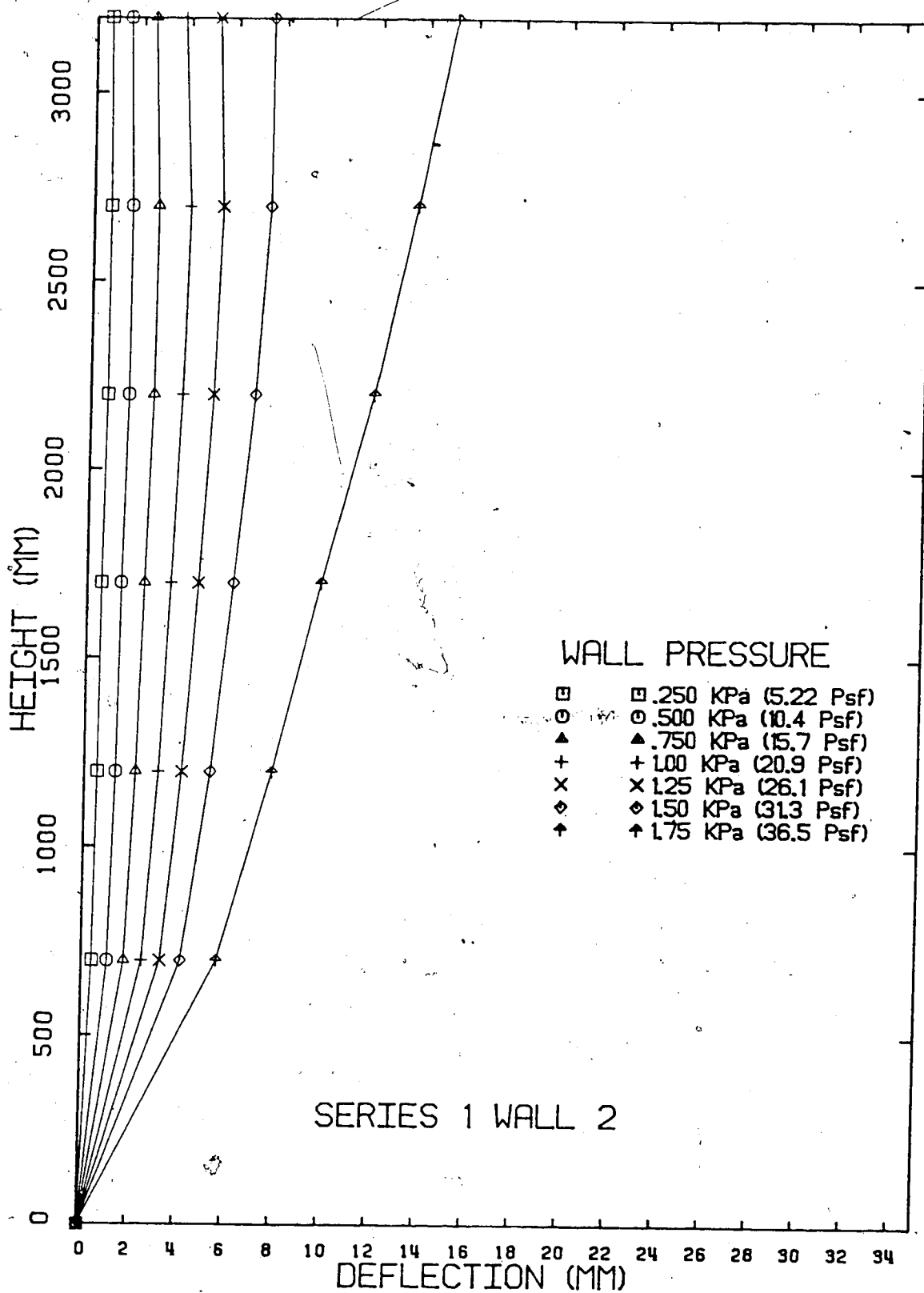


Figure B-3 Brick Veneer Deflections - Series No.1 Wall No.2

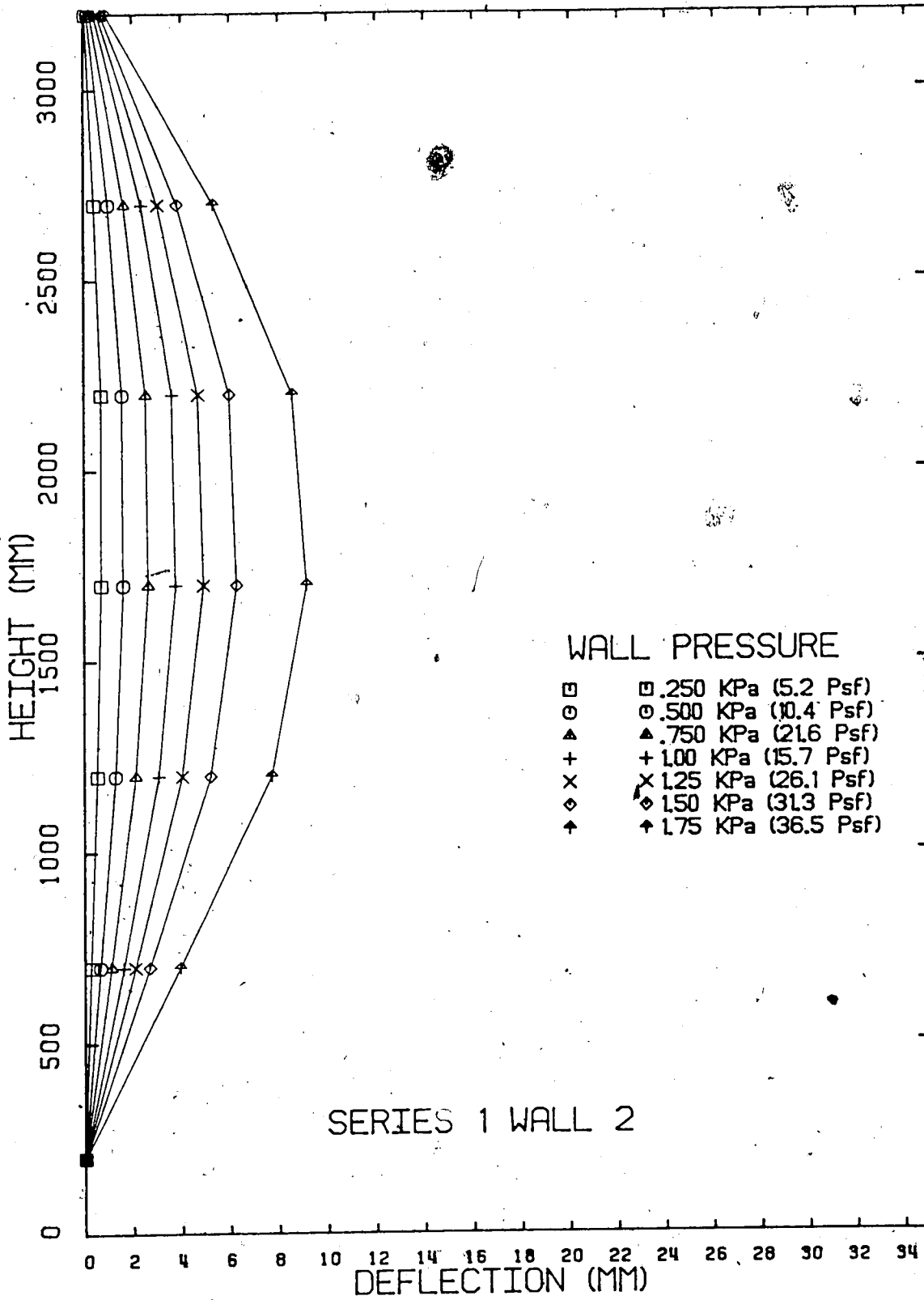


Figure B-4 Stud Wall Deflections - Series No.1 Wall No.2

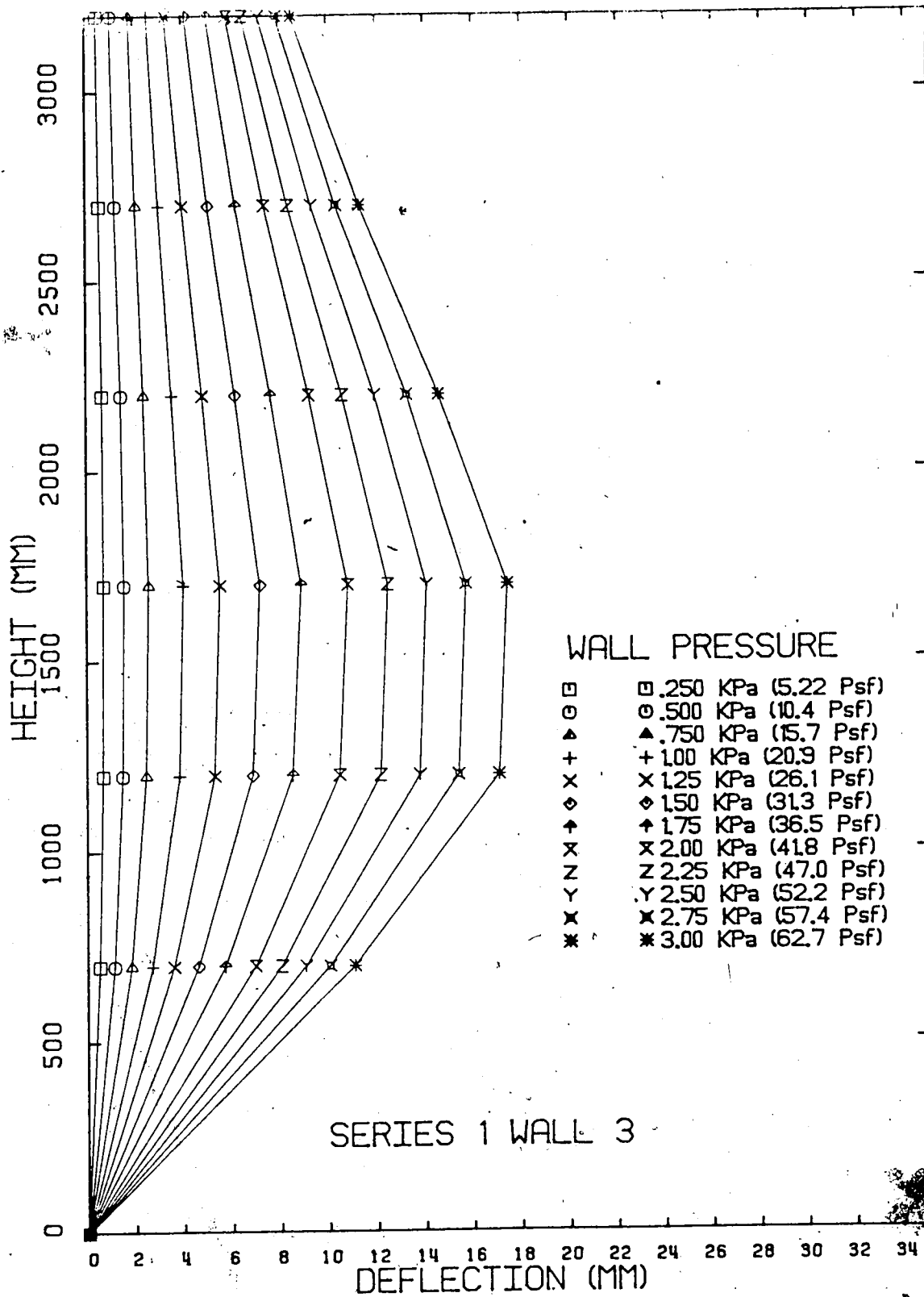


Figure B-5 Brick Veneer Deflections - Series No.1 Wall No.3

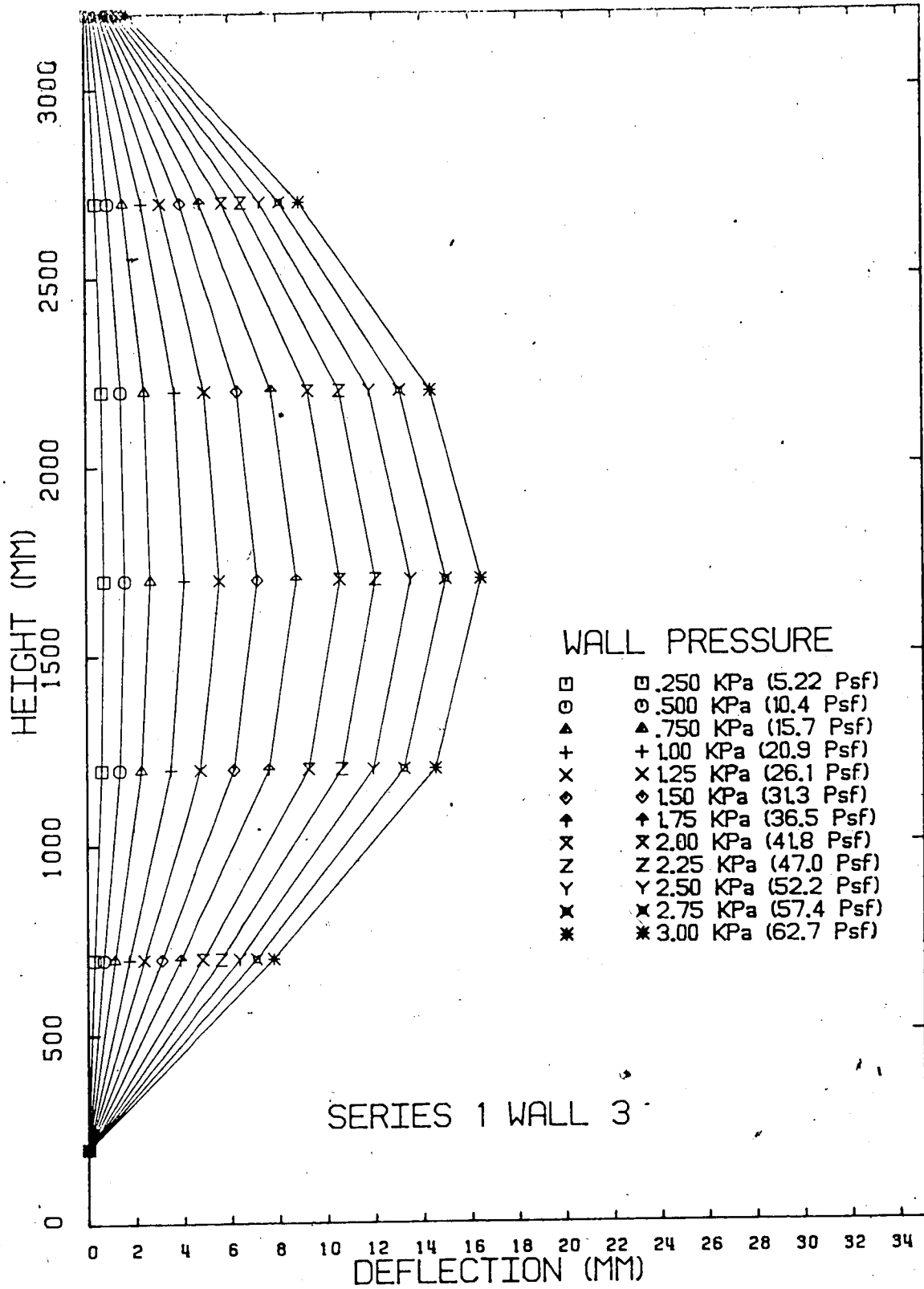


Figure B-6 Stud Wall Deflections - Series No.1, Wall No.3

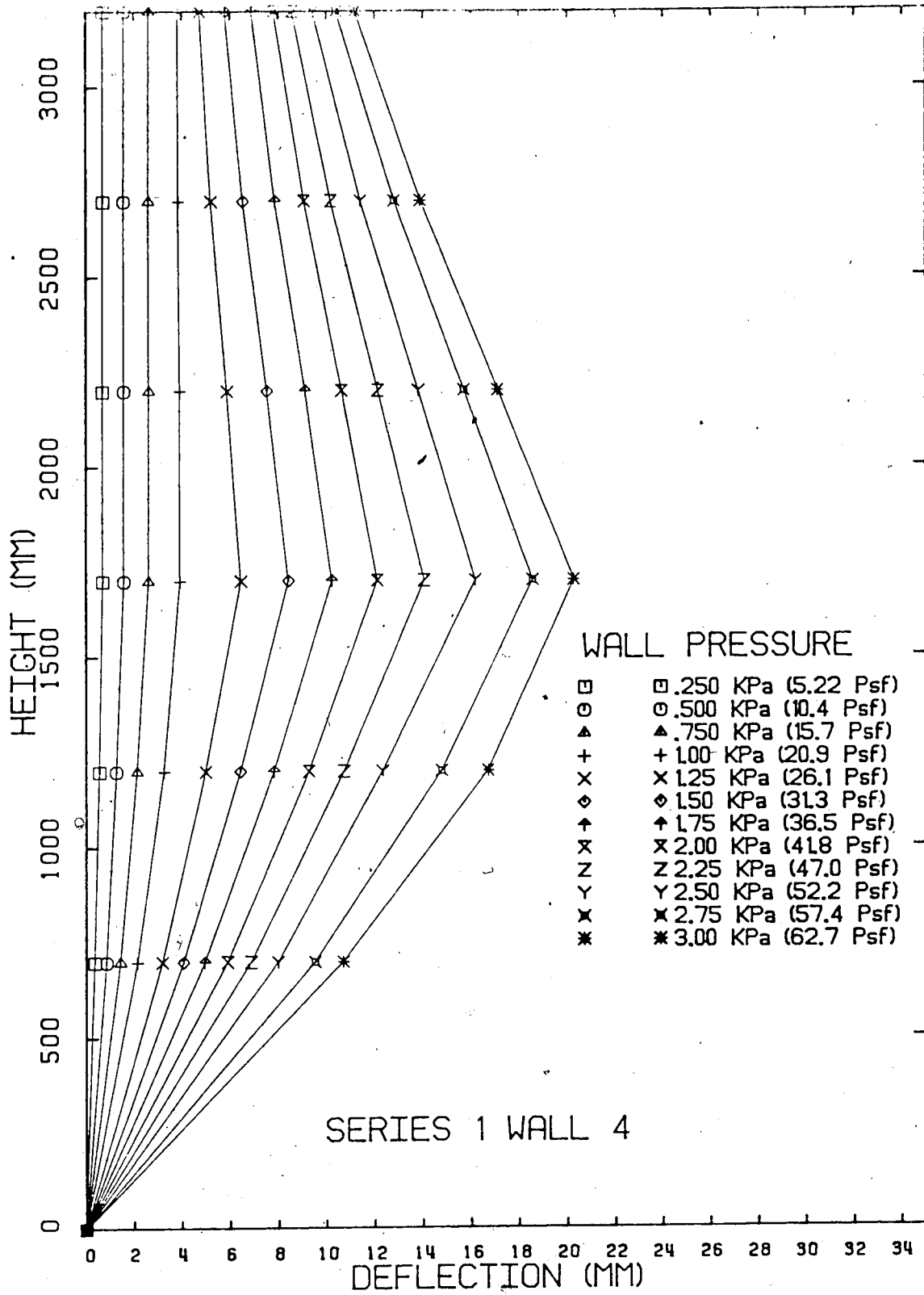


Figure B-7 Brick Veneer Deflections - Series No.1 Wall No.4

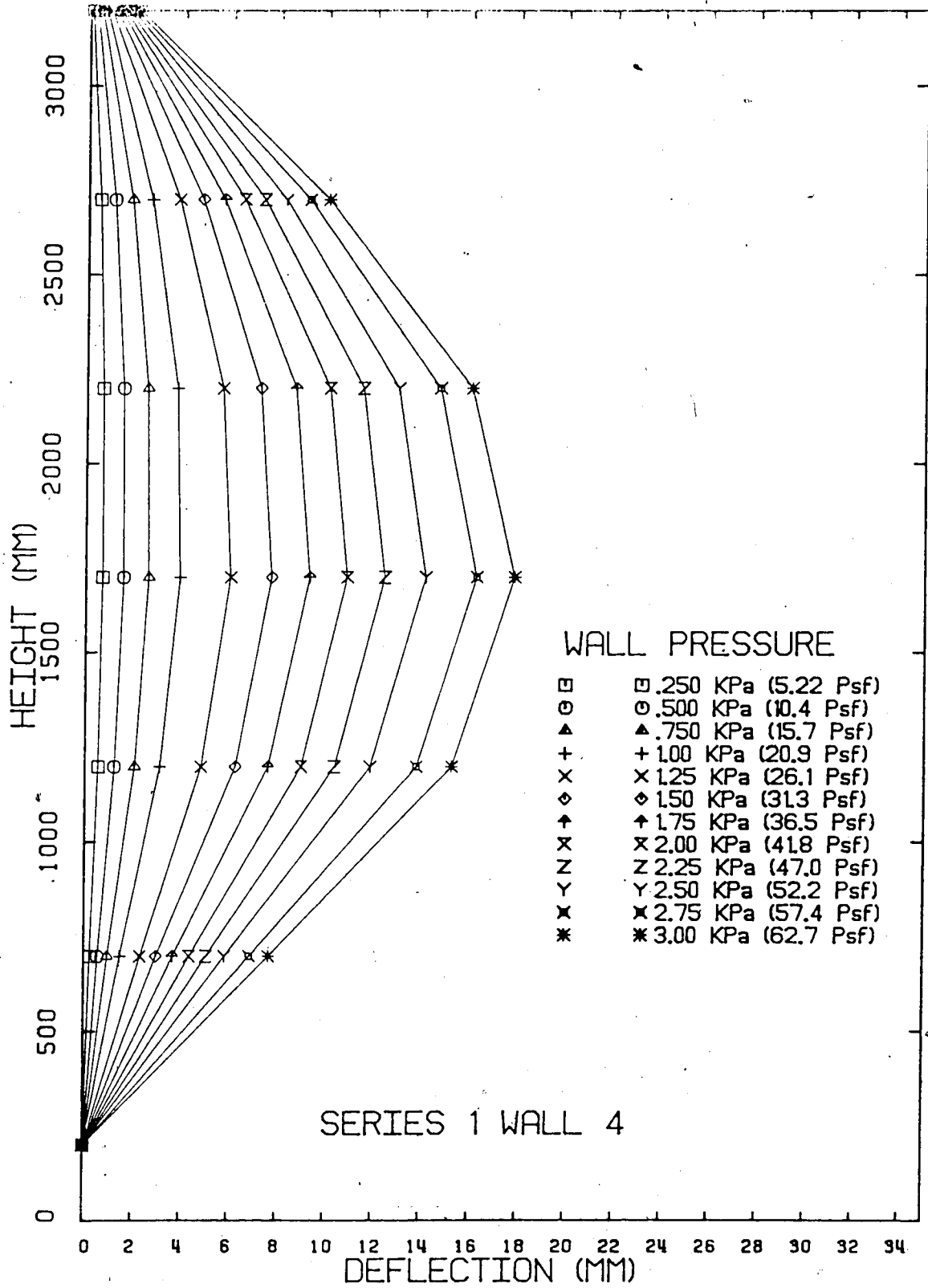


Figure B-8 Stud Wall Deflections - Series No.1 Wall No.4

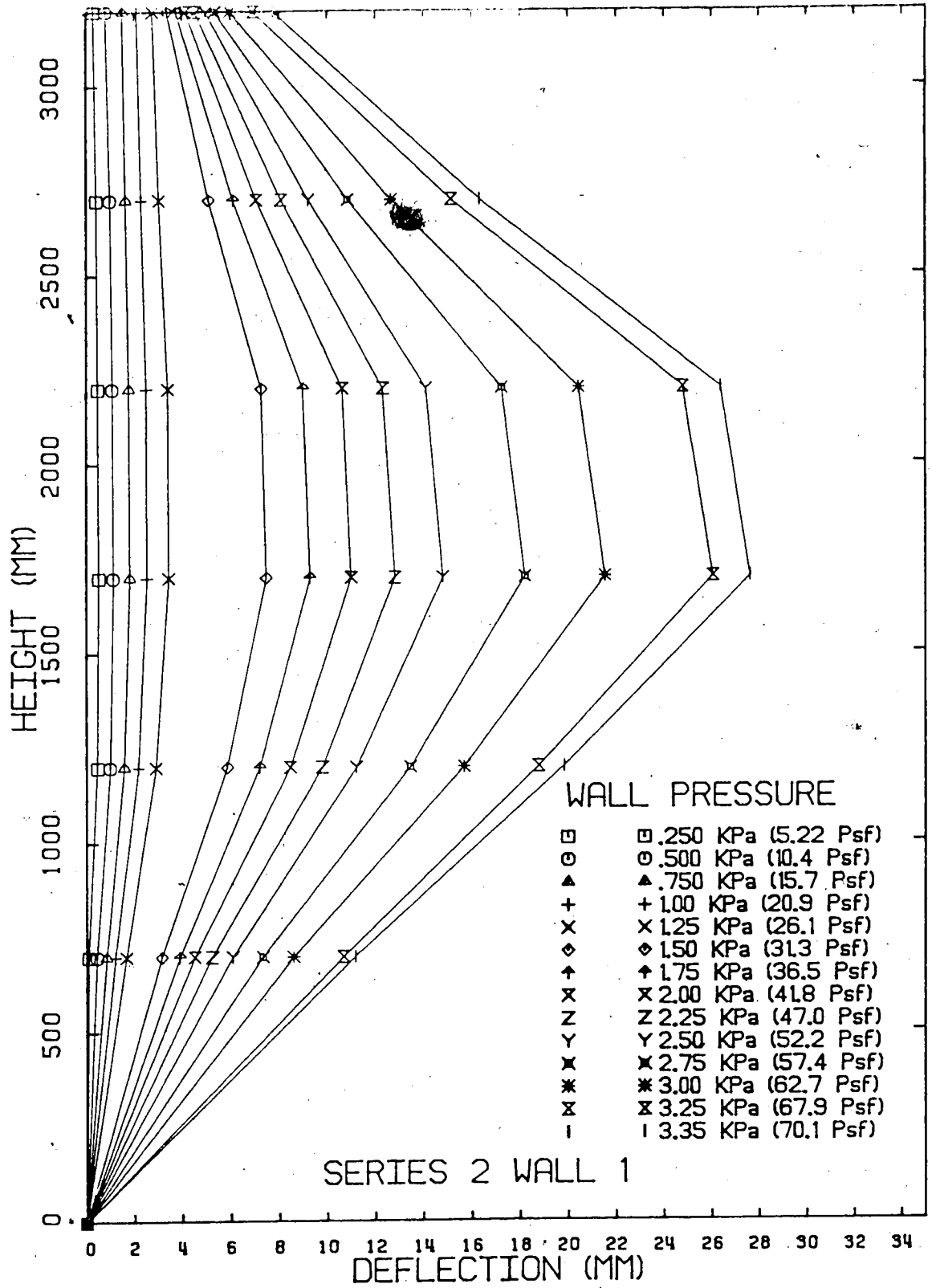


Figure B-9 Brick Veneer Deflections - Series No.2 Wall No.1

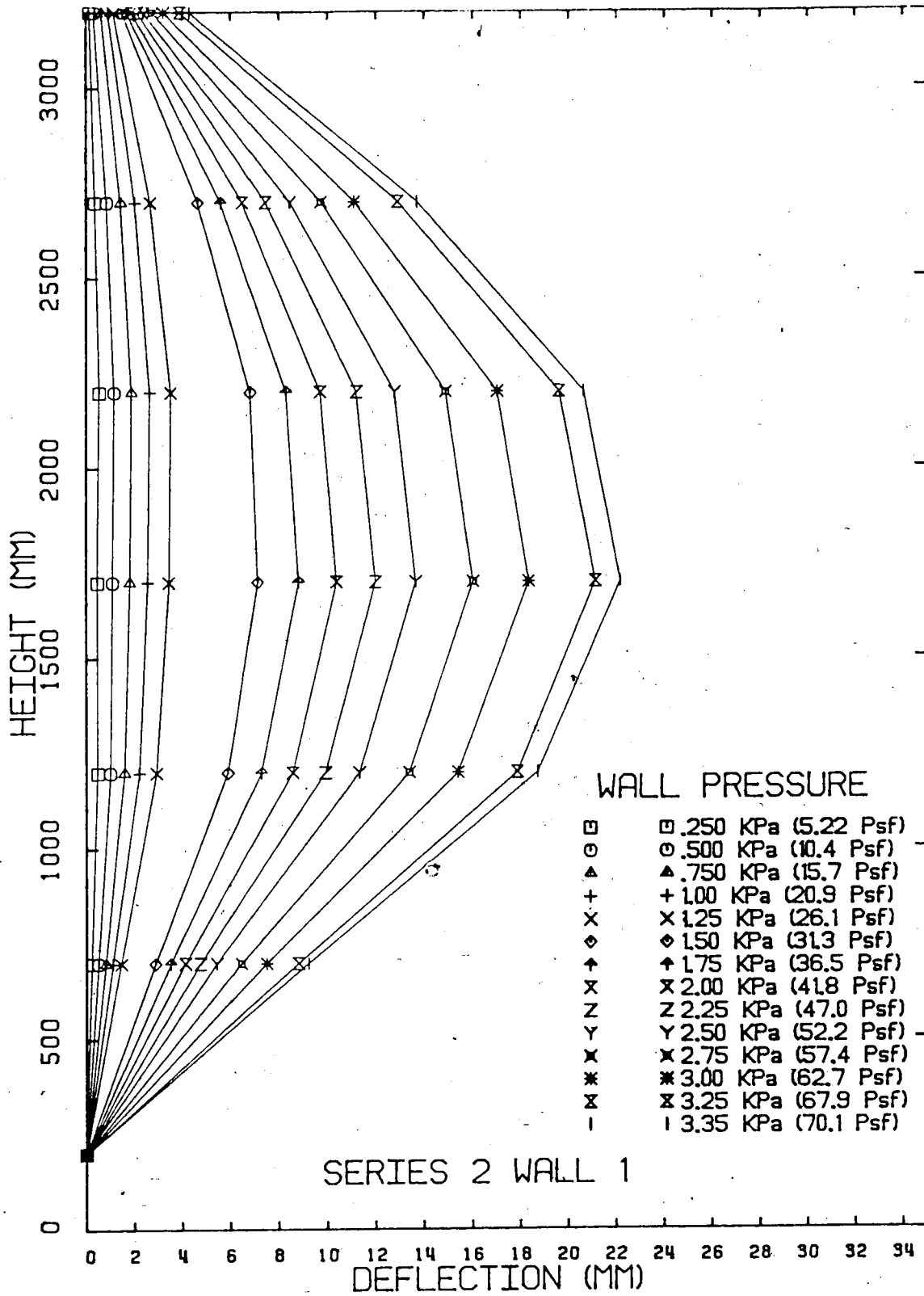


Figure B-10 Stud Wall Deflections - Series No.2 Wall No.1

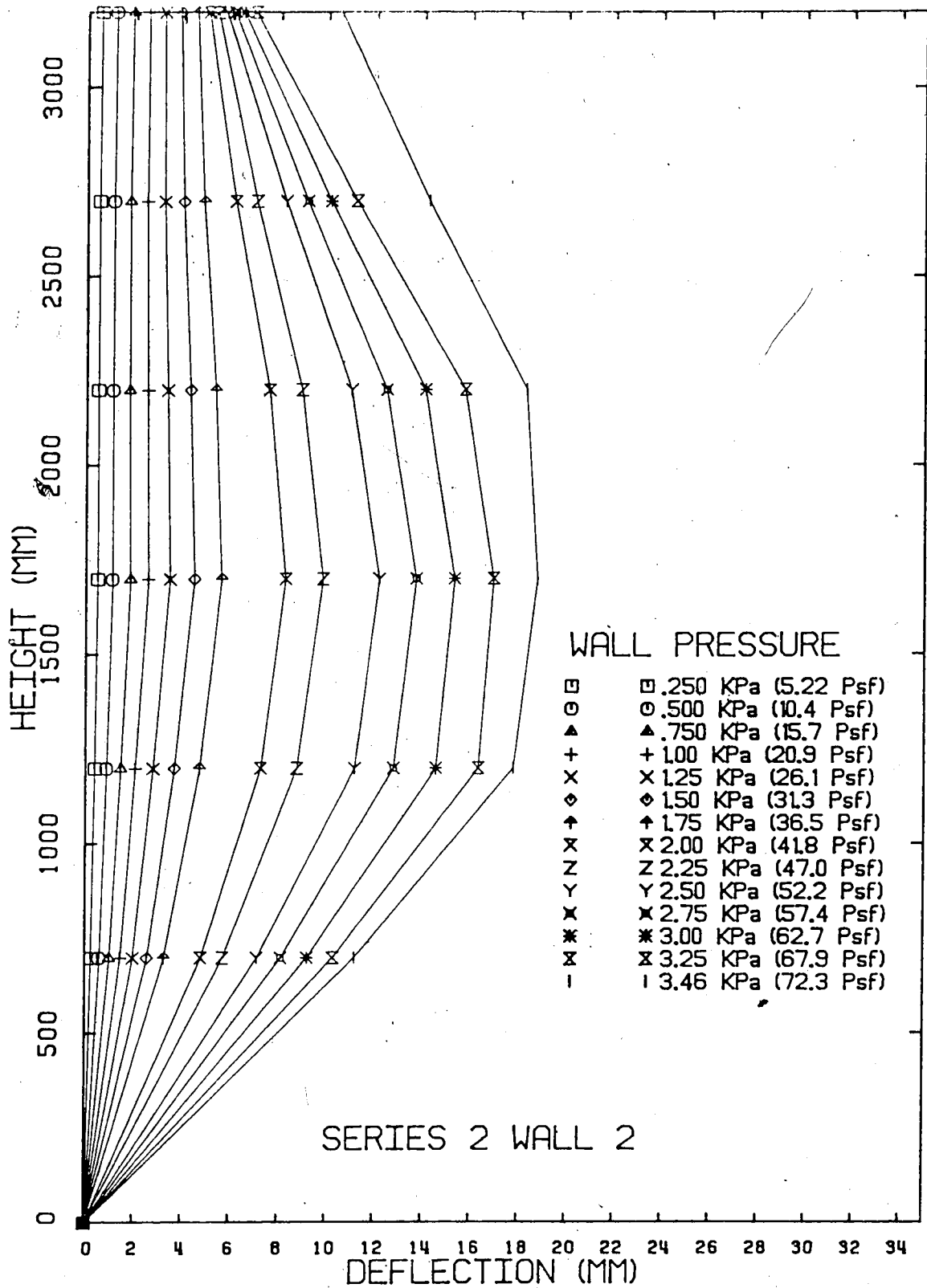


Figure B-11 Brick Veneer Deflections - Series No.2 Wall No.2

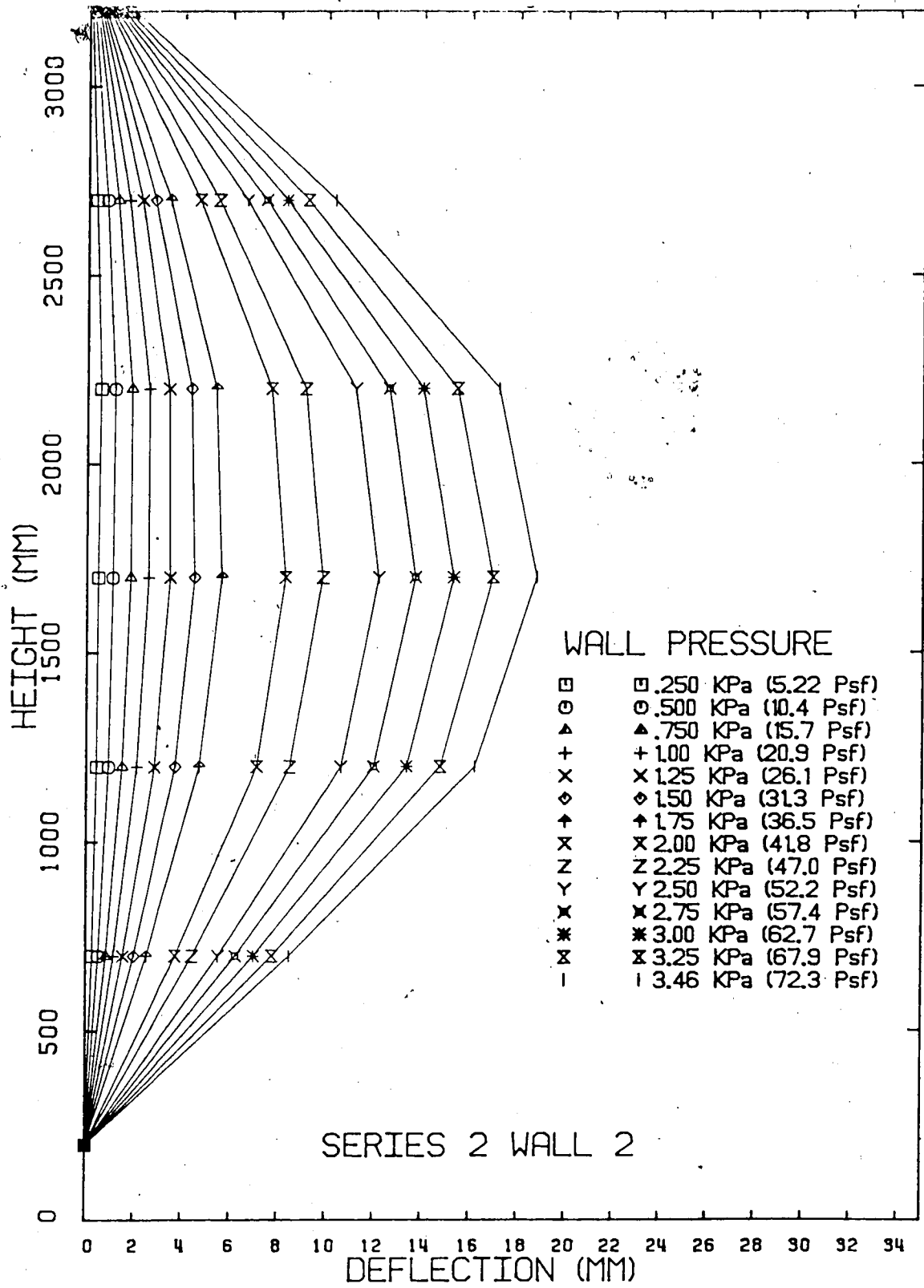


Figure B-12 Stud Wall Deflections - Series No.2 Wall No.2

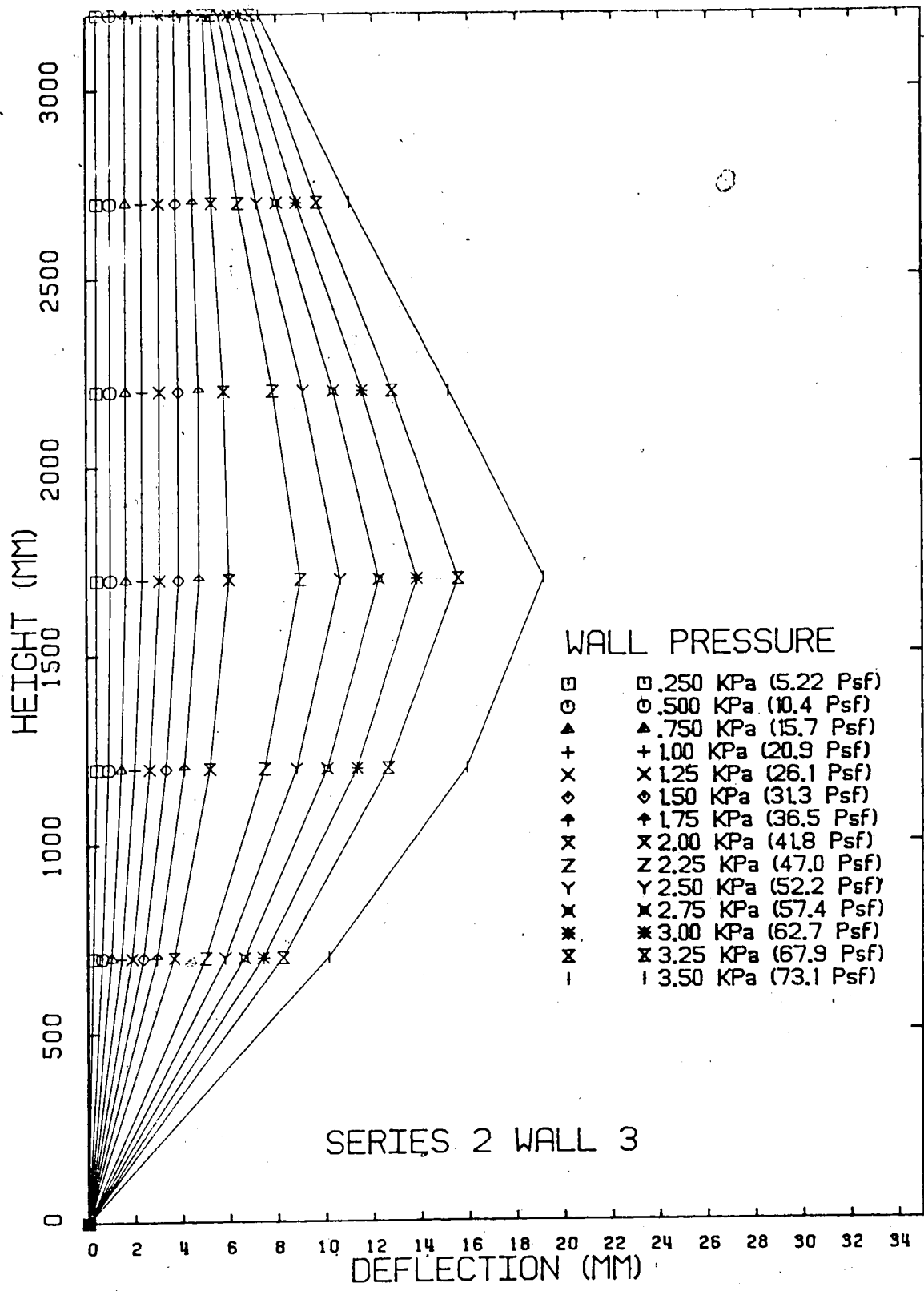


Figure B-13 Brick Veneer Deflections - Series No.2 Wall, No.3

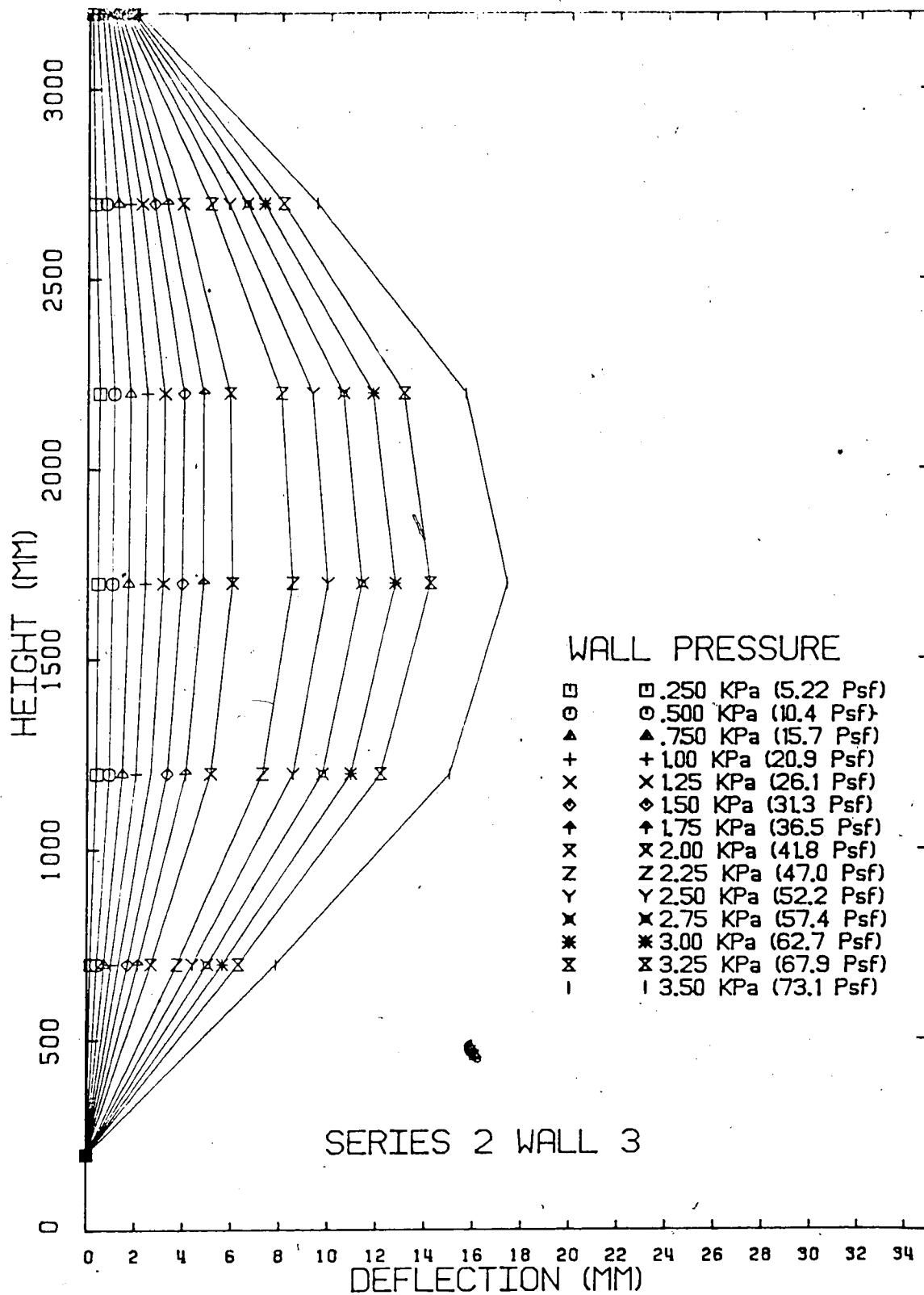


Figure B-14 Stud Wall Deflections - Series No.2 Wall No.3

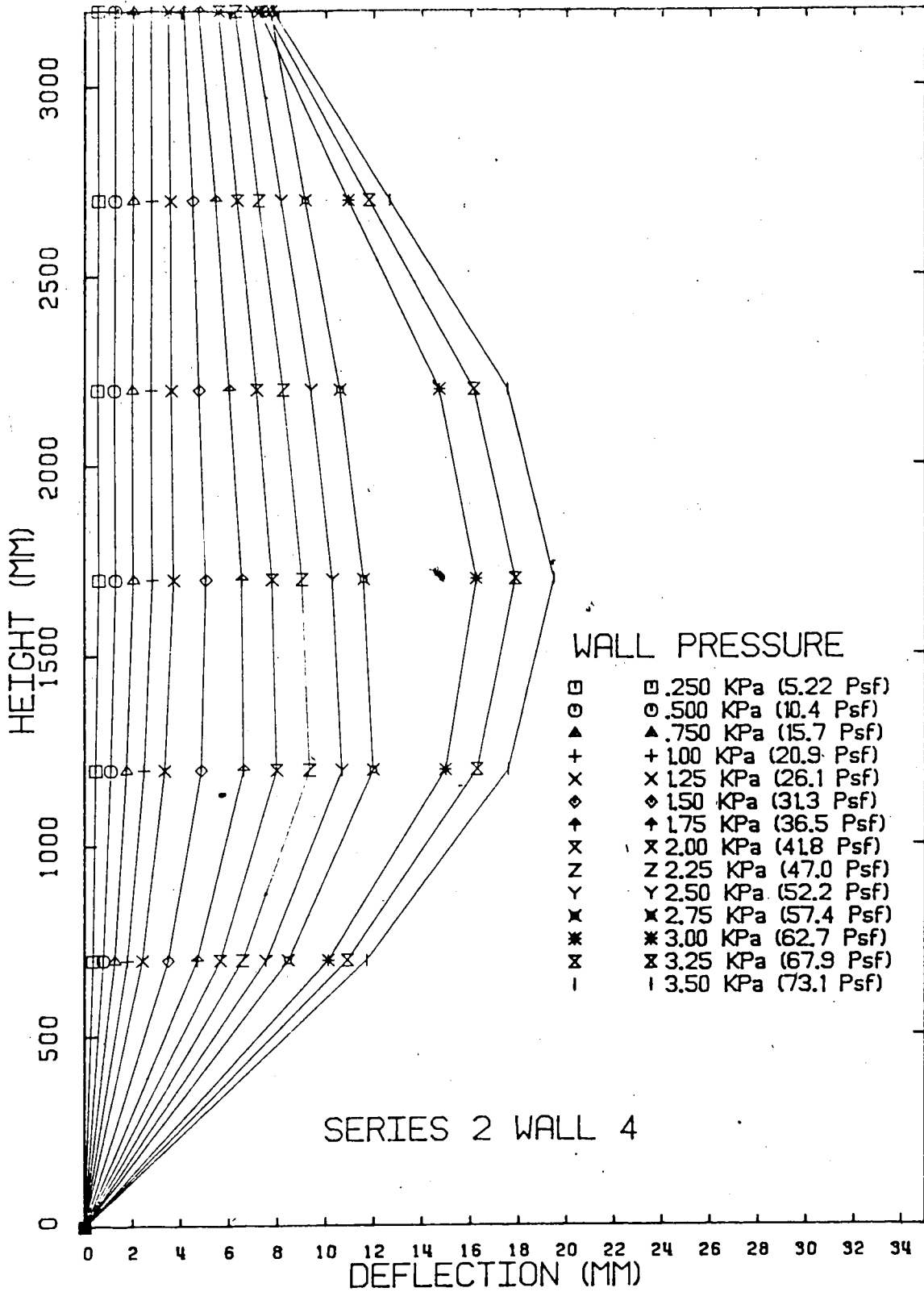


Figure B-15 Brick Veneer Deflections - Series No.2 Wall No.4

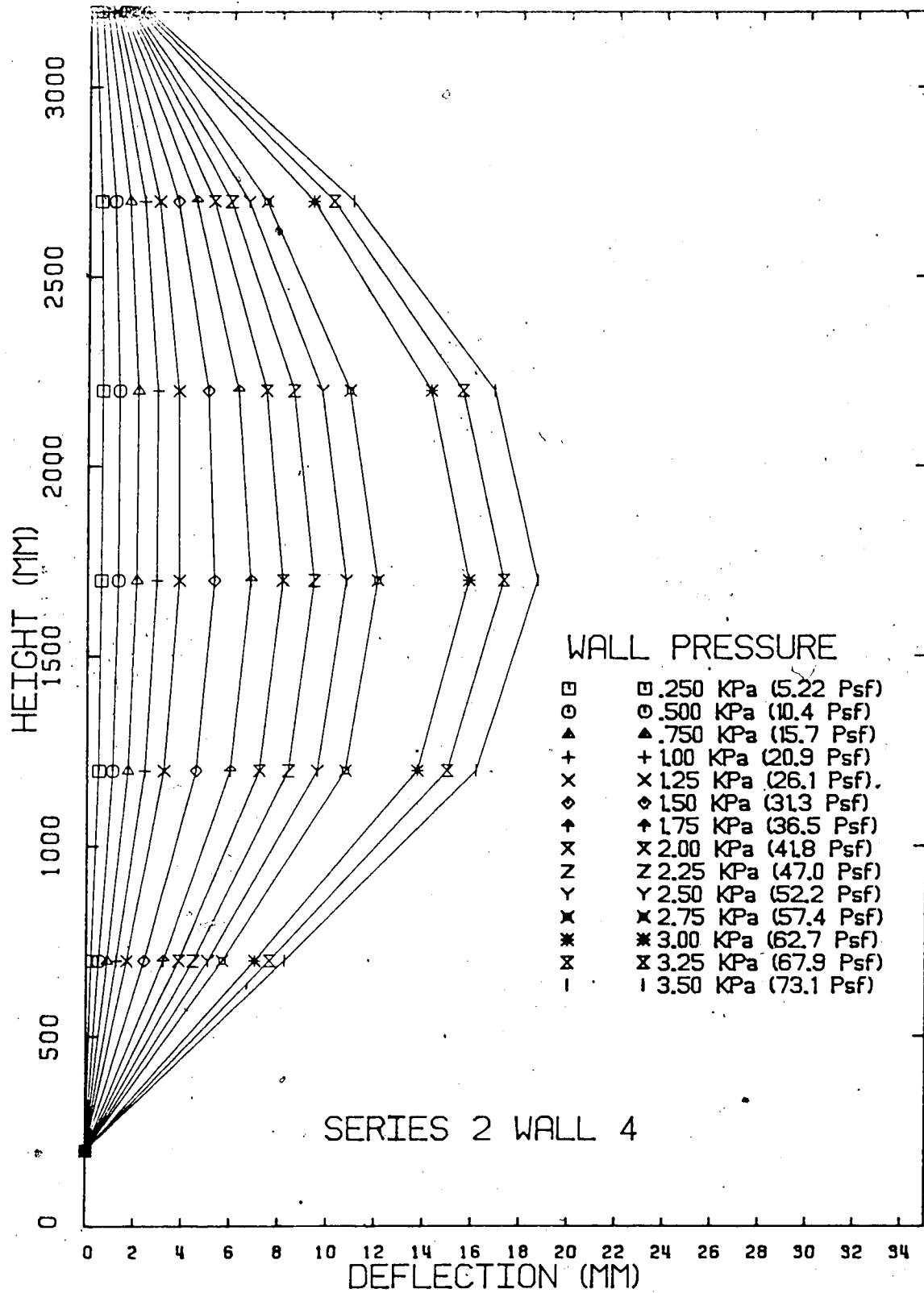


Figure B-16 Stud Wall Deflections - Series No.2 Wall No.4

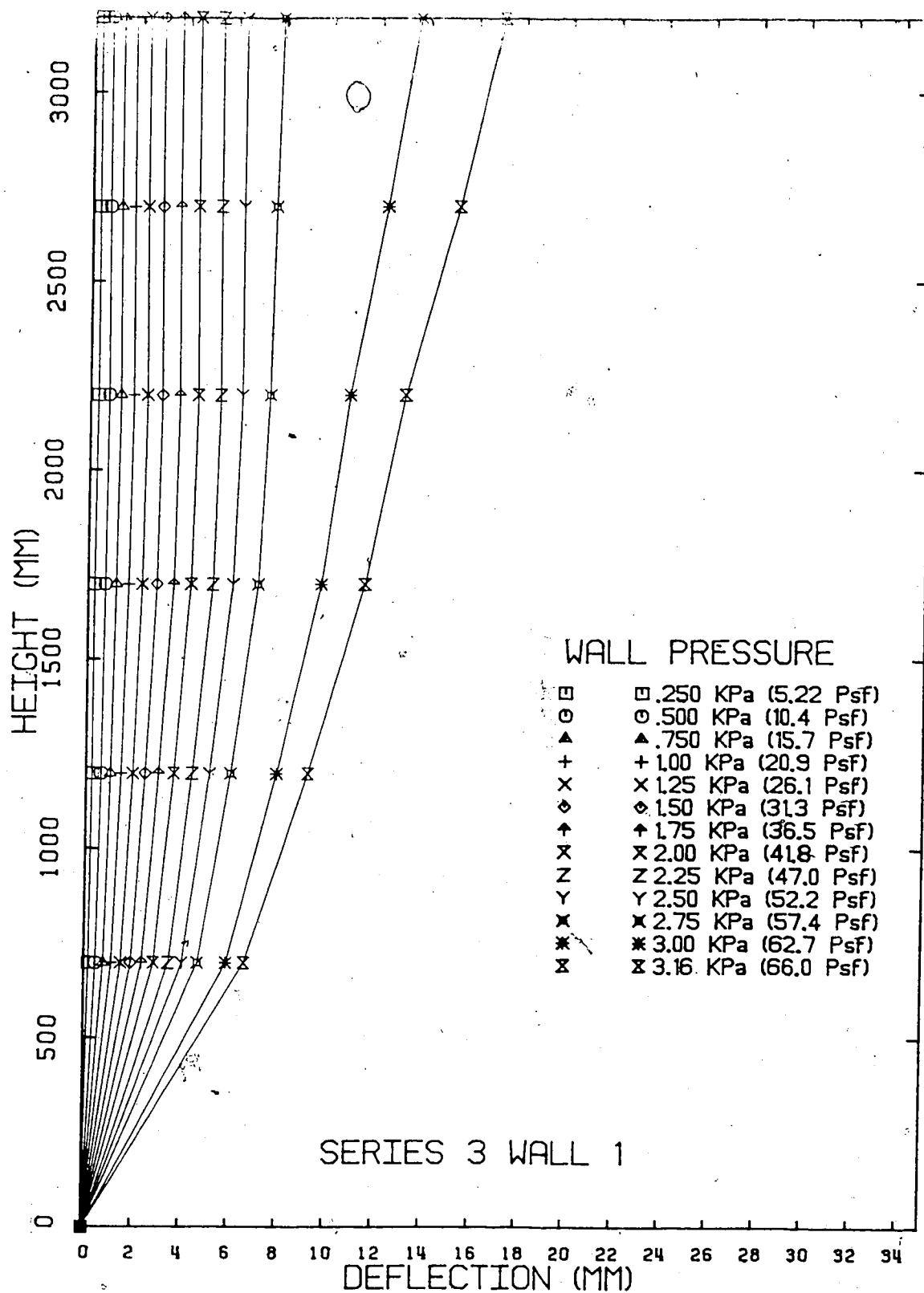


Figure B-17 Brick Veneer Deflections - Series No.3 Wall No.1

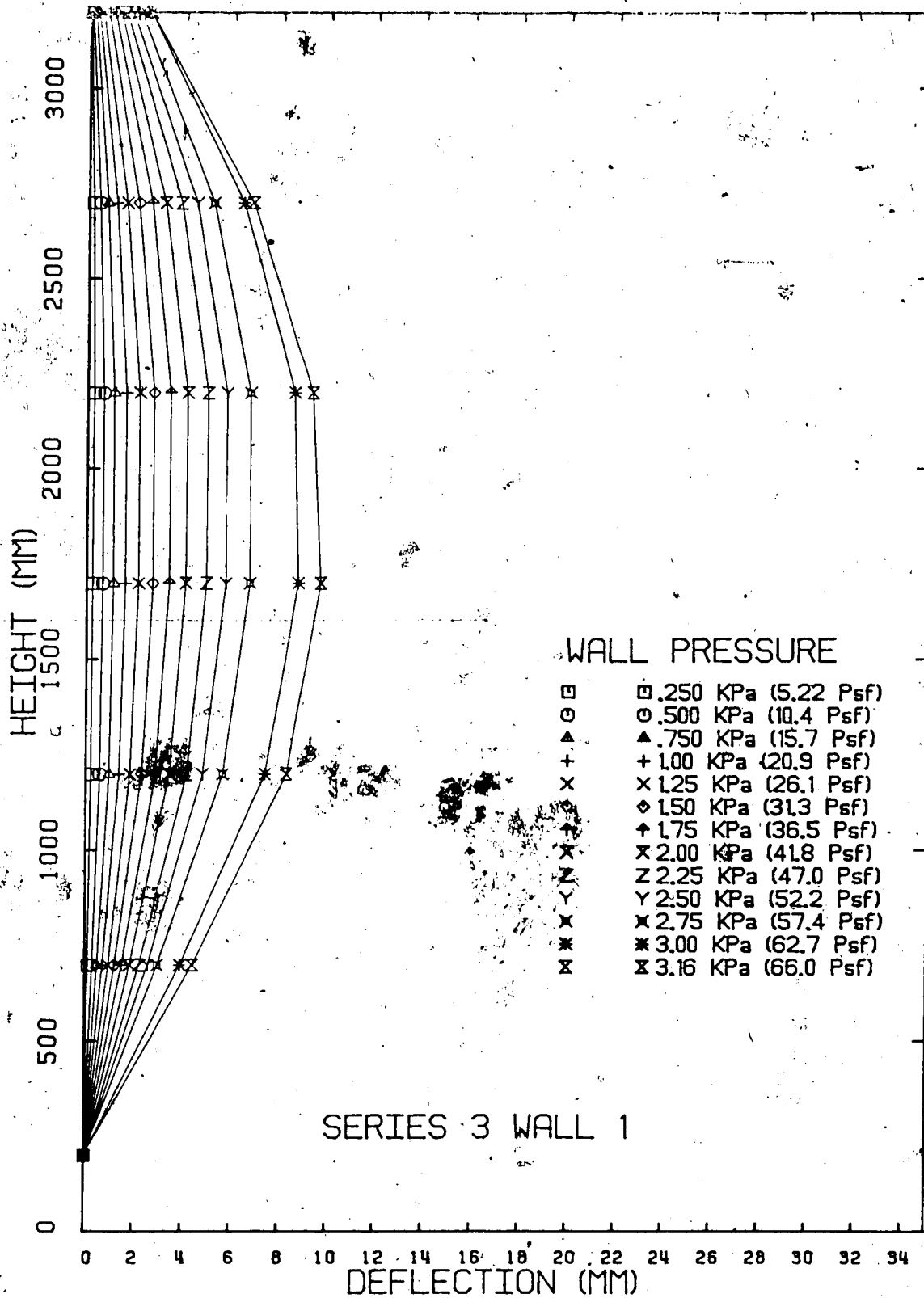


Figure B-18 Stud Wall Deflections - Series No.3 Wall No.1

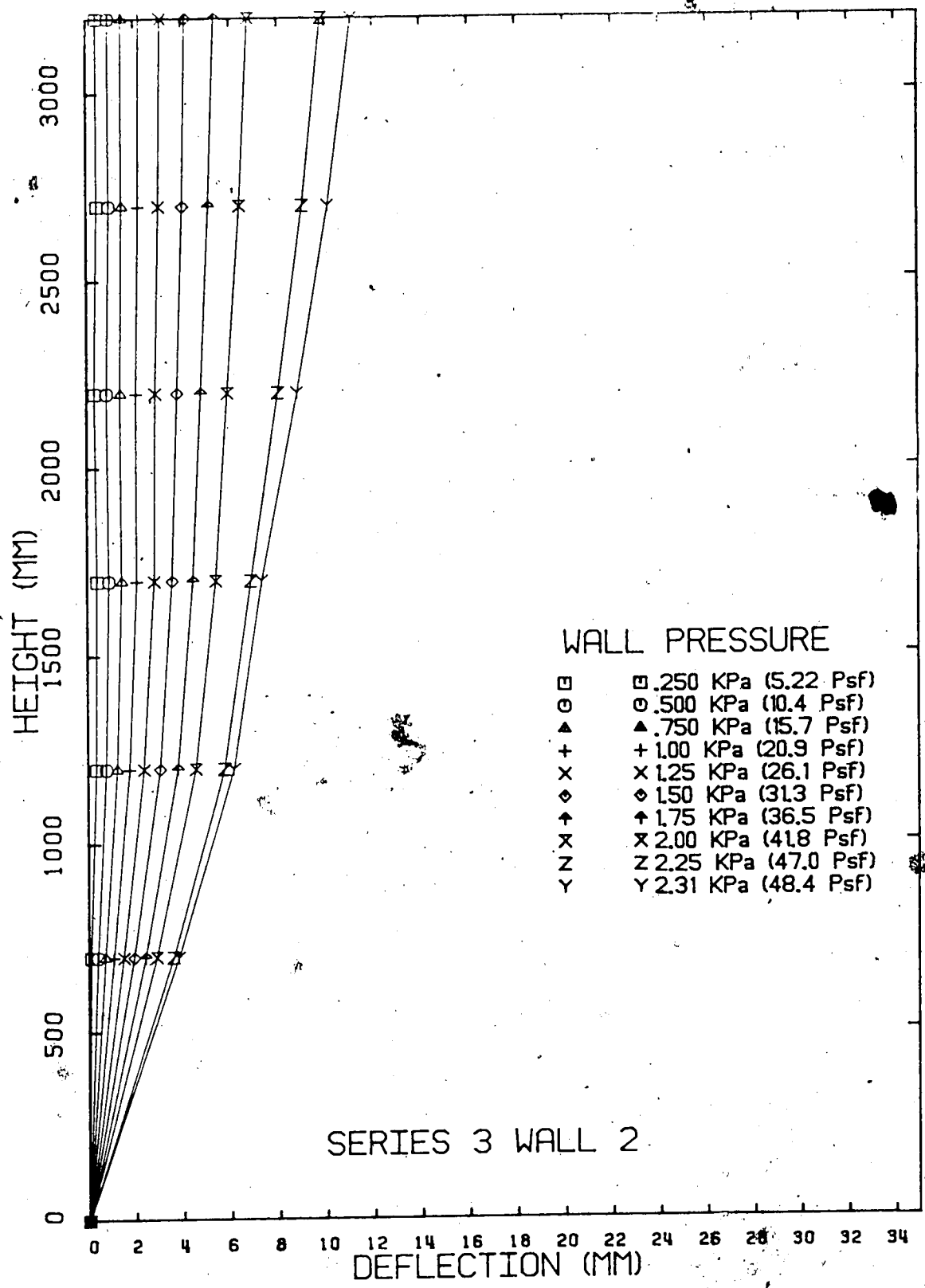


Figure B-19 Brick Veneer Deflections - Series No.3 Wall No.2

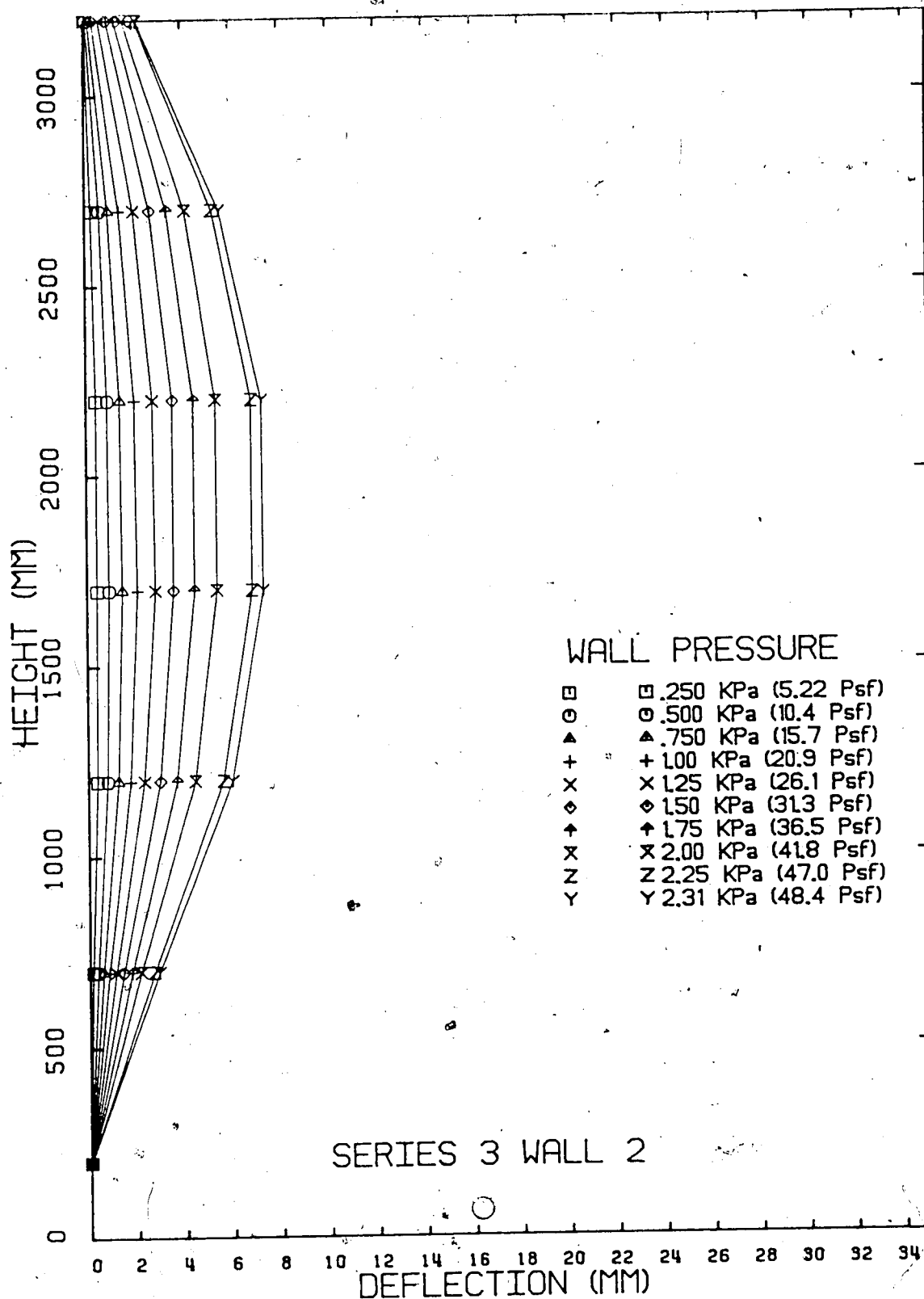


Figure B 20 Stud Wall Deflections - Series No.3 Wall No.2

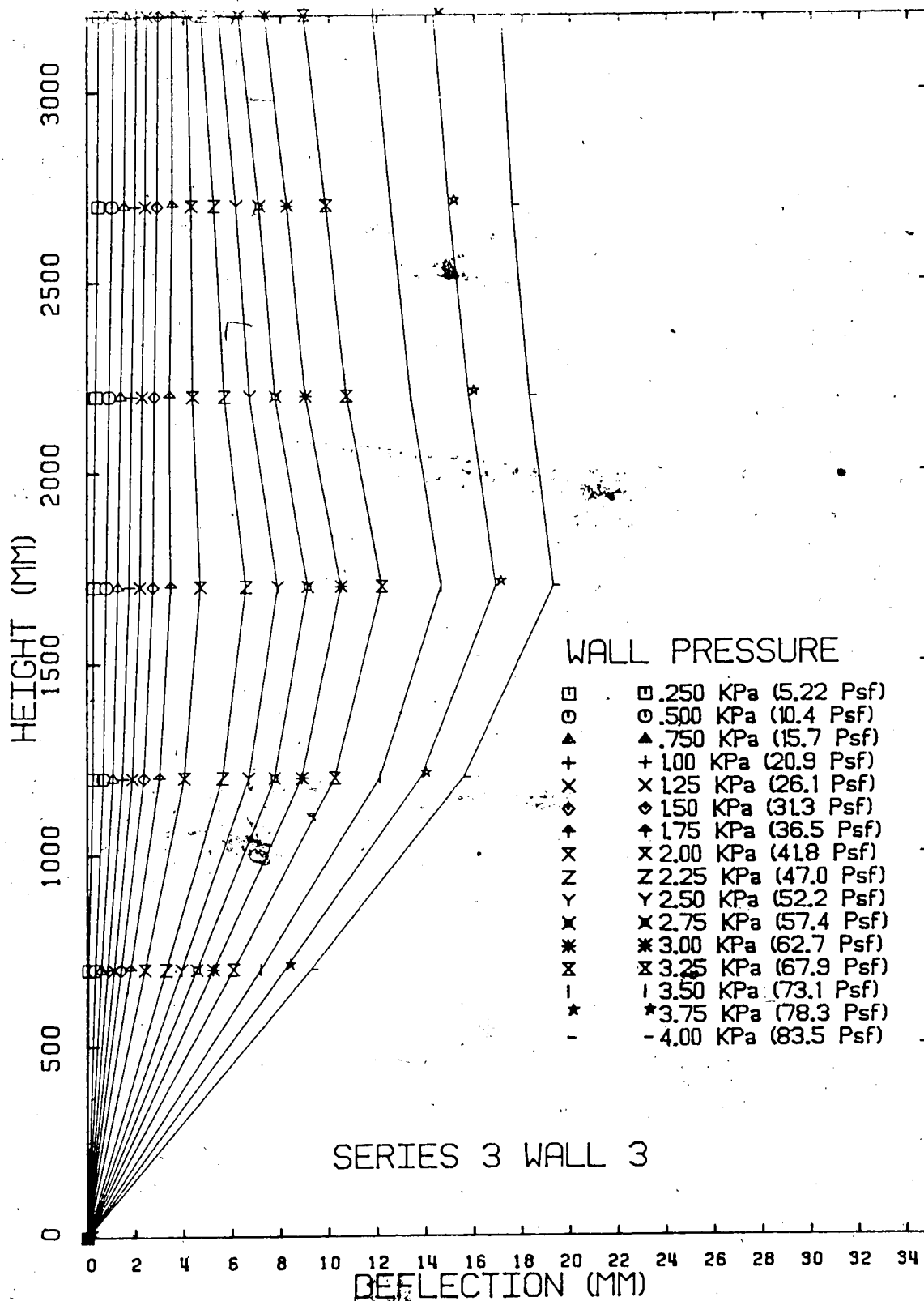


Figure B-21 Brick Veneer Deflections - Series No.3 Wall No.3

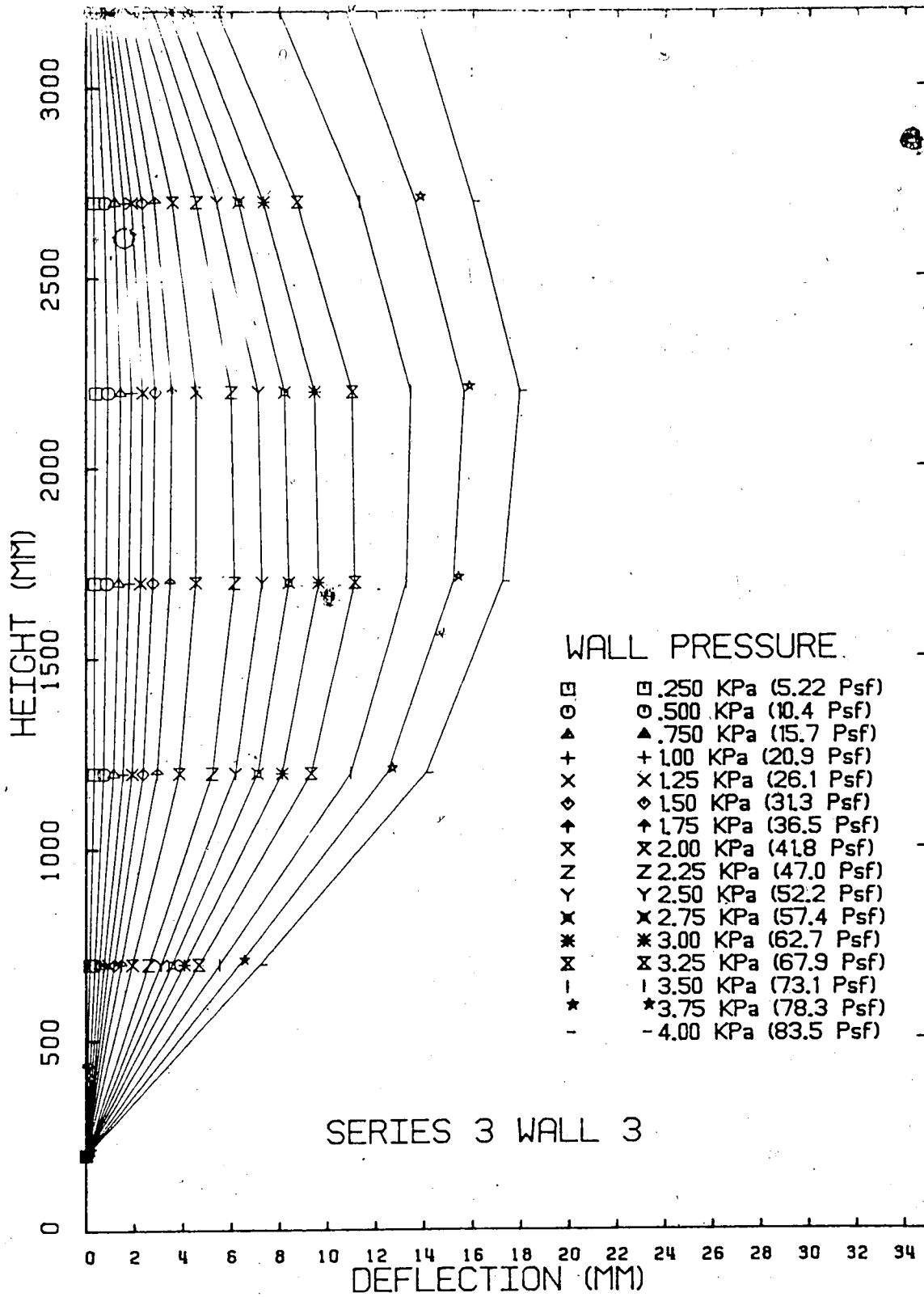


Figure B-22 Stud Wall Deflections - Series No.3 Wall No.3

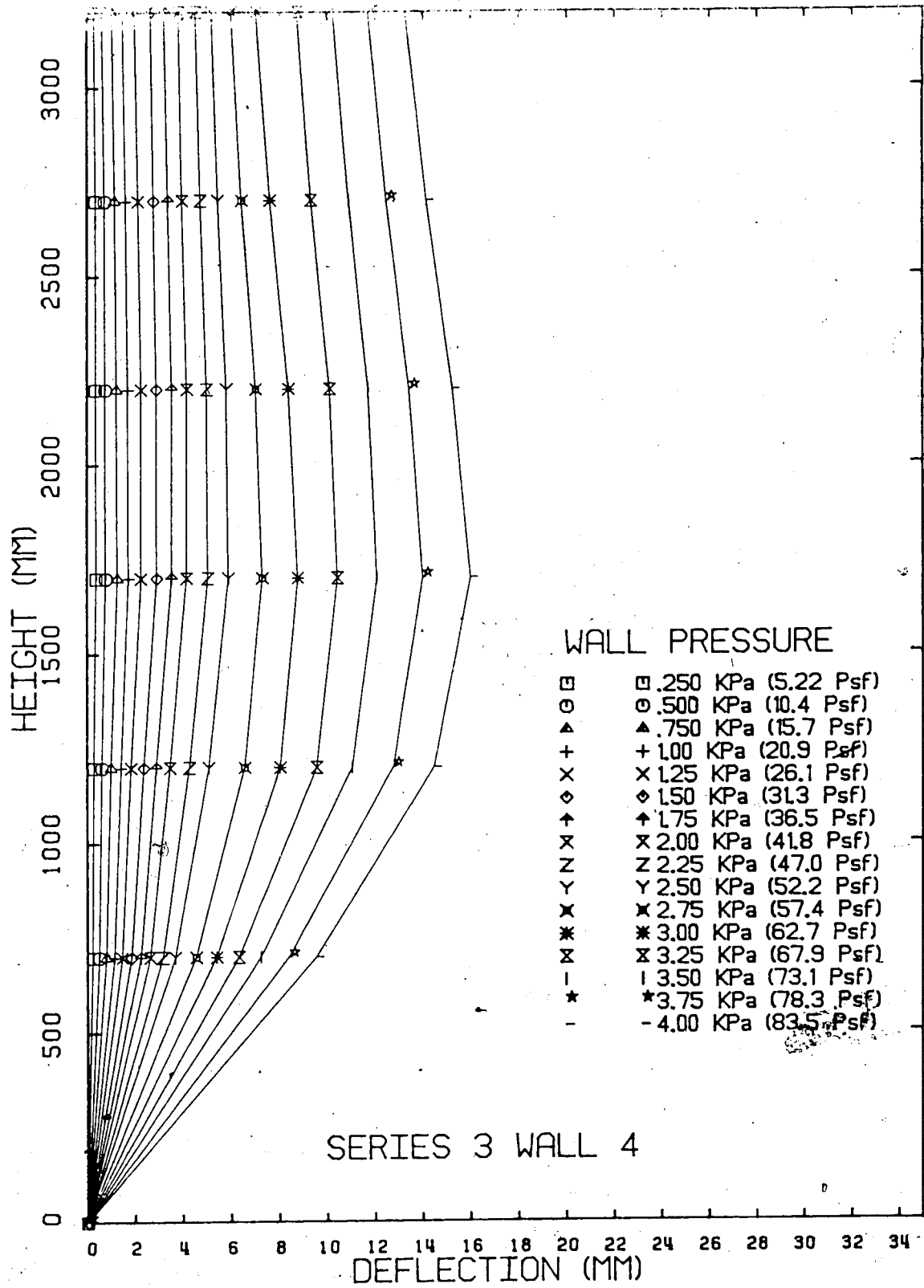


Figure B-23 Brick Veneer Deflections - Series No.3 Wall No.4

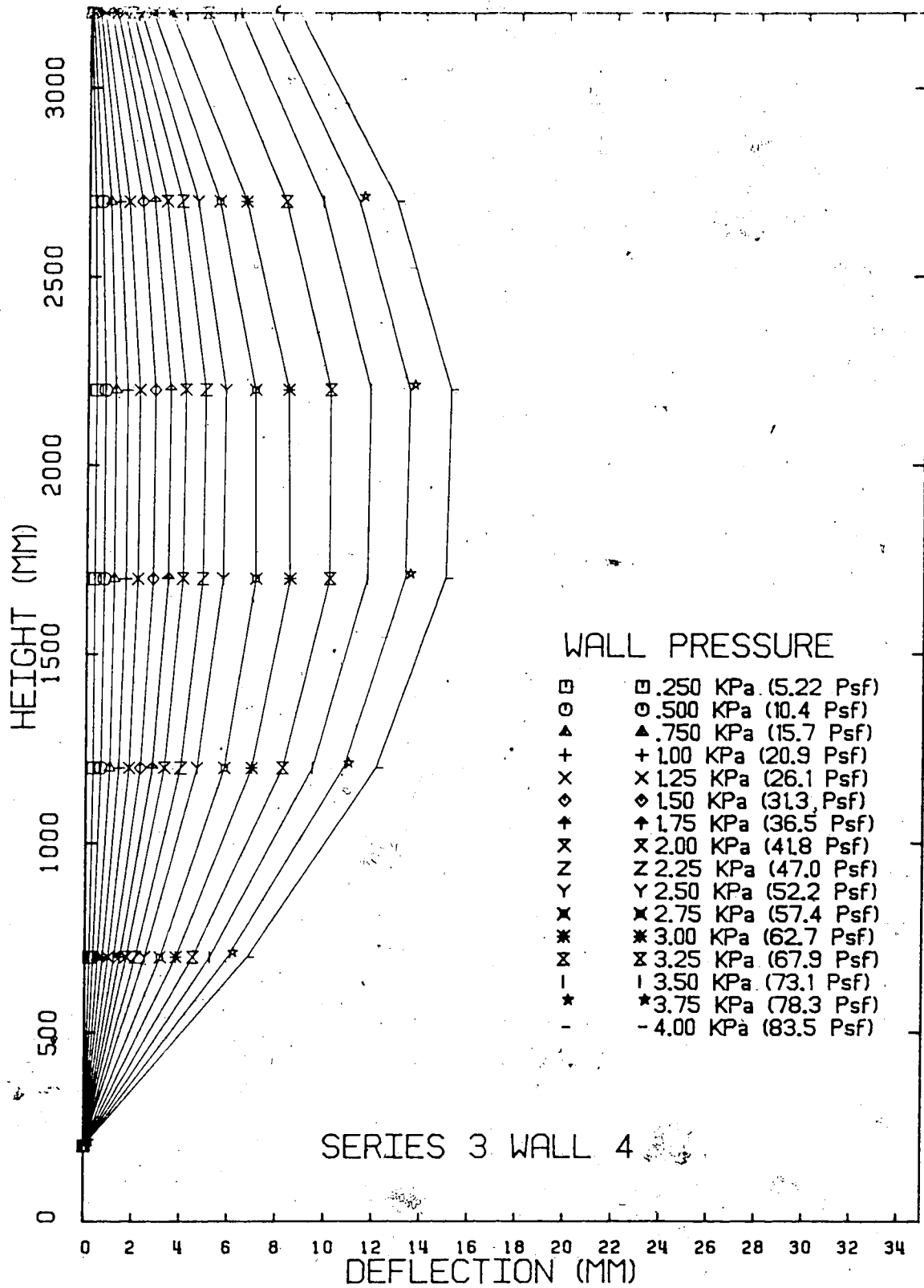


Figure B-24 Stud Wall Deflections - Series No.3 Wall No. 4

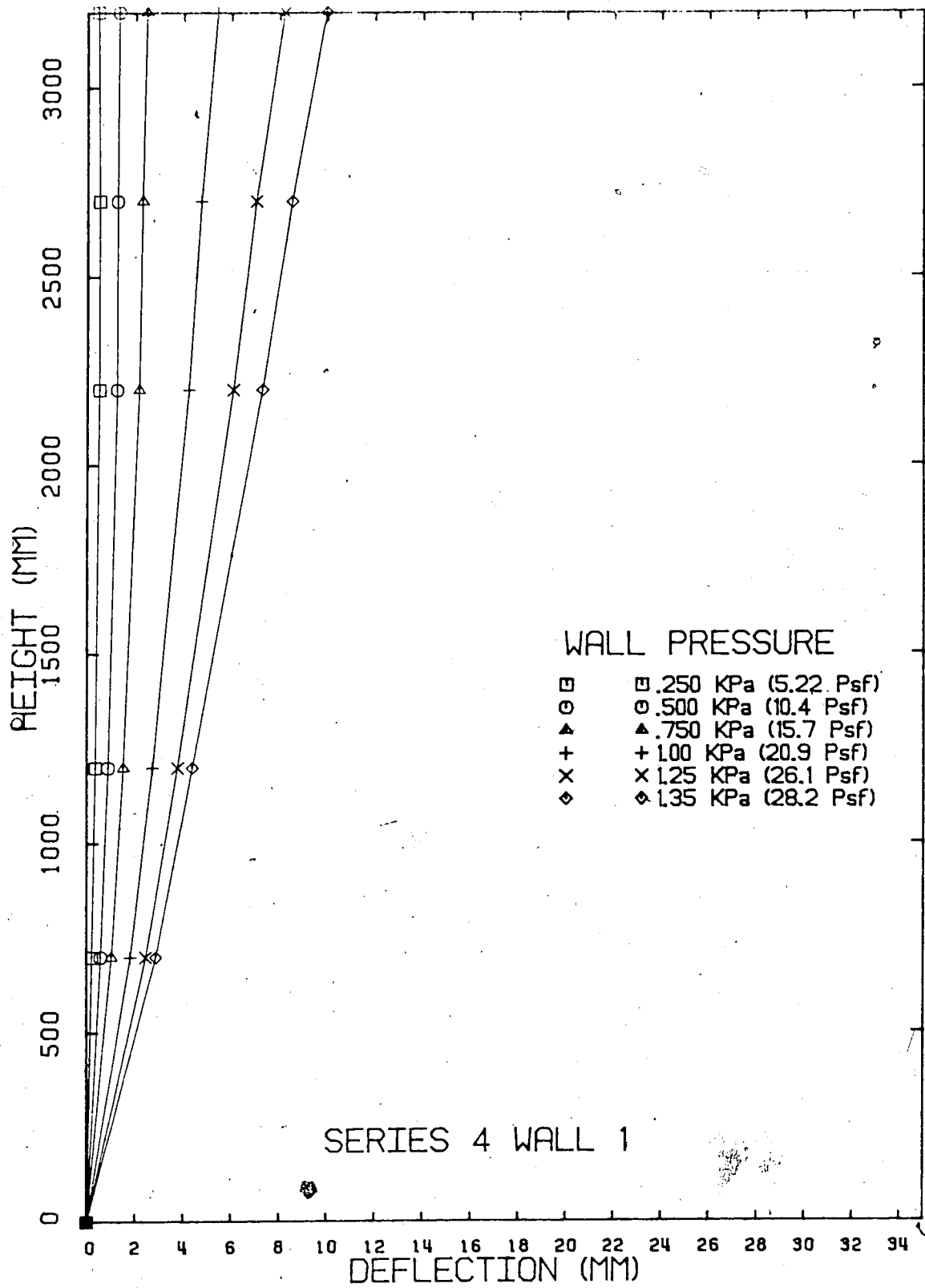


Figure B-25 Brick Veneer Deflections - Series No.4 Wall No.1

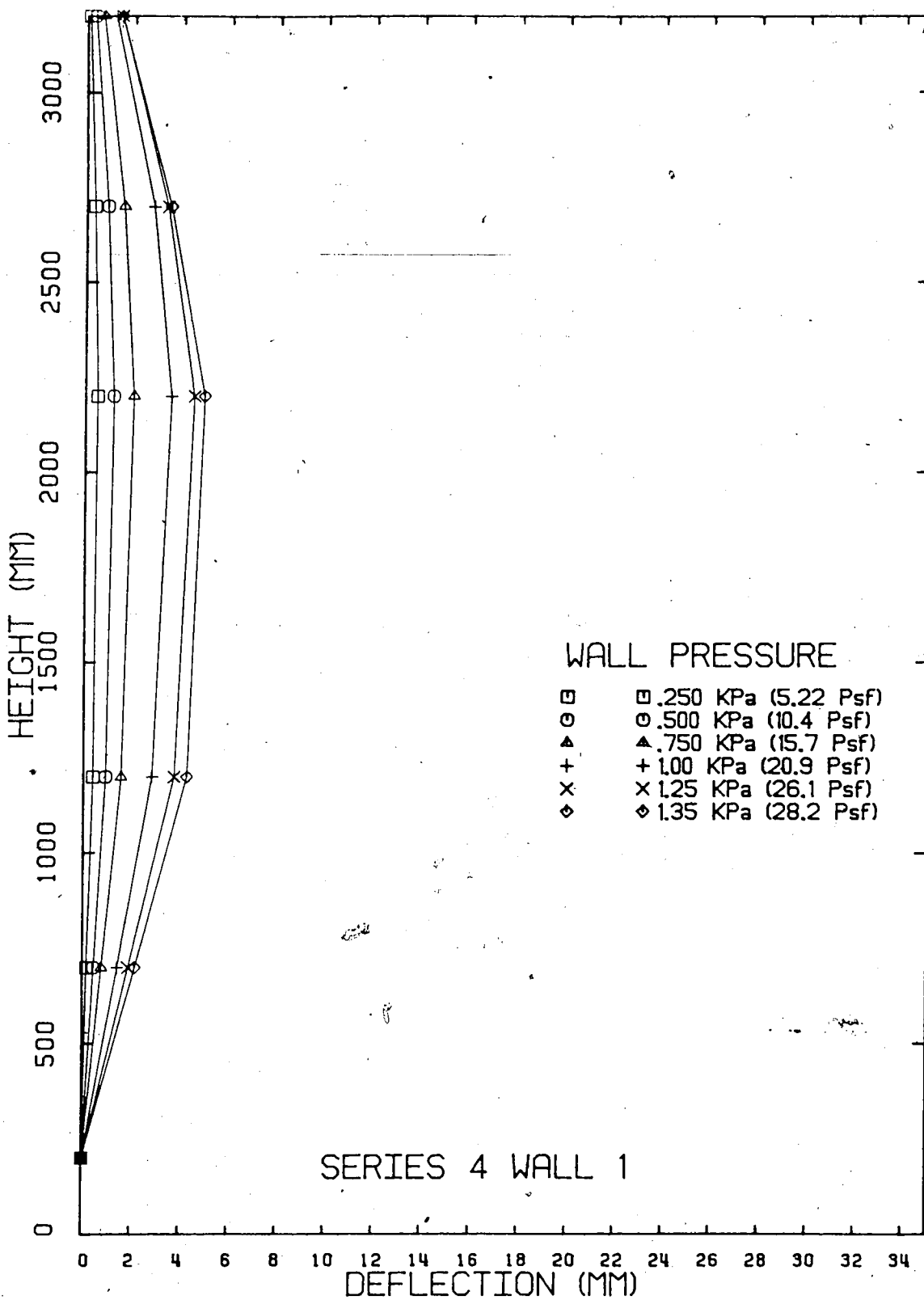


Figure B-26 Stud Wall Deflections - Series No.4 Wall No.1

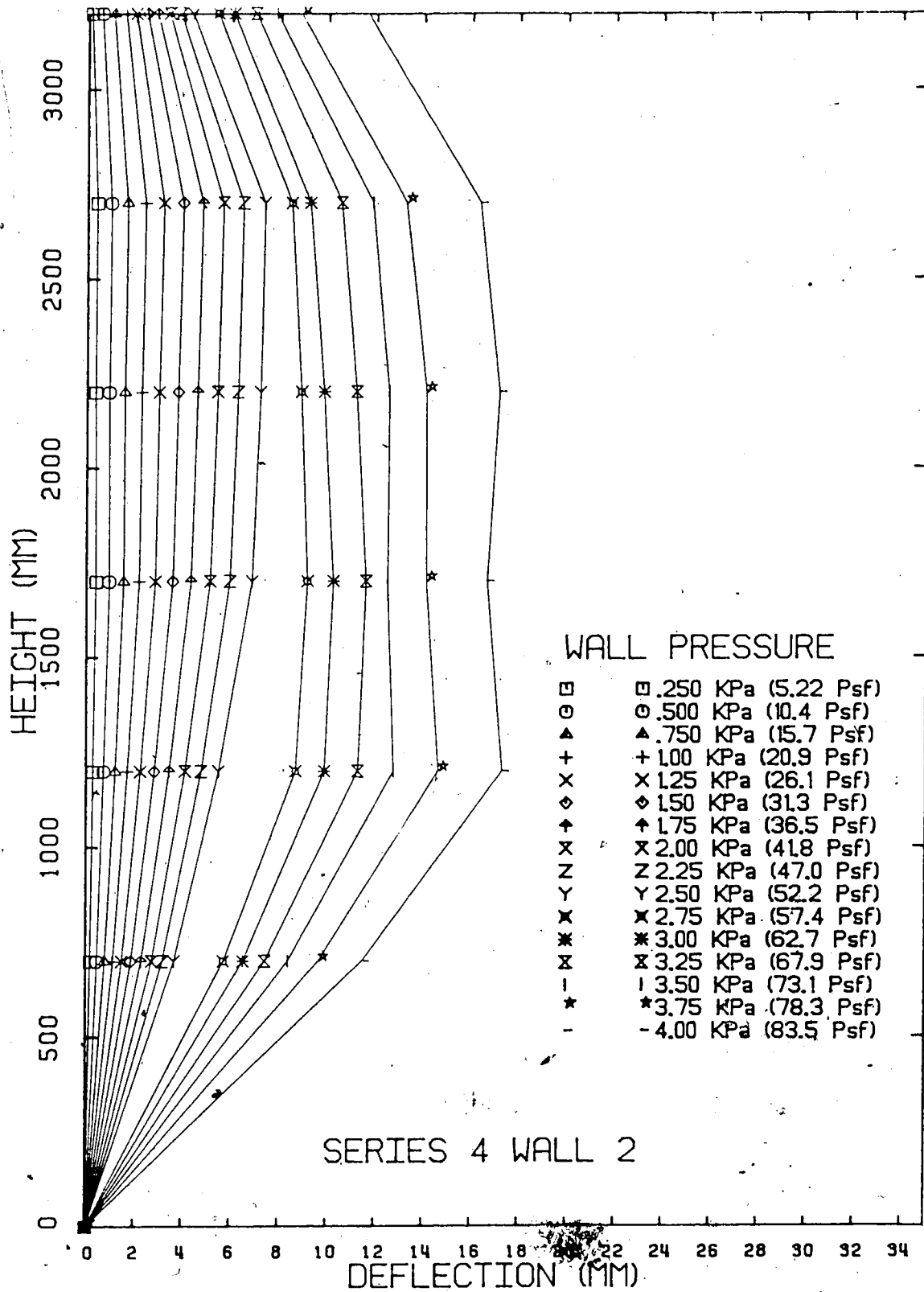


Figure B-27 Brick Veneer Deflections - Series No.4 Wall No.2

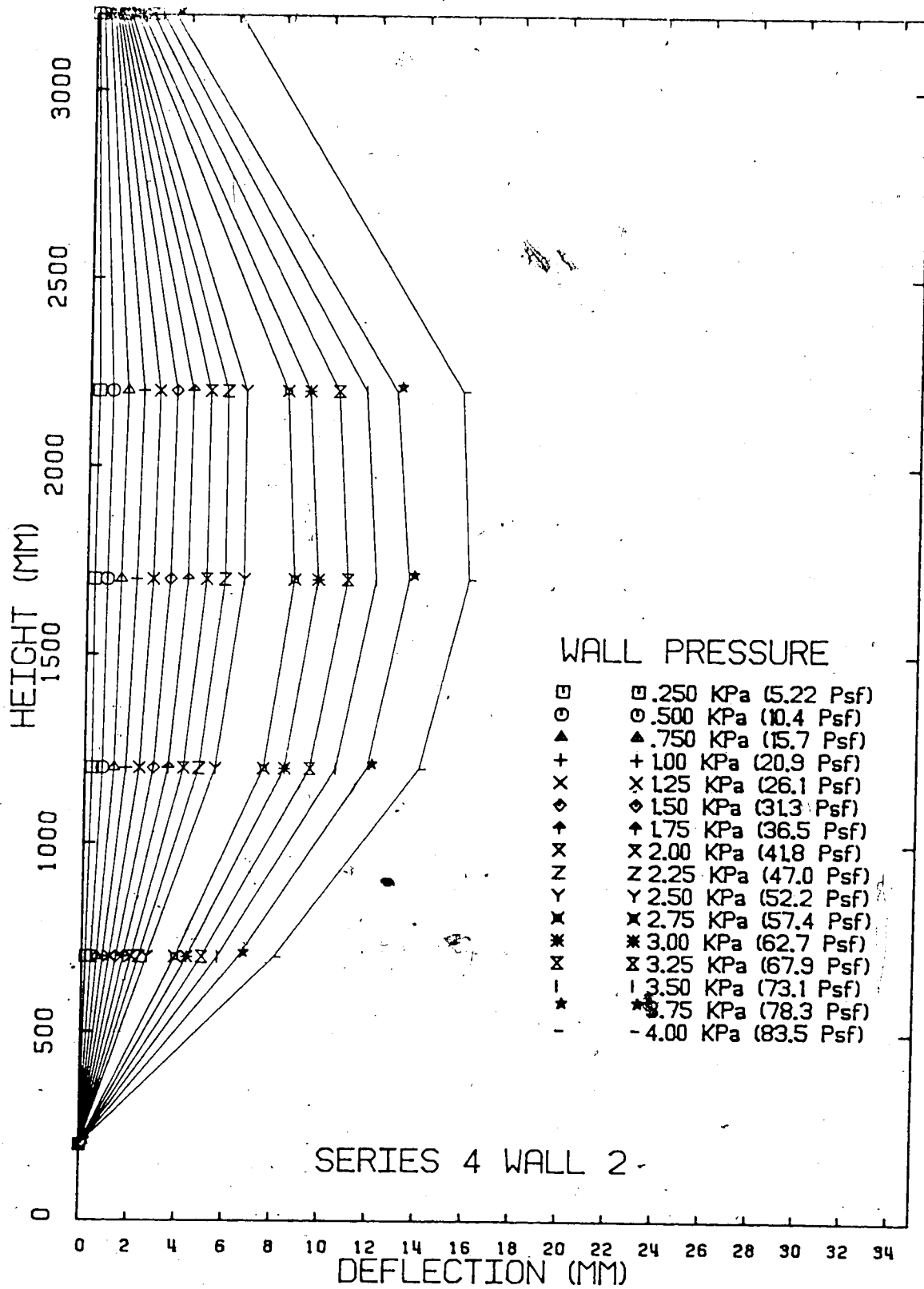


Figure B-28 Stud Wall Deflections - Series No.4 Wall No.2

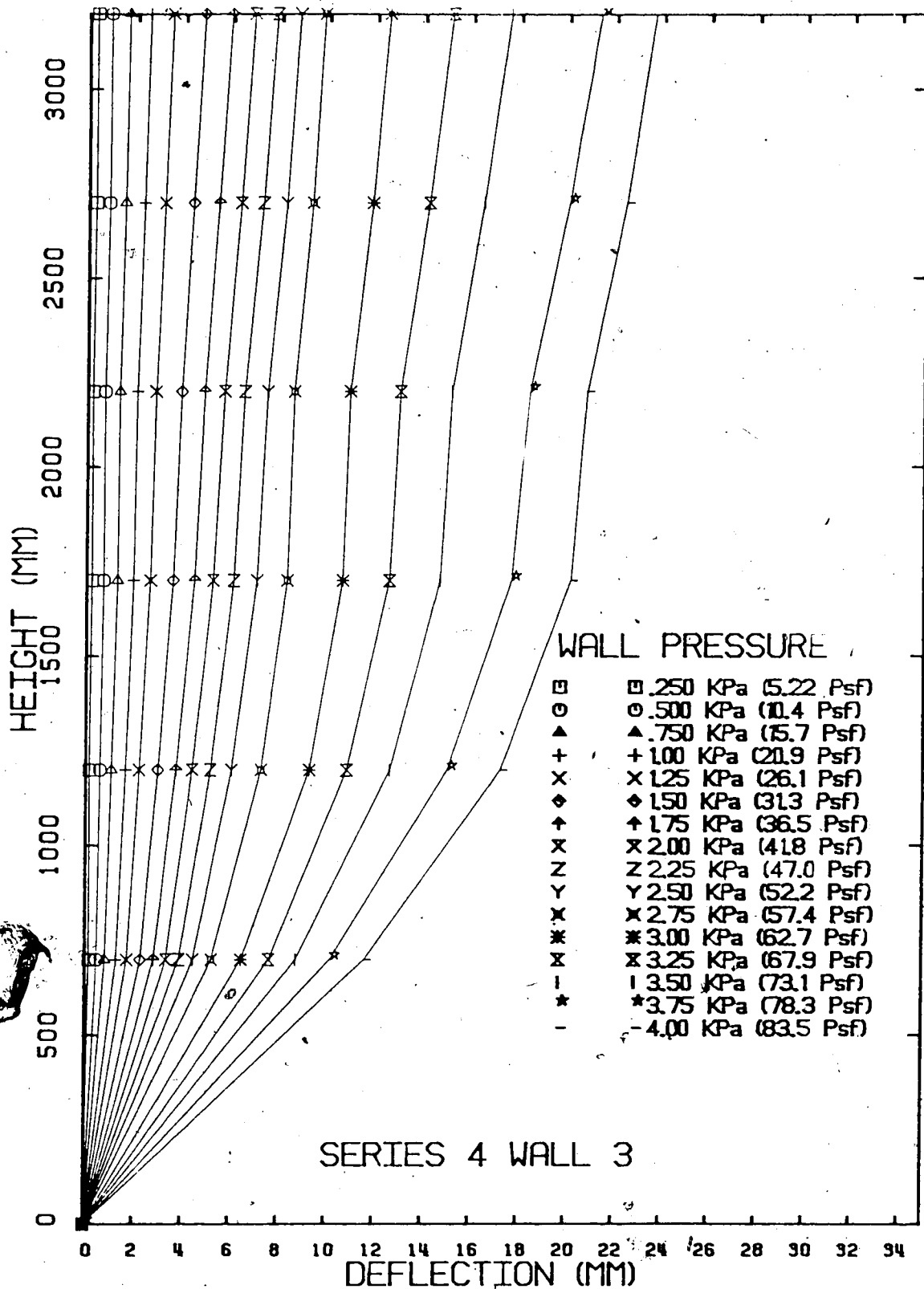


Figure B-29 Brick Veneer Deflections - Series No.4 Wall No.3

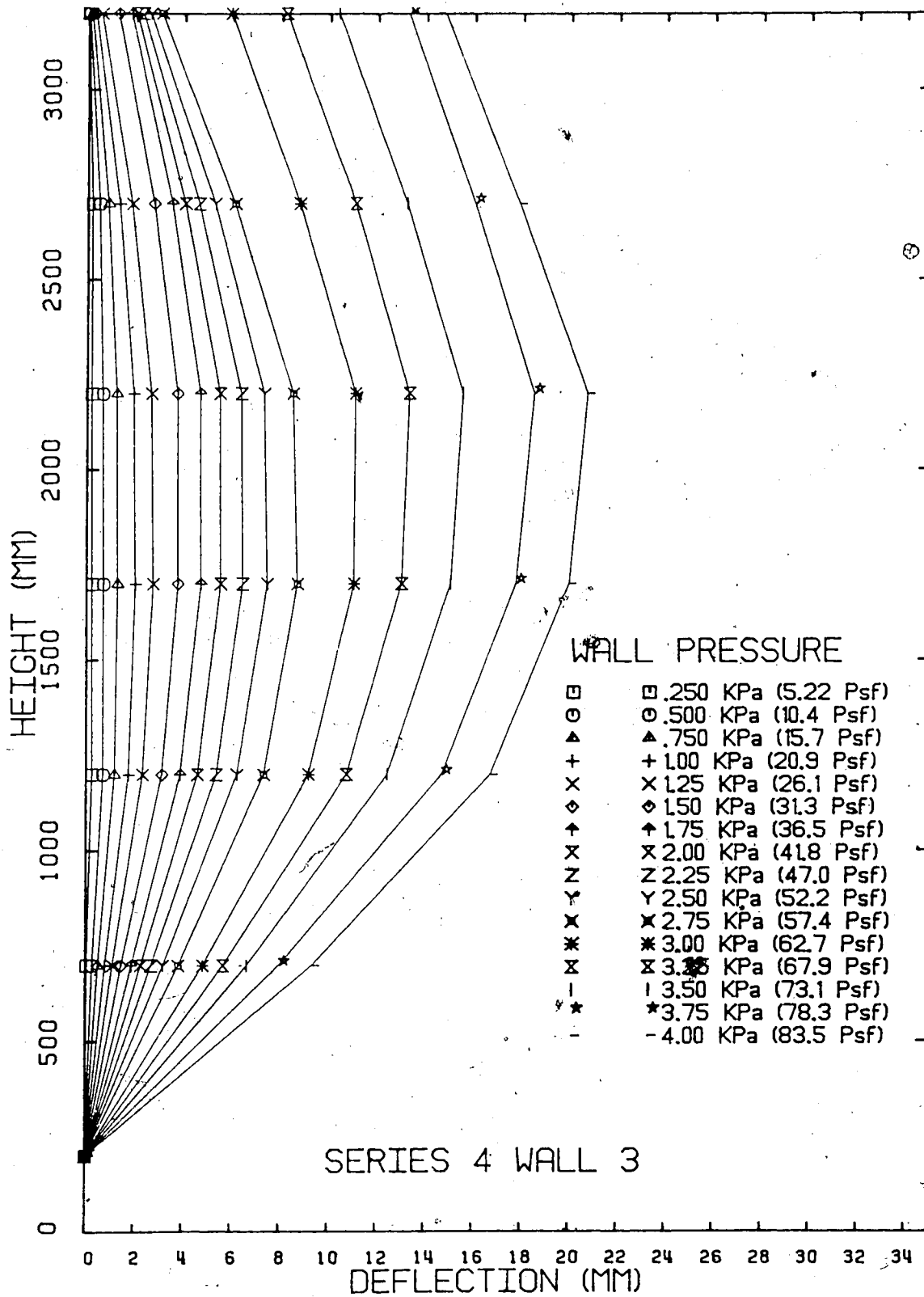


Figure B-30 Stud Wall Deflections - Series No.4 Wall No.3

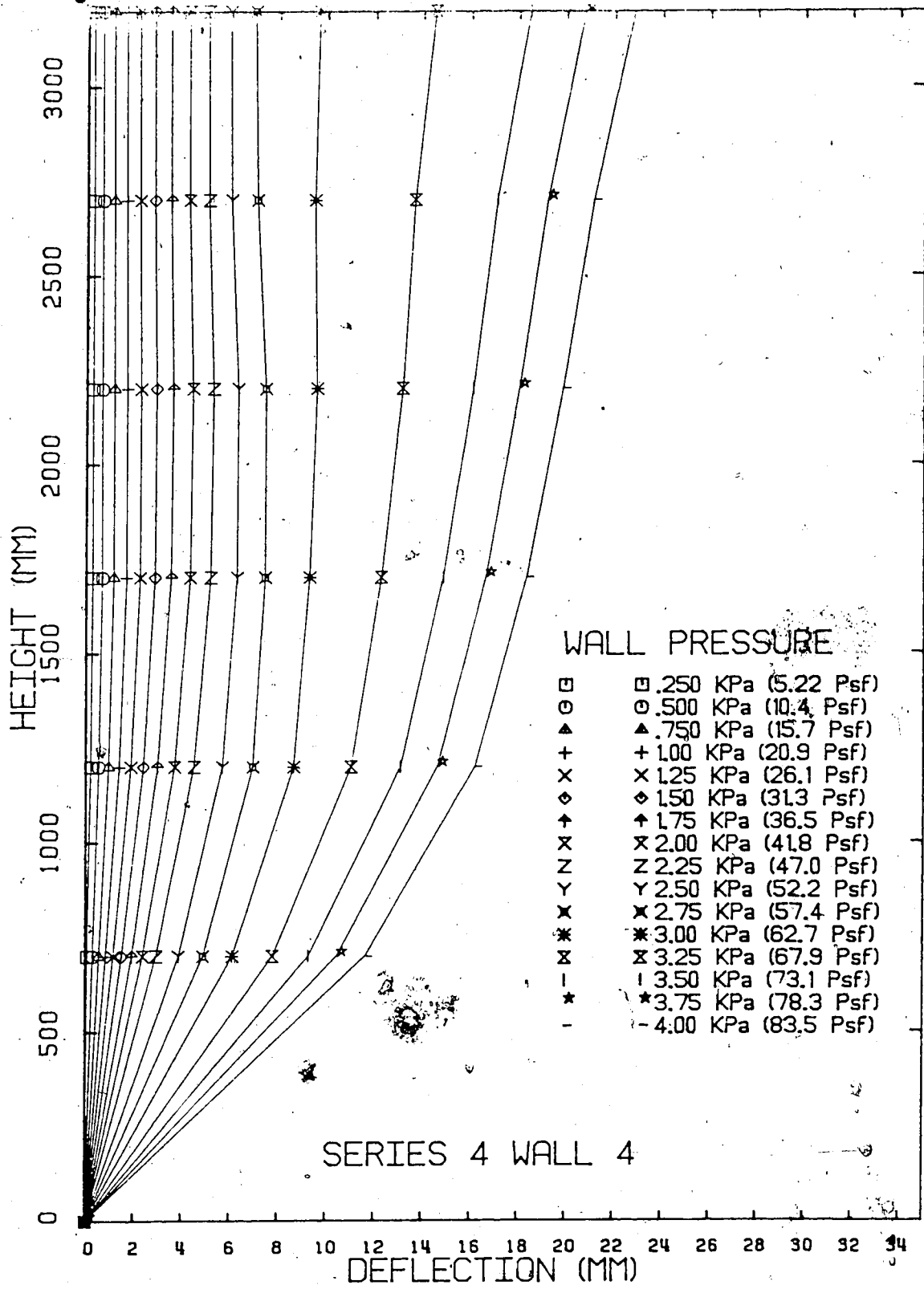


Figure B-3: Brick Veneer Deflections - Series No.4 Wall No.4

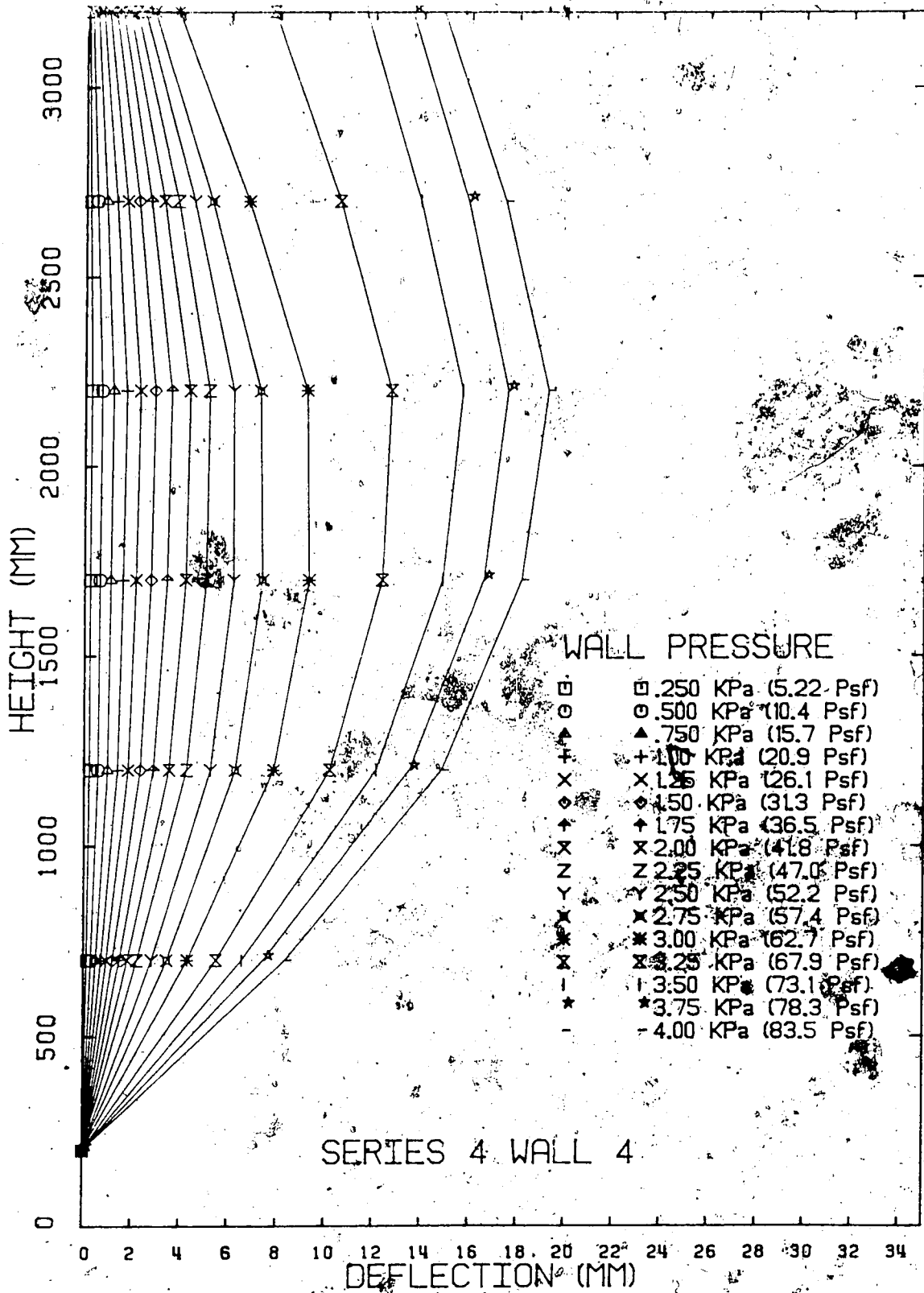


Figure B-32 Stud Wall Deflections - Series No.4 Wall No.4

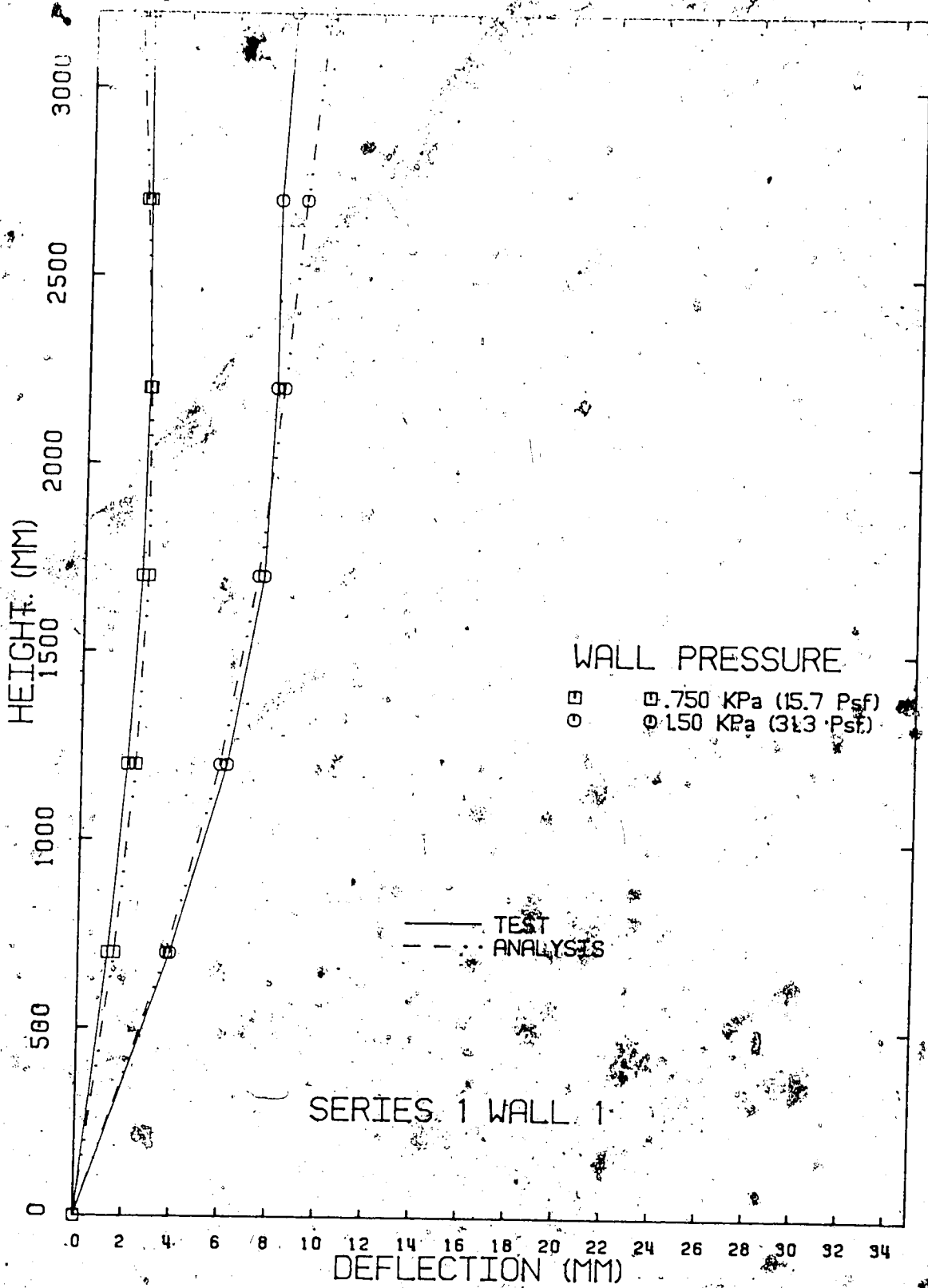


Figure B-33 Brick Veneer Deflections - Series No. 1 Wall No. 1

With Analysis

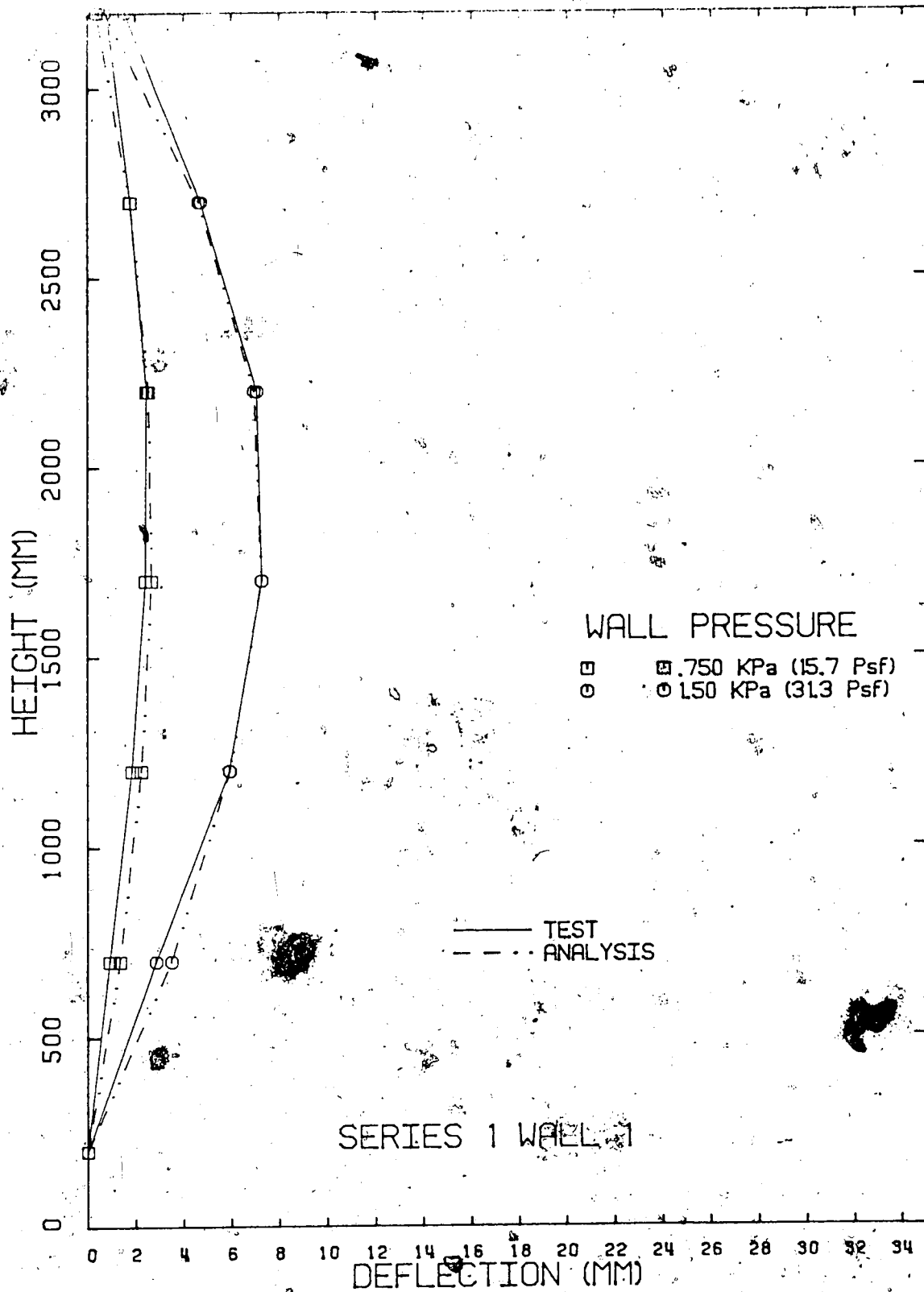


Figure B-34 Stud Wall Deflections - Series No. 1 Wall No. 1

With Analysis

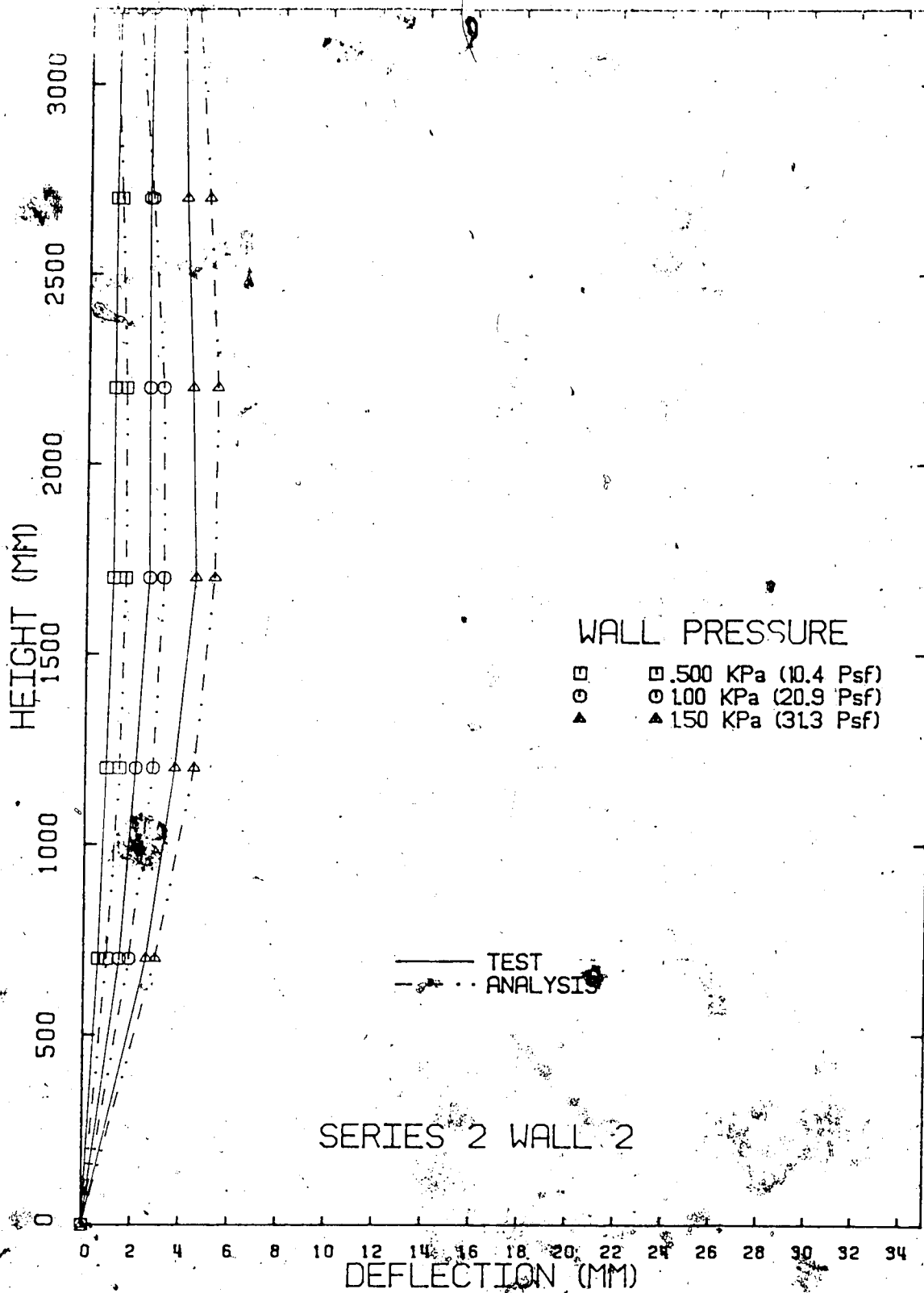


Figure B-35 Brick Veheer Deflections - Series No.2 Wall No.2
With Analysis

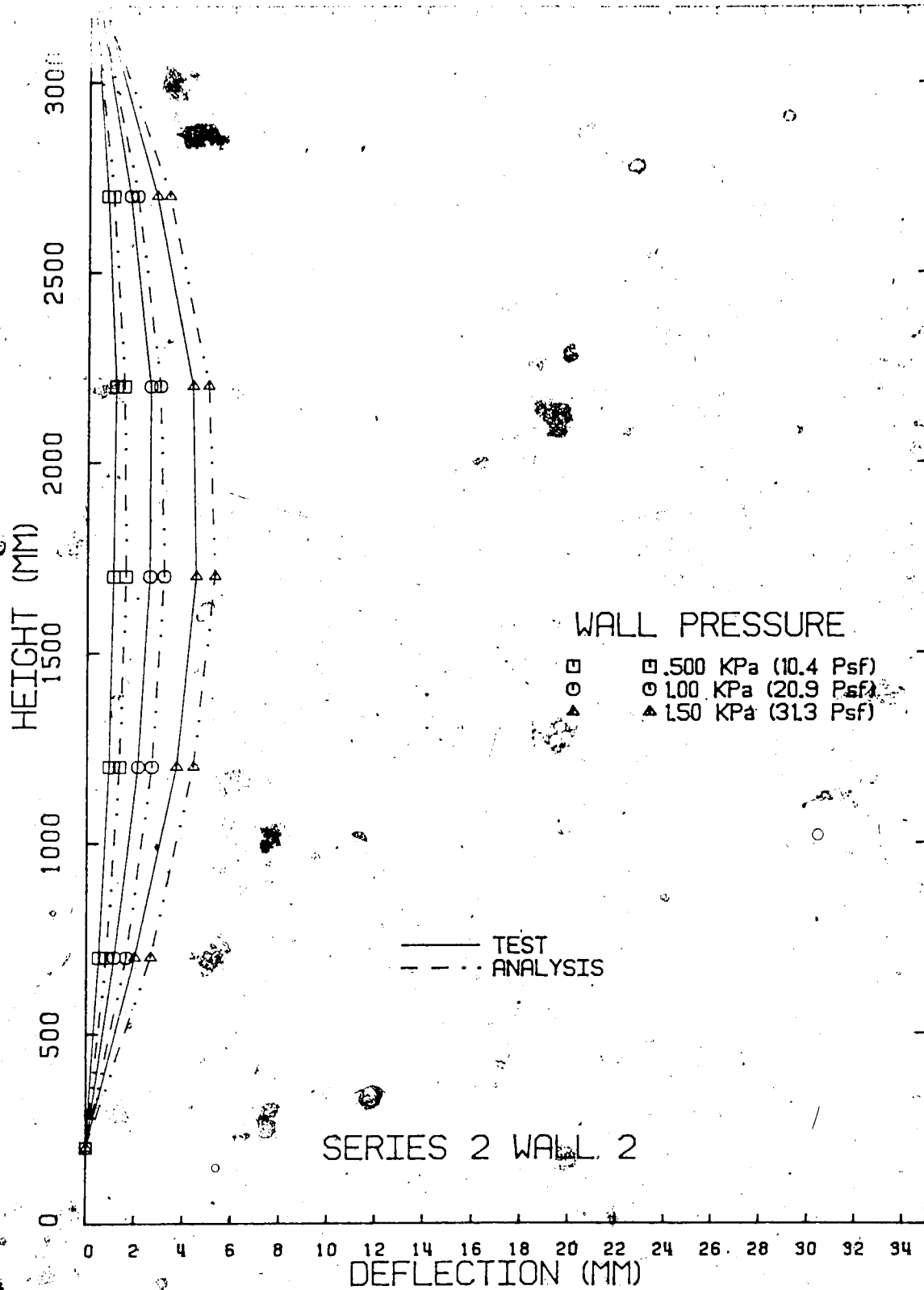


Figure B-36 Stud Wall Deflections - Series No. 2 Wall No. 2

With Analysis

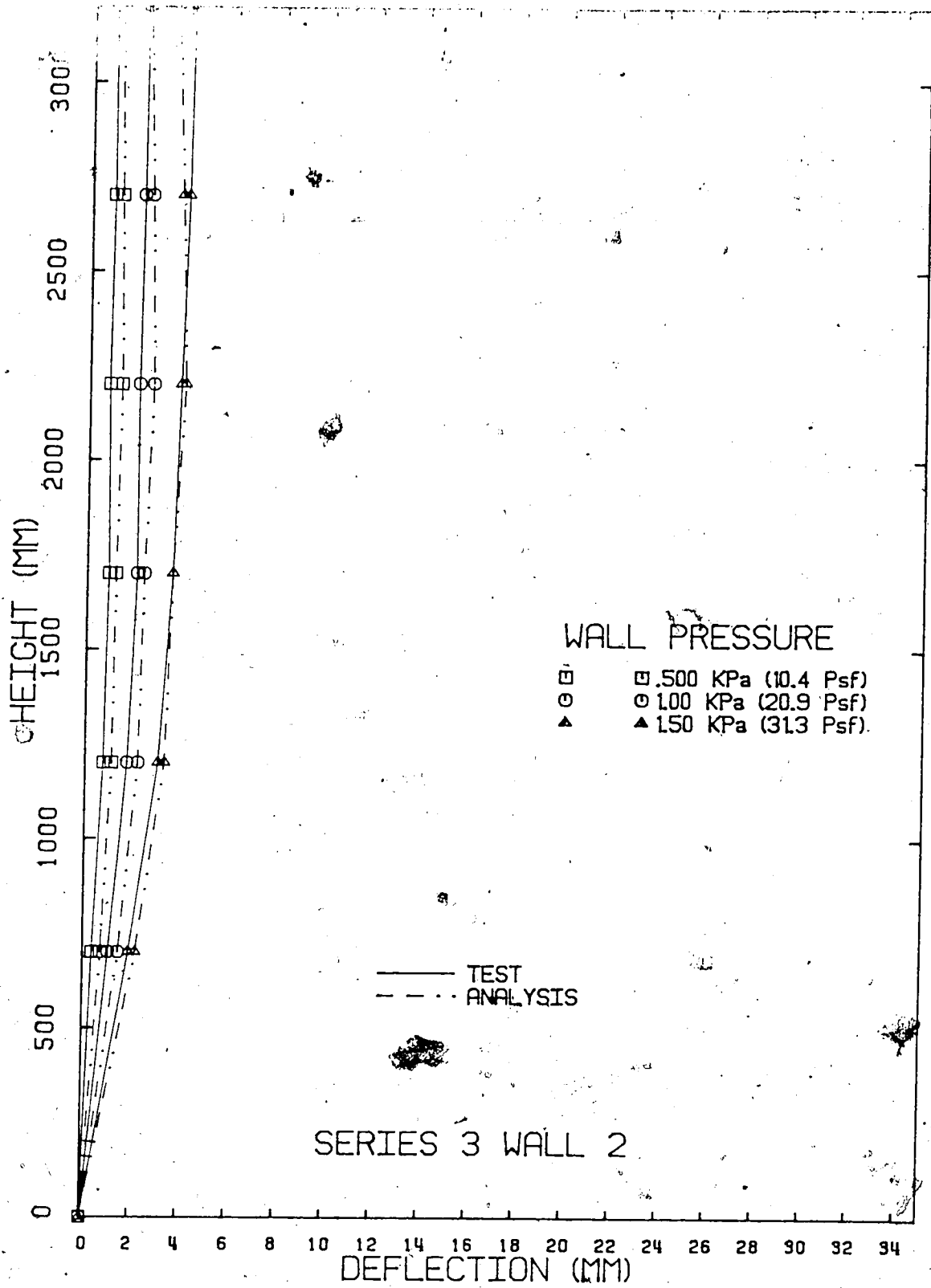


Figure B-37 Brick Veneer Deflections - Series No.3 Wall No.2

With Analysis

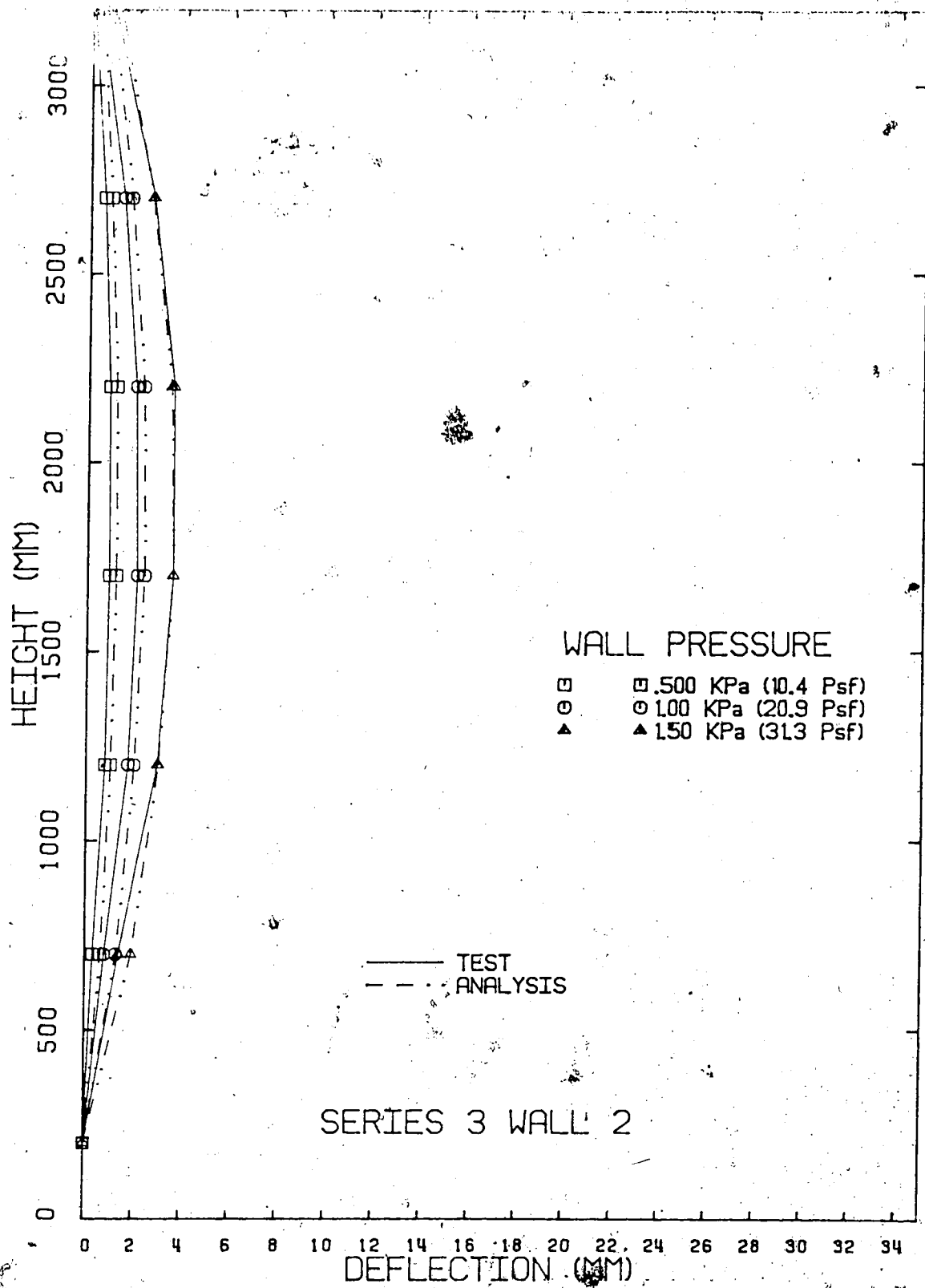


Figure B-38 Stud Wall Deflections - Series No. 3 Wall No. 2
With Analysis

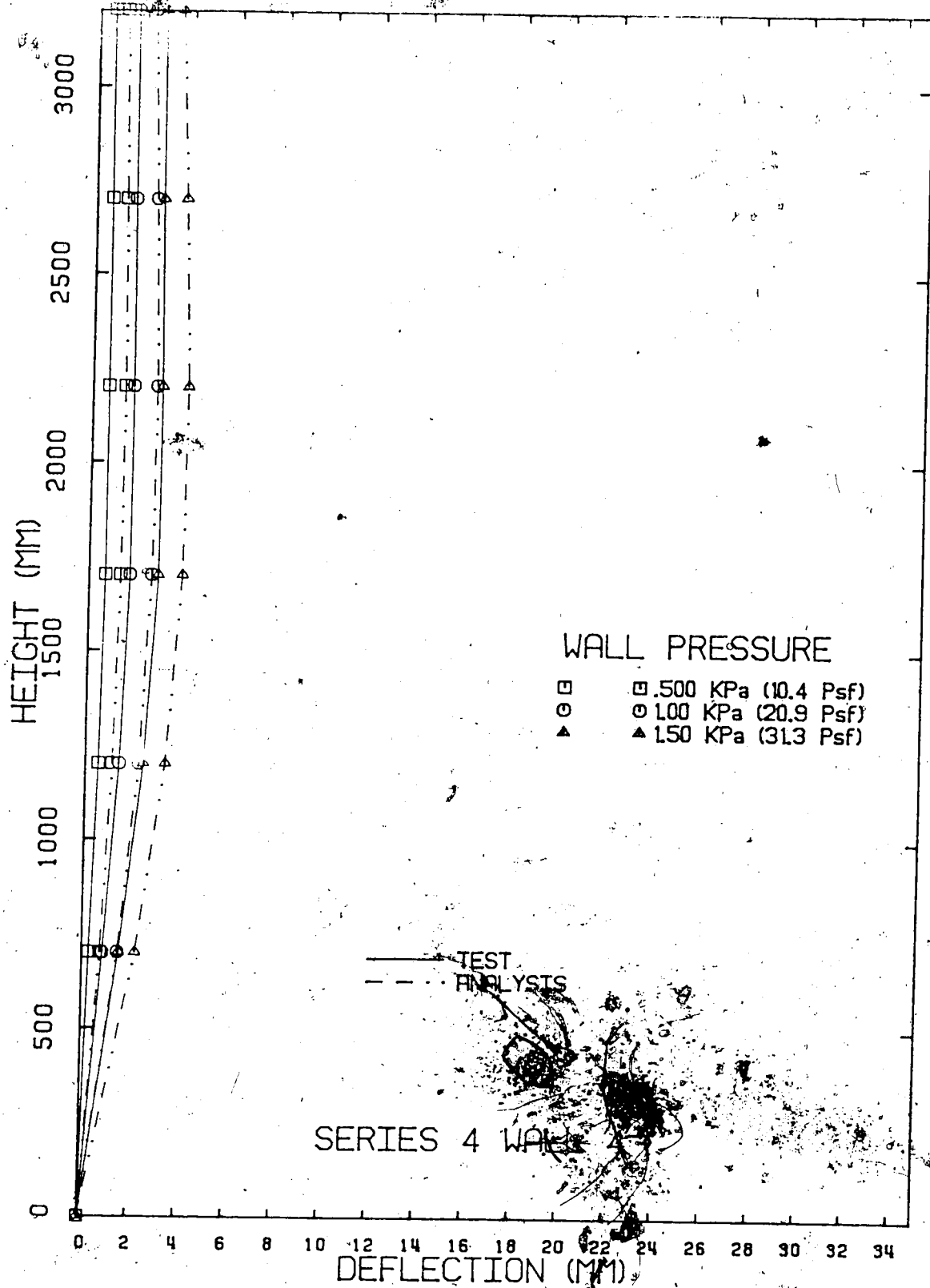


Figure B-39 Brick Veneer Deflections -- Series No. 4 Wall No. 4
With Analysis

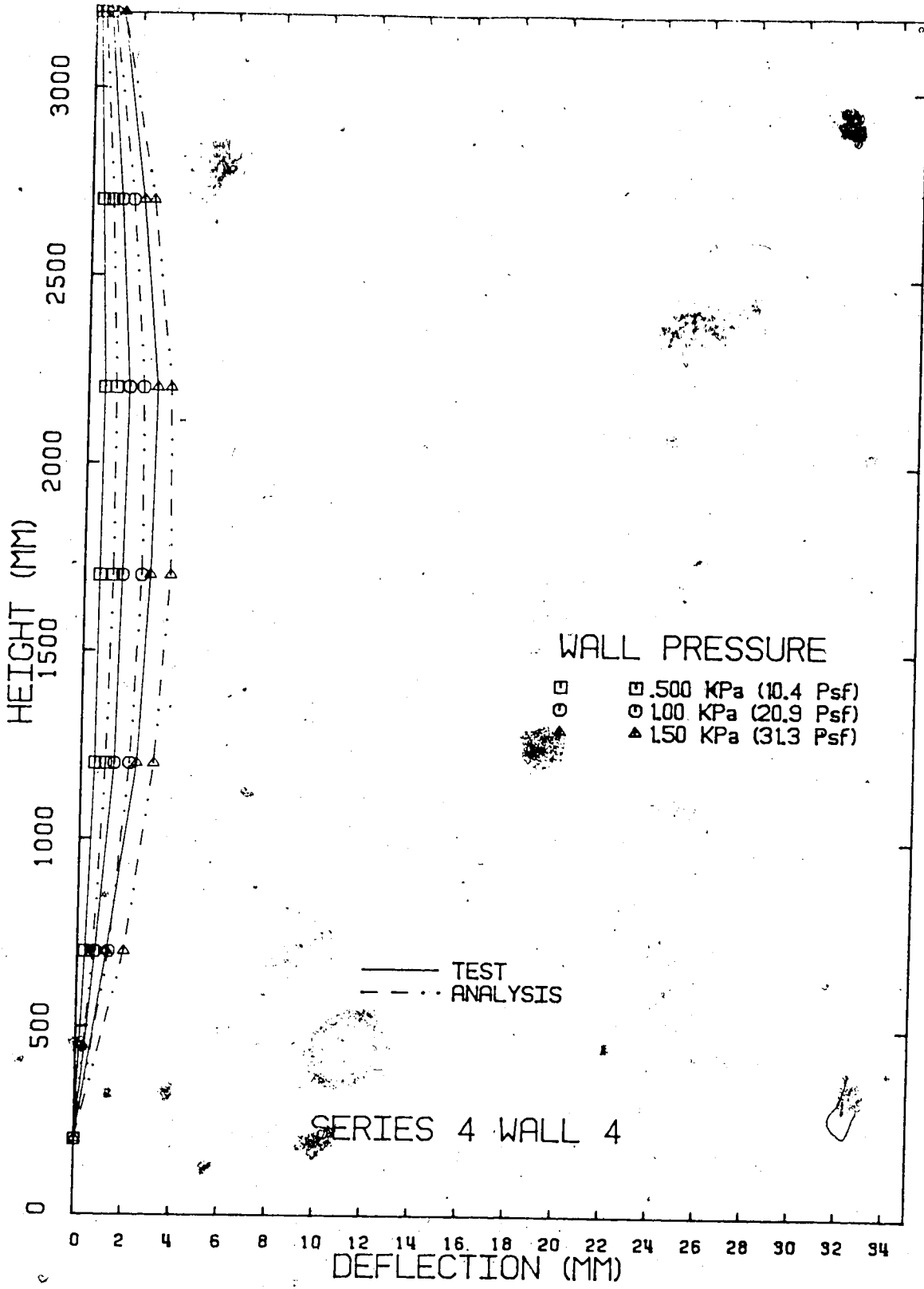


Figure B-40 Stud Wall Deflections - Series No.4 Wall No.4.
With Analysis